Faculty of Medicine and Health Sciences
School of Medicine

Investigating the Role of CD24 in Metastatic Colorectal Cancer

Abdullah Sulaiman Alsulaiman
MSc (Molecular Genetics)

Under the supervision of Professor Mohammad Ilyas

Thesis submitted to the University of Nottingham for the

Degree of Doctor of Philosophy

Declaration

This thesis entitled 'Investigating the Role of CD24 in Metastatic Colorectal Cancer' has been composed by Abdullah Alsulaiman, and I confirm that the work presented in this thesis is my own, unless otherwise mentioned. No part of this thesis has been submitted for any degree, diploma or any other type of qualification at any other institution.

Abdullah Sulaiman Alsulaiman

Acknowledgment

I must thank **ALLAH** who gave me countless blessings; one of them is the completion of this piece of work.

First and foremost, I would like to express my great gratitude to my mother, wife, daughter, sons and brothers for their love, emotional support and encouragement and their patience and confidence in me during the time we spent at Nottingham.

My thanks expressed to Medical services of armed forces at Saudi Arabia –Riyadh for their financial support to achieve a higher degree.
I would like to thank all the staff members of The School of Medicine and Division of Pathology whom taught and assisted me during my first year. I want to extend my deep gratitude to Professor Peter Altevogt for providing me with CD24 Antibody as a gift for four years. My deepest special thanks to my colleagues for their help, to progress my knowledge and research's skills during the practical period.

Above all, my sincere gratitude to my supervisor Prof. Mohammad Ilyas for his guidance, enthusiastic encouragement and practical assistance that he offered me throughout the PhD years.

Dedication

This thesis is dedicated to my wife and my children. For my wife, I cannot find enough words to express my deepest gratitude for her continuous patience, support, love and endless confidence in me. My children were really supportive and were a true source of motivation for me, as I can always see the bright future in them.

Abbreviations

AAP	Acetaminophen.
ALL	Acute lymphocytic leukaemia.
BCA	Bicinchoninic Acid Protein.
Ca19-9	Cancer antigen 19-9/Carbohydrate antigen 19-9.
CD	Cluster of differentiation.
CD24	Cluster of differentiation 24 or heat stable antigen.
CEA	Carcinoembryonic antigen.
CHX	Cyclohexamide.
CLR	C-type lectin receptors.
Conc.	Concentration.
CRC	Colorectal carcinoma.
CSC	Cancer stem cells.
C-Src	Cellular Src kinase.
Cten	COOH-terminal tensin-like protein/TNS4
CXCR	Chemokine Receptor.
ECM	Extracellular Matrix.
EGFR	Epidermal Growth Factor Receptor.
EMT	Epithelial Mesenchymal transition.
FAK	Focal adhesion Kinase.
GPI ANCHOR	Glycosyl Phosphatidylinosito Anchor.
HMGB1	High Mobility Group Box 1 Protein.
HSP90	Heat shock protein 90.
ILK	Integrin linked Kinase.
Notch1	Notch homolog 1, translocation-associated (Drosophila)
NICD	Notch intracellular domain
KDa.	Kilo Daltons.
LCAM/CD171	Liver Cell Adhesion Molecule.
mAb	monoclonal Antibody.
MALDI-MS	Matrix-assisted laser desorption/ionization- Mass spectrophotometry.
MET	Mesenchymal epithelial transition.
MSCs	Mesenchymal stem cells.

NCL	Necrotic cell lysate.
NLRs	NOD like receptors.
NOD	Nucleotide-binding oligomerization domain.
ORF	Open Reading frame.
PBS	Phosphate Buffered Saline.
PCR	Polymerase Chain Reaction.
PTB	Phosphotyrosine-binding domain.
PTEN	Phosphatase and tensin homolog.
RAGE	Receptor for Advanced Glycation End products.
SDM	Site-directed mutagenesis
SH2	Src homology domain 2.
SIGLECS	Sialiac acid binding Immunoglobulin like lectins.
SLE	Systemic lupus erythematosus
STAT3	Signal Transducer and Activator of Transcription 3.
TBS	Tris-buffered saline
TCF/LEF	T-cell factor/lymphoid enhancer factor.
TLR	Toll like receptors.
TNFα	Tumour necrosis factor alpha.
UC	Ulcerative colitis.
UTR	Untranslated Region.

Abstract

CD24 is a small (81 amino acids) GPI anchored protein which is involved in promoting cell motility and stemness and may be a part of the metastatic process. It is a heavily glycosylated molecule and contains numerous O-glycosylation sites together with two N-glycosylation sites. N-glycosylation is thought to be important in protein function, and therefore, the aim of this study is to (a) investigate the importance of N-glycosylation in the function of CD24, (b) identify other potentially functional sites in CD24 by deletion mapping, (c) define downstream targets of CD24, and (d) identify the extrinsic signals of which activate CD24.

(a) Through site-directed mutagenesis, we changed the glycosylated residues N32 (ACC to CAA) and Q52 (AAT to CAG) in CD24. Mutating each of these sites individually, when compared to pCCD24^{WT} (wild-type CD24), caused a partial reduction in ability to induce cell motility and cell invasion (cell motility p=0.0001 cell invasion p=0.0001) and, unexpectedly, resulted in significantly enhanced cell proliferation (p=0.0001). Mutation of both sites resulted in a near loss of motility induction and retained cell proliferation. (b) We mapped the functional sites of CD24 by deleting seven amino acid segments of the whole of the mature peptide. Apart from the N-glycosylation sites, no other functional domains were identified which altered cell motility or proliferation. (c) Previously, in our lab it has been shown that Cten is downstream motility-inducing target of CD24. We hypothesised that CD24 may signal through the Notch pathway since Notch1 has an important role in maintaining CSCs. Results showed that forced expression of CD24 upregulates Notch1 and Cten whilst knockdown of CD24 causes loss of Notch1 and Cten expression. However, forced expression of CD24 with simultaneous knockdown of Notch1

resulted in failure to induce Cten. (d) CD24 is reported to act as a ligand of P-selectin. We found that stimulating CD24 expressing cell lines induced with P-selectin induced cell motility ($p=0.0011$) and caused an increased in the protein expression of downstream targets of CD24. Stimulating cell lines expressing CD24 with mutant glycosylation sites resulted in a failure to induce motility or CD24 targets.

We conclude, the removal of the N-glycosylation sites in CD24 resulted in a loss of cell migration and invasion, thereby suggesting the importance of these sites in mediating the migration and invasion functions of CD24. Unexpectedly, these mutations also appeared to stimulate cell proliferation, suggesting that wild type CD24 can functionally inhibit cell proliferation. Deletion mapping did not reveal any other functional sites on the mature CD24 suggesting that O-glycosylation is relatively affecting the glycosylation in the biology of CD24. Notch1 was to be an important downstream target of CD24 and a regulator of Cten. The binding of P-selectin with CD24 resulted in increased motility of CD24 which is also dependent on N-glycosylation.

Conference Communication

A. Presentations and Conference Communications

A Alsulaiman and M Ilyas. Investigation of the role of N-glycosylation of CD24 in colorectal cancer (2016). NCRI Cancer Conference. Poster presentation.

Contents

1. GENERAL INTRODUCTION 1

1.1 COLORECTAL CANCER 2

1.1.1 MOLECULAR PATHOGENESIS OF CRC 2

1.1.2 CHROMOSOMAL INSTABILITY (CIN) 4

1.1.3 MICROSATELLITE INSTABILITY 5

1.1.4 CIMP AND "SERRATED" PATHWAY 6

1.1.5 THERAPEUTIC INTERVENTION 7

1.2 CANCER METASTASIS 8

1.2.1 STEP OF METASTASIS 8

1.2.2 TARGETING METASTASIS 14

1.3 CD24 16

1.3.1 OVERVIEW AND GENE STRUCTURE 16

1.3.2 EXPRESSION OF CD24 IN NORMAL TISSUES 17

1.3.3 ROLE OF CD24 IN AUTOIMMUNE DISEASE 18

1.3.4 ROLE OF CD24 IN IMMUNE SYSTEM 19

1.3.5 EXPRESSION OF CD24 IN CANCER 20

1.3.6 CD24 AS CANCER STEM CELL MARKER 21

1.3.7 CD24 GLYCOSYLATION 21

1.3.8 CD24 POST-TRANSLATION MODIFICATION 25

1.3.9 CD24 LIGANDS 26

1.4 DOWNSTREAM TARGETS 27

1.4.1 NOTCH1 27

1.4.2 CTEN 28

1.4.3 FAK 30

1.4.4 ILK 30

1.5 AIMS AND HYPOTHESIS 31

2. MATERIALS AND METHODS 32

2.1 CELL CULTURE 33

2.1.1 CELL VIABILITY MAINTENANCE 34

2.1.2 CELL LINES SUB-CULTURE 34

2.1.3 CELL COUNTING 34

2.2 TRANSFECTION OF CELL LINES 35

2.2.1 GENE FORCED EXPRESSION 35

2.2.2 GENE KNOCKDOWN 35

2.2.3 CO-TRANSFECTION 36

2.3 CELL TREATMENT 37

2.3.1 CYCLOHEXIMIDE 37

2.3.2 RECOMBINANT P-SELECTIN 38

2.4 WESTERN BLOTTING 38

2.4.1 PROTEIN EXTRACTION AND QUANTIFICATION . 38

2.4.2 NEURAMINIDASE DIGESTION 39

2.4.3 SDS POLYACRYLAMIDE GEL ELECTROPHORESIS 39

2.4.4 TRANSFER OF SEPARATED PROTEINS 40

2.4.5 IMMUNO-DETECTION OF PROTEINS 40

2.5 CO-IMMUNOPRECIPITATION 42

2.6 FLOW CYTOMETRY AND CD24 EXPRESSION 42

2.7 TOTAL RNA (RIBONUCLEIC ACID) EXTRACTION 43

2.7.1 ASSESSMENT OF RNA INTEGRITY 44

2.8 COMPLEMENTARY DNA (C. DNA) GENERATION 44

2.9 REAL-TIME POLYMERASE CHAIN REACTION 46

2.9.1 PRIMER DESIGN 46
2.9.2 PCR REACTION 47
2.10 SITE DIRECTED MUTAGENESIS AND MAPPING OF CD24 49
2.10.1 PRIMERS DESIGN 50
2.10.2 STANDARD PCR 51
2.10.3 AGROSE GEL ELECTROPHORESIS 52
2.10.4 DNA EXTRACTION FROM AGAROSE GEL 52
2.10.5 LIGATION AND BACTERIAL TRANSFORMATION 53
2.10.6 DNA ISOLATION AND PLASMID MINI-PREP .. 54
2.10.7 MUTATION SCREENING BY HIGH RESOLUTION MELTING (HRM) 55
2.10.8 DIRECT SEQUENCING 56
2.11 MUTATION PROFILING 56
2.11.1 PCR 56
2.11.2 HIGH RESOLUTION MELTING 58
2.12 FUNCTIONAL STUDIES 58
2.12.1 PRESTO BLUE PROLIFERATION ASSAY 58
2.12.2 CELL MIGRATION ASSAY 58
2.12.3 MATRIGEL INVASION ASSAY 59
2.13 STATISTICAL ANALYSIS 60

3. INVESTIGATING THE ROLE OF N-GLYCOSYLATION IN THE REGULATION OF CD24 FUNCTION 61

3.1 INTRODUCTION 62
3.2 RESULT 63
3.2.1 CONSTRUCTION OF pCCD24^{N36Q} PLASMID 63
3.2.2 CONSTRUCTION OF pCCD24^{N52Q} PLASMID 69
3.2.3 CONSTRUCTION OF pCCD24$^{N36, 52Q}$ PLASMID 74

3.2.4 PROTEIN EXPRESSION OF pCCD24^{N36Q,} pCCD24^{N52Q}, AND pCCD24$^{N36, 52Q}$ 79

3.2.5 THE ONCOGENIC FEATURES 82

3.3 DISCUSSION: 89

4. MAPPING THE FUNCTIONAL SITES IN THE REGULATION OF CD24 93

4.1 INTRODUCTION 94

4.2 RESULT 95

4.2.1 CONSTRUCTION OF pCCD24$^{\Delta 7.1}$ PLASMID..... 95

4.2.2 CONSTRUCTION OF pCCD24$^{\Delta 7.2}$ PLASMID..... 99

4.2.3 CONSTRUCTION OF pCCD24$^{\Delta 7.3}$ PLASMID... 103

4.2.4 CONSTRUCTION OF pCCD24$^{\Delta 4.4}$..... 107

4.2.5 PROTEIN EXPRESSION OF pCCD24$^{\Delta 7.1,}$ pCCD24$^{\Delta 7.2,}$ pCCD24$^{\Delta 7.3,}$ AND pCCD24$^{\Delta 4.4.}$ 111

4.2.6 THE ONCOGENIC FEATURES 113

4.3 DISCUSSION: 116

5. SIGNALLING PATHWAY OF CD24.....118

5.1 INTRODUCTION 119

5.2 RESULT: 120

5.2.1 CD24 REGULATES NOTCH1 120

5.2.2 CD24 REGULATES NOTCH1 AT TRANSCRIPTIONAL LEVEL 123

5.2.3 CD24 STABILISES NOTCH1 125

5.2.1 CD24 PHYSICALLY INTERACTS WITH NOTCH1128

5.2.1 NUCLEAR/ CYTOPLASMIC LOCALISATION OF CD24 AND NOTCH1 130

5.2.2 FUNCTIONAL INTERACTION BETWEEN CD24 AND NOTCH1 131
5.2.3 NOTCH1 REGULATES CTEN 133
5.2.4 THE CD24-NOTCH1-CTEN PATHWAY 136
5.3 DISCUSSION: 138

6. EXTRINSIC SIGNALLING OF CD24 143

6.1 INTRODUCTION 144
6.2 RESULT: 145
6.2.1 STIMULATING OF SW620 WITH RECOMBINANT P-SELECTIN 145
6.2.2 P-SELECTIN ENHANCES THE CELL MOTILITY . 146
6.2.3 CTEN MEDIATES CD24/P-SELECTIN INDUCED MOTILITY 147
6.2.4 THE CD24/P-SELECTIN PATHWAY 149
6.3 DISCUSSION 151

7. GENERAL DISCUSSION 153

7.1 INTRODUCTION 154
7.2 KEY FINDINGS 154
7.2.1 REMOVAL OF THE N-GLYCOSYLATION OF CD24 CAUSED A FAILURE TO INDUCE THE CELL MOTILITY 154
7.2.2 THE O-GLYCOSYLATION ARE NOT THE FUNCTIONAL PARTS OF CD24 159
7.2.3 NOTCH1 IS AN IMPORTANT MOLECULE IN CD24 SIGNALLING 160
7.2.4 P-SELECTIN STIMULATES CD24 163
7.3 CONCLUSION 164

7.4 Potential strengths 165
7.5 Potential weakness 165
7.6 Future suggestion and recommendation 165

8. REFERNCES 167

9. APPENDICES 178

9.1 Vector map of His Topo Cloning Vector 3.1..... 179
9.2 BCA protein assay Kit standard preparation guidelines.... 180
9.3 Cell line mutation profiling..... 181

Index of figures

Figure 1-1 : The classical CIN adenocarcinoma sequence. *[5].* 4
Figure 1-2 : Epithelial cell junctions. 10
Figure 1-3: a simplified model for the structure of human CD24 protein [68] 17
Figure 1-4 : Simplified diagram showing the glycosylation sites of CD24 [90]. 21
Figure 1-5 : Steps of protein N-glycosylation. (112) 22
Figure 1-6 : CD24 and common sugars on the human cell surface [102]. 25
Figure 1-7: Activation of NOTCH signalling. 28
Figure 2-1: A representative example of qPCR. 48
Figure 2-2 : Site directed mutagenesis flow chart. 49
Figure 3-1 : Simplified model structure of CD24 glycosylation [68]. 62
Figure 3-2: PCR optimization of pCCD24^{N36Q} primer. 63
Figure 3-3 : PCR product of primers for creating pCCD24^{N36Q}. 64
Figure 3-4: Gel electrophoresis of the ten the extracted plasmids. 65
Figure 3-5: The HRM result and the comparison of the wild type and pCCD24^{N36Q} 66
Figure 3-6: Sequencing of pCCD24^{N36Q} 67
Figure 3-7 : Blast 2 analysis of pCCD24^{WT} and pCCD24^{N36Q}. 68
Figure 3-8 : PCR optimization of pCCD24^{N36Q}. 69
Figure 3-9 : PCR product of primers for creating pCCD24^{N52Q}. 70
Figure 3-10 : Gel electrophoresis of the ten the extracted plasmids. 70
Figure 3-11 : The HRM result and the comparison of the wild type and pCCD24^{N52Q} 71
Figure 3-12 : Sequencing of pCCD24^{N52Q} 72
Figure 3-13 : Blast 2 analysis of pCCD24^{WT} and pCCD24^{N52Q}. 73
Figure 3-14: PCR product of pCCD24^{N36,52Q}. 74
Figure 3-15: Gel electrophoresis of the ten the extracted plasmids. 75
Figure 3-16: The HRM result and the comparison of the wild type and mutant 76

FIGURE 3-17: SEQUENCING OF pCCD24$^{N36, 52Q}$.....77
FIGURE 3-18 : BLAST 2 ANALYSIS OF pCCD24^{WT} AND pCCD24^{N36,52Q}.....78
FIGURE 3-19: THE PROTEIN EXPRESSION OF pCCD24^{N36,} pCCD24^{N52}, AND pCCD24^{N36,52Q}.....80
FIGURE 3-20 : PROTEIN EXPRESSION FOLLOWING NEURAMINIDASE DIGESTION.....82
FIGURE 3-21 : THE EFFECT OF pCCD24^{N36Q}, pCCD24^{N52Q}, pCCD24^{N36,52Q} ON THE CELL PROLIFERATION IN HCT116.....84
FIGURE 3-22 : THE EFFECT OF pCCD24^{N36Q} , pCCD24^{N52Q}, AND pCCD24^{N36,52Q} ON THE CELL MIGRATION.....86
FIGURE 3-23 : THE EFFECT OF pCCD24^{N36Q}, pCCD24^{N52Q} ,AND pCCD24^{N36,52Q} ON THE CELL INVASION.....88
FIGURE 4-1: MODEL STRUCTURE OF CD24 GLYCOSYLATION [68].....94
FIGURE 4-2: PRIMER OPTIMIZATION OF pCCD24$^{\Delta 7.1}$.....95
FIGURE 4-3: GEL ELECTROPHORESIS OF THE TEN THE EXTRACTED PLASMIDS.....96
FIGURE 4-4 : SEQUENCING OF pCCD24$^{\Delta 7.1}$.....97
FIGURE 4-5 : BLAST 2 ANALYSIS OF pCCD24^{WT} AND pCCD24$^{\Delta 7.1}$.....98
FIGURE 4-6 : PRIMER OPTIMIZATION OF pCCD24$^{\Delta 7.2}$.....99
FIGURE 4-7 : GEL ELECTROPHORESIS OF THE TEN THE EXTRACTED PLASMIDS.....100
FIGURE 4-8 : SEQUENCING OF pCCD24$^{\Delta 7.2}$.....101
FIGURE 4-9 : BLAST 2 ANALYSIS OF pCCD24^{WT} AND pCCD24$^{\Delta 7.2}$.....102
FIGURE 4-10 : PRIMER OPTIMIZATION OF pCCD24$^{\Delta 7.3}$.....103
FIGURE 4-11 : GEL ELECTROPHORESIS OF THE TEN THE EXTRACTED PLASMIDS.....104
FIGURE 4-12 : SEQUENCING OF pCCD24$^{\Delta 7.3}$.....105
FIGURE 4-13 : BLAST 2 ANALYSIS OF pCCD24^{WT} AND pCCD24$^{\Delta 7.3}$.....106
FIGURE 4-14 : PRIMER OPTIMIZATION OF pCCD24$^{\Delta 4.4}$.....107
FIGURE 4-15 : GEL ELECTROPHORESIS OF THE TEN THE EXTRACTED PLASMIDS.....108
FIGURE 4-16 : SEQUENCING OF pCCD24$^{\Delta 4.4}$.....109
FIGURE 4-17 : BLAST 2 ANALYSIS OF pCCD24^{WT} AND pCCD24$^{\Delta 4.4}$.....110
FIGURE 4-18 : THE PROTEIN EXPRESSION OF pCCD24$^{\Delta 7.1}$, pCCD24$^{\Delta 7.2}$, pCCD24$^{\Delta 7.3}$, AND pCCD24$^{\Delta 4.4}$.....112
FIGURE 4-19 : THE EFFECT OF pCCD24$^{\Delta 7.1}$, pCCD24$^{\Delta 7.2}$, pCCD24$^{\Delta 7.3}$, AND pCCD24$^{\Delta 4.4}$ ON THE CELL PROLIFERATION IN HCT116.....114
FIGURE 4-20: THE EFFECT OF pCCD24$^{\Delta 7.1}$, pCCD24$^{\Delta 7.2}$, pCCD24$^{\Delta 7.3}$, AND pCCD24$^{\Delta 4.4}$ ON THE CELL MOTILITY.....115
FIGURE 5-1: CD24 AND REGULATION OF NOTCH1.....122
FIGURE 5-2: CD24 REGULATES NOTCH1 AT TRANSCRIPTIONAL LEVEL.....124
FIGURE 5-3: CD24 STABILISES NOTCH1.....127
FIGURE 5-4: THE PHYSICAL INTERACTION BETWEEN CD24 AND NOTCH1.....129
FIGURE 5-5: NUCLEAR AND CYTOPLASMIC FRACTIONATION.....130
FIGURE 5-6: THE RELATIONSHIP BETWEEN CD24 AND NOTCH1.....133
FIGURE 5-7: NOTCH1 AND REGULATION OF CTEN.....135
FIGURE 5-8: THE CD24-NOTCH1-CTEN PATHWAY.....137
FIGURE 5-9 : SCHEMATIC OF THE NOTCH1-RBP-J κ -HES1 SIGNALING NETWORK..140
FIGURE 5-10 : SCHEMATIC DIAGRAM FOR PROPOSED LINK BETWEEN CD24 –NOTCH1-CTEN-FAK-ILK.....142
FIGURE 6-1: STIMULATING SW620 WITH DIFFERENT P-SELECTIN CONCENTRATIONS.....145
FIGURE 6-2 : THE EFFECT OF P-SELECTIN ON THE CELL MIGRATION.....146
FIGURE 6-3 : THE EFFECT OF CTEN ON CD24/P-SELECTIN SIGNALLING.....148

FIGURE 6-4: CD24/P-SELECTIN PATHWAY.....150
FIGURE 9-1 : THE SCREENING OF CRC CELL LINES FOR A MUTATION IN KRAS EXON2. 182
FIGURE 9-2 : THE SCREENING OF CRC CELL LINES FOR A MUTATION IN KRAS EXON4. 183
FIGURE 9-3 : THE SCREENING OF CRC CELL LINES FOR A MUTATION IN BRAF EXON 11. 184
FIGURE 9-4 : THE SCREENING OF CRC CELL LINES FOR A MUTATION IN BRAF EXON 15. 185
FIGURE 9-5 : THE SCREENING OF CRC CELL LINES FOR A MUTATION IN PIK3CA EXON 20.....186
FIGURE 9-6 : THE SCREENING OF CRC CELL LINES FOR A MUTATION IN PTEN EXON 3. 187
FIGURE 9-7 : THE SCREENING OF CRC CELL LINES FOR A MUTATION IN TP53 EXON 6. 188

Index of Tables

TABLE 2-1: CELL LINES WITH THEIR CHARACTERISTICS.....33
TABLE 2-2 : THE SEQUENCES OF THE SIRNAS AND THE REFERENCE SEQUENCE NUMBER (NM) OF THE GENES MRNA.....37
TABLE 2-3: THE SOURCES OF THE ANTIBODIES AND THE WORKING CONDITIONS WHEN USED IN WESTERN BLOT. 41
TABLE 2-4 : MASTER MIX MADE FOR THE REVERSE TRANSCRIPTION REACTION. 45
TABLE 2-5 : MASTER MIX MADE FOR THE RT- NEGATIVE REACTIONS. 45
TABLE 2-6 : RT- PCR PRIMER SEQUENCES. 46
TABLE 2-7 : MASTER MIX FOR QPCR 48
TABLE 2-8 : THE SEQUENCE OF THE PRIMERS, WHICH WERE PRODUCED FROM EUROFINS MWG OPERON . A) SITE DIRECTED MUTAGENESIS (CHANGE THE AMINO ACID ASPARAGINE TO GLUTAMINE) AND B) MAPPING THE FUNCTIONAL SITES OF CD24 BY DELETING THE MATURE PEPTIDE.....51
TABLE 2-9 : *MUTATION PROFILING PRIMER SEQUENCES.* 57
TABLE 9-1 : THE MUTATION STATUS OF CRC CELL LINES FOR COMMONLY MUTATED GENES IN CRC.....181

1. General Introduction

1.1 Colorectal cancer

CRC is a major health issue, it is the third most commonly diagnosed malignancy in the UK and worldwide 1.2 million people are diagnosed annually. The number of patients diagnosed with the disease has increased, likely due to improvements in screening and detection methods. Despite this, mortality rates have gradually fallen to 600,000 deaths per year worldwide which may also be attributed to earlier detection and better treatment options. CRC is more prevalent in men and as with most cancers, the prevalence increases with age. The incidence is greater in western countries, namely Europe, United States and Oceanic countries but it is on the increase in other counties as they adopt a more westernised lifestyle [1, 2]. Patient prognosis has seen a recent improvement in developed countries although there is still an imperative need to understand the stages in malignant transformation to circumvent the high mortality associated with CRC [2].

1.1.1 Molecular pathogenesis of CRC

Almost all CRC is adenocarcinoma and arises from the uncontrolled proliferation of epithelial cells of the colon and rectum. CRCs are generally sporadic and develop from a benign precursor lesion known as an adenoma. This may progress into a malignant cancer which can invade through the bowel wall and into surrounding tissues, namely the abdomen and pelvis. With further progression, tumour cells will metastasise to the local lymph nodes and then to distant sites such as the liver. Genetic instability underpins the development of CRC. Progression from normal epithelium through

to adenoma, cancer and ultimately metastasis is driven by gene mutations that correspond to histologic changes [3]. Approximately 70-85% of cases arise as a result of chromosome instability (CIN) [4]. Comprising the majority of cases, CIN is characterised by deletions or amplifications of chromosomal regions. The classical multi-hit model for this process states that sequential Adenomatous polyposis coli (*APC*), *KRAS*, chromosome region 18q and Tumour protein p53 (*TP53*) mutations, among others, allows for progression from adenoma to advanced metastatic disease (figure 1-1) [5]. The microsatellite instability (MSI) route to carcinogenesis is characterised by mutations or loss of function in the DNA mismatch repair enzymes including MutL homolog 1 (*MLH1*), MutL homolog 2 (*MLH2*), MutL homolog 6 (*MLH6*) or PMS2 postmeiotic segregation increased 2 (*PMS2*). Alterations of these genes leads to defective repair of insertional or deletional mutations (Indels) occurring at microsatellite sequences which, causes the accumulation of mutations in these regions [6]. Approximately 15% of CRCs follow this route to carcinogenesis [7]. CRCs may also arise through the CpG island methylator phenotype (CIMP) pathway in which methylation of the promoter regions of tumour suppressor genes encourages uncontrolled cell growth. The CIMP pathway is often associated with MSI, for example, MLH1 is often inactivated through promoter hypermethylation [8]. In addition to those

discussed, a number of other classifications and molecular subtypes of CRC have been proposed [9, 10].

Although most cases of CRC are sporadic, hereditary disease forms also occur. Familial adenomatous polyposis (FAP) is characterised by CIN [11]. Hereditary non-polyposis colorectal cancer (HNPCC) follows the MSI route to carcinogenesis [12, 13]. However, colorectal carcinogenesis is complex with additional genes and molecular pathways further implicated in disease progression.

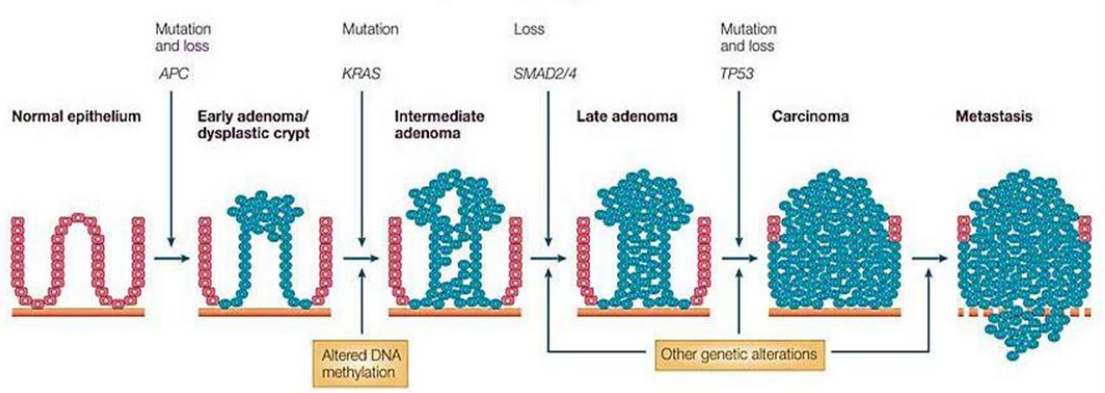


Figure 1-1 : The classical CIN adenocarcinoma sequence. *Progression from normal epithelium to metastasis is driven my gene mutations. The classical CIN adenocarcinoma sequence states that sequential genomic alterations in APC, KRAS, chromosomal region 18q and TP53 drive carcinogenesis [5].*

1.1.2 Chromosomal instability (CIN)

CIN (Chromosomal instability) is the most common genetic defect. It has been reported in approximately 50 to 85% of all cases [14], [15]. CIN is recognised by aneuploidy and even structural alterations to chromosomes. It is usually assessed by DNA flow-cytometry [16]. Mutation in the APC gene occurs early during the development of polyps. Kras mutations arise during the intermediate - late adenomas stage. TP53 and deletion of 18q occur

with the transition to malignancy. SMAD2 and SMAD4 are located on 18q, which contains the Deleted in Colorectal Cancer (DCC) gene. SMAD2 and SMAD4 are involved in the TGF-β signalling pathway [17] . It is well-established that CRC cases with CIN are associated with a much poorer prognosis [18]. Deletion in chromosome 5, 18q, or 17p and gain in 8q, 13q, and 20q are frequently reported in CRC.

1.1.3 Microsatellite instability

Microsatellite instability is a common feature in several cancers such as gastric and ovarian cancer as well as CRC [19]. Microsatellites are short repeat nucleotide sequences that are present throughout the whole genome. The mismatch repair (MMR) system contains at least seven different proteins (MLH1, MLH3, MSH2, MSH3, MSH6, PMS1, and PMS2) that form heterodimeric proteins. These heterodimers recognize and repair mismatch errors during DNA replication. Any mutations that reduce the efficacy of the MMR system would predispose to the development of MSI [20] .Germline mutations in the MMR genes can also lead to MSI and can cause Hereditary Non Polyposis CRC (or Lynch syndrome) [21]. Promoter hypermethylation is another pathway that has been identified, which can also inhibit the MMR system by silencing the MMR genes. This seems to be the mechanism that underlies loss of MMR in sporadic MSI tumours. Specifically, a high degree of MLH1 promoter hypermethylation and consequent silencing of this gene has been noted in sporadic tumours with MSI [22] . Target genes for MSI are involved in various critical cell functions, including cell signalling, apoptosis, and DNA repair. The MSI pathway differs from the CIN pathway in that MSI cases display a normal karyotype with exceptional molecular genetic characteristics [16]. Most research groups identify MSI as the presence of at least 30% unstable loci,

present among a panel of five mononucleotide markers, BAT-25, BAT-26, NR-21, NR-24, and MONO-27, which are known to have a high sensitivity and specificity [23]. MSI positive tumours have also been subdivided into MSI high (MSI-H) and MSI-low (MSI-L) depending on the quantitative differences in the degree of instability. Tumours with 10–29% unstable loci are designated as MSI low. Patients with MSI positive tumours tend to have a better prognosis than those with CIN tumours [24]. Although MSI CRC tumours have a distinct feature compared to the Microsatellite stability (MSS), there is an overlap between the two groups especially in the MSI-L group. This overlap may be due to the categorisation of MSI-L [25], which is still questionable. Contradictory results have been published regarding the clinical and histological outcome between MSI-L and MSS cases [26]. Therefore, these results may be explained by the use of a non-conclusive cut-off to distinguish between MSS and MSI–L cases. It could be argued that there is no convincing evidence showing molecular and physiological differences between CRC MSS and MSI-L. Thus, if the differences between features are minor; we may be able to only refer to MSI-H as MSI.

1.1.4 CIMP and "serrated" pathway

The CpG island methylator phenotype (CIMP) is the third pathway in the progression of CRC [27], [28]. Hypermethylation of the CpG dinucleotide sequences located within the promoter region is seen in genes associated with cell cycle regulation, angiogenesis, DNA repair, apoptosis, invasion and adhesion. This hypermethylation causes a loss of gene expression. In one study, 20%-30% of CRC were found to have the CIMP phenotype, and it has been reported that the CIMP CRCs are similar to MSI CRCs regarding clinical features [29], [30], [31]. The CIMP phenotype can be categorized

into CIMP-high and CIMP-low based on the number of methylated markers. In CIMP-high CRC, the *BRAF* mutation has a major role in increasing the cell growth, carcinogenesis progression, and high colon cancer specific mortality [32]. Nevertheless, the CIMP-high tumours are associated with low colon cancer mortality regardless of *BRAF* mutation [32]. Notably, 90% of CRC cases involving sessile serrated adenoma (SSA) contain *BRAF* V600E mutations .An early event in the serrated pathway is the *BRAF* mutation and its forced expression results in a state known as senescence. *BRAF* mutations in SSA are usually found in the early hyperplastic polys, which is the serrated precursors, or in the advanced dysplastic serrated polyp. [33], [34],[35]. It was recently demonstrated that when a *KRAS* mutation appears, it is associated with low markers of methylation, which is called CIMP-low, and with no gain of function of the PIK3CA and mutations in the DNA repair gene methylguanine methyltranferase (MGMT) [31], [36], [37].

1.1.5 Therapeutic intervention

The management of CRC is dependent on the tumour stage and the molecular classification may also direct therapy. Treatment for early CRC commonly comprises complete tumour removal although adjuvant chemotherapy or radiation therapy may be required for locally advanced disease. Few therapeutic options exist for advanced, metastatic disease. Surgery together with neoadjuvant and/or adjuvant therapy may be used to eradicate the tumour. Treatment options include 5-fluorouracil (5-FU), initially effective against tumours displaying chromosomal instability and anti-EGFR therapy, which has also shown success, although rendered ineffective in those with mutated downstream target genes such as the commonly mutated *KRAS* and *BRAF* [38]. However, as with many anti-cancer therapies, resistance may arise through

downstream mutation. For more advanced metastatic disease, palliative treatment is often the only option. Considering this, it is critical that improved therapies are made available for late stage CRCs.

1.2 Cancer metastasis

1.2.1 Step of metastasis

The majority of cancer related deaths are attributed to metastatic disease. Consequently, it is imperative that the pathways involved in metastatic spread are understood [39]. For a cell to establish tumour growth at a secondary site it must successfully undergo a sequential, coordinated series of events accomplished by the acquisition of molecular alterations. Metastasis is an inefficient process that is completed by only a minority of cells but, once achieved; it has a dramatic, negative impact on patient prognosis.

1.2.1.1 Distribution of cancer cells

In order to metastasise, the cell firstly must detach from the primary tumour. Epithelial cell architecture is maintained by cell to cell junctions namely adherens junctions, tight junctions, gap junctions and desmosomes. Furthermore, epithelial cells are anchored to the underlying extracellular matrix (ECM) via focal adhesions and hemidesmosomes (figure 1-2). The process of EMT occurs early in cancer metastasis and is a process whereby epithelial cells display phenotypic plasticity by adopting a mesenchymal phenotype, which endows the cell with greater invasive capabilities. During EMT, the loss of adhesion is governed

by changes in the expression of cell adhesion molecules that make up these cell junctional complexes. Epithelial cells experience loss of basolateral to apical polarity and adopt front to back polarity, as displayed by mesenchymal cells. Furthermore, cytoskeletal rearrangements induce morphological cell changes to form cell protrusions including lamellopodia and filopodia to aid cell motility [40]. EMT pathways promote the formation of invadopodia that secrete proteolytic enzymes including matrix metalloproteases (MMPs) to facilitate ECM degradation. [41]. Further actin structural rearrangements promote stress fibre formation to facilitate cell migration. Interaction with the surrounding stroma is postulated to aid the invasion-metastasis cascade [42].

Epithelial cells invade through the basement membrane into the ECM, either collectively or as single cells, by amoeboid movement characterised by squeezing through matrix barriers or mesenchymal migration, which is characterised by ECM breakdown [43]. The mode of migration may be influenced by the microenvironment and it is possible that cells can undergo mesenchymal amoeboid transition (MAT) and vice versa to adapt to variations in the microenvironment [44]. Conversion between the different transitional states is associated with further molecular changes but this is not well understood.

Following local invasion, if successful, cancer cell intravasation into nearby blood vessels and lymphatics is facilitated by the 'leaky'

neovasuclar system [45]. Extravasation into the distant tissue is aided by the expression of growth factors and cytokine signalling. Cytokines may act as chemoattractants, for example, the chemokine receptor CXCR4 is expressed by cells derived from numerous tumour types and promotes migration towards target tissues that secrete its cognate ligand [46, 47]. Moreover, the cell must undergo this obstacle of events whilst evading the immune responses.

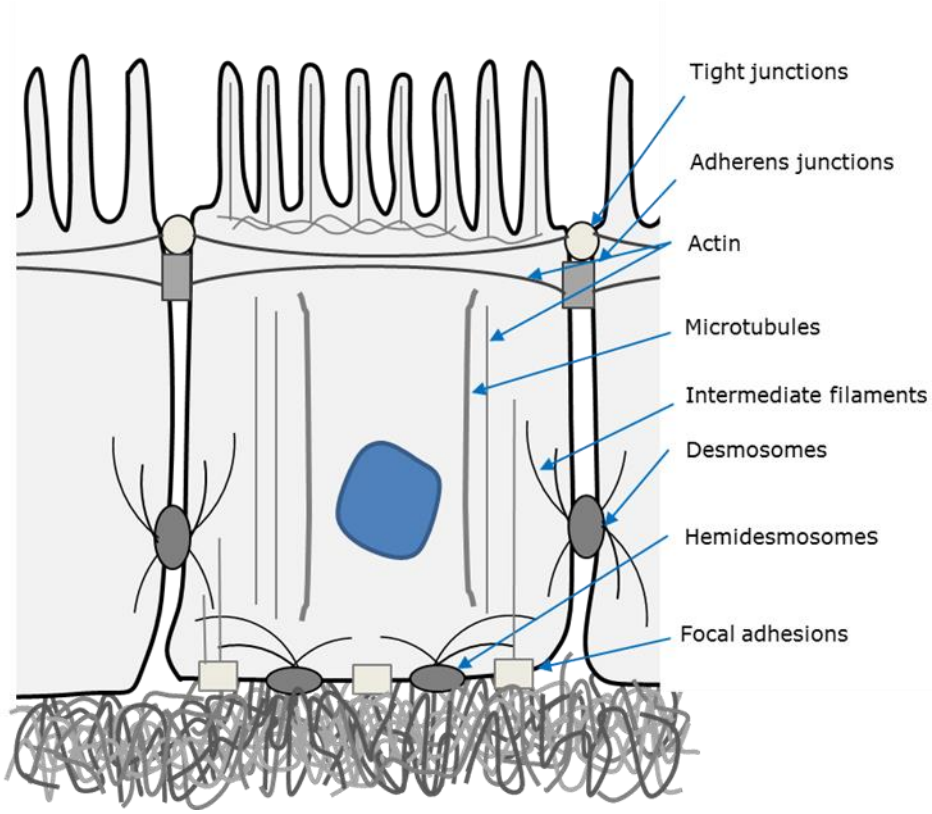


Figure 1-2 : Epithelial cell junctions. Epithelial cell structure is maintained by cell-cell and cell-ECM junctions. Tight junctions form regions of cell-cell attachment near the apical surface and are maintained by Claudins, Occludin and ZO proteins. Adherens junctions mediate cell-cell attachment via cadherin molecules which link via catenins to the actin cytoskeleton. Desmosomes form strong attachments to the intermediate filaments of neighbouring cells. Focal adhesions and hemidesmosomes mediate cell-ECM adhesion.

1.2.1.2 Metastatic settlement

Upon reaching the target site, survival in a new, hostile environment is the next obstacle for the tumour cell to overcome. Initially, cells may form micrometastasis under these unfavourable conditions before progression to clinically detectable tumour growth. It is postulated that the reversal of EMT, mesenchymal to epithelial transition (MET), may occur to seed metastasis. This is demonstrated by the re-expression of epithelial markers and the loss of mesenchymal markers in metastatic tumours. EMT transcription factors can supress cell proliferation and reversal of this may promote tumour cell proliferation at the secondary site [48, 49]. Together with the stimulation of angiogenic processes, clinically detectable macroscopic tumour metastases may prevail.

Metastases have a tendency to form in particular tissues dependant on the tumour type. This could just be a passive process dependent on tissue proximity to the primary tumour but accumulating evidence suggests that biological mechanisms permit secondary tumour growth at particular sites. The 'seed and soil' hypothesis states that tumour cells establish secondary tumour growth in particular distant tissues dependent on the environment of that tissue and its compatibility [50]. Theories also suggest that the cell can secrete factors that prime the new environment ready for the cell's arrival [51].

1.2.1.3 Cancer stem cell in metastasis

It has been proposed that only a subset of cells have the ability to establish clinically detectable metastasis and, those that have this ability, have attributes of stem cells, or cancer stem cells (CSCs). Stem cells have self-renewal property and therefore can establish secondary growth at the distant site however it is likely that further attributes of stem cells promote metastatic growth. Cells in primary tumours that display high expression of stem cell markers show a higher tendency to metastasis and depletion of these cell pools abrogates metastasis [52, 53]. Furthermore, the induction of EMT has been linked to the CSC concept. EMT programmes co-induce stem-cell pathways and those cells that are able to metastasise are coined 'migrating stem cells'. [54]. In CRC, cells at the invasive tumour front were shown to have reduced expression of epithelial cell junction marker E-cadherin, and therefore thought to have undergone EMT. These cells were in an undifferentiated state, a feature of stem cells. Additionally, they displayed nuclear expression of β-catenin which is a feature of active Wnt signalling that maintains the stem cell compartment in the normal intestinal epithelium. These were phenotypically distinct from the cells in the centre of the tumour that displayed high expression of E-cadherin and an absence of β-catenin in the nucleus. Interestingly, differentiated cells were present in the corresponding liver metastasis suggesting that MET had occurred at the metastatic site

[48]. Further evidence supports the involvement of CSCs in EMT. The induction of EMT in human mammary epithelial cells was associated with the expression of mesenchymal markers. In addition, the induction of MET also gave rise to a population of cells with properties of breast stem cells defined by $CD44^{high}/CD24^{low}$ marker expression. Cells that had undergone EMT were also more efficient at mammosphere growth, another property of stem cells [55]. Recent evidence supports the view that CSCs may be involved in EMT processes however; it is not known whether pathways promoting metastasis are always linked to stem cell properties. Using alternative models, others have shown the uncoupling of EMT and cell stemness [56]. It is clear that advances have been made in trying to determine the molecular pathways associated with metastatic spread however the complexity of events it entails precludes full understanding. It is evident that EMT processes play a central role and it is likely that this is driven by the induction of stem cell pathways.

1.2.2 Targeting metastasis

It is estimated that 90% of deaths arising from cancer do so as a result of metastasis [39]. Thus, there is a critical need to use the knowledge of molecular mechanisms to develop therapies to target this process. Additionally, as many of the steps in metastasis are common among cancers, it would seem a logical and a worthwhile process to target. However, despite its clinical relevance, the current success of antimetastatic drugs is poor.

Most current anti-cancer therapies target the primary tumour however, there are some therapies that target molecules involved in metastatic spread. Bevacizumab, for example, targets vascular endothelial growth factor (VEGF) and is administered alongside chemotherapy for the advanced treatment of a number of tumour types. Since VEGF is involved in the promotion of angiogenic processes, its inhibition could potentially prevent the growth of metastatic tumours by restricting the bloody supply [57]. Moreover, therapies against other metastatic pathways are under investigation, including inhibitors of Axl (a tyrosine kinase involved in EMT signalling), which reduced the metastatic burden of breast tumours in animal models and is demonstrating success in a number of tumour types [58, 59]. It is clear that despite the clinical significance of metastasis, the development of therapies targeting these pathways is limited. The drug discovery process may be facilitated by further understanding of the complex series of

molecular events involved. The molecular changes that may contribute to metastasis are next reviewed.

1.3 CD24

1.3.1 Overview and gene structure

In 1978, Springer revealed that rat monoclonal antibodies M1/75 and M1/69 recognised CD24 [60]; it was termed a heat-stable antigen due to its heat resistance. Subsequently, in 1990, CD24 was found to encode a small protein in mature form with only 31 amino acids. The CD24 is a small, heavily glycosylated protein which attaches to a cell's membrane via a GPI anchor. It is a single exon gene located on chromosome 6q21 which encodes 81 amino acid. Serine and threonine account for half of the amino acid [61], [62], [63].

The potential sites of O- glycosylation are serine and threonine, and the potential site of N- glycosylation is asparagine. Variable glycosylation of CD24 has been suggested as the reason for the variation in its molecular weight. Half of the 81 amino acids in a mature CD24 protein are potentially targeted for either N or O linked oligosaccharides [63], [64]. The diversity of functions and glycosylation was partly responsible for that actions in genetically and immunologically analysis. CD24 acts as a receptor for P-selectin and it is fundamentally expressed in a wide range of epithelial and non- epithelial cell types. [65]. Recently, high CD24 expression was found to be associated with poor outcomes in colorectal cancer. [66, 67]. Many studies have shown that CD24 has several ligands, and specificity of the ligands appears to be dependent on the context of the cells due to highly variable glycosylation. For example, colonization and cancer-cell rolling to lung tissue is promoted by CD24 when fucose transferase VII alters CD24 into a P-selectin ligand. Signal transduction is mediated by CD24 by engaging the family of Src protein tyrosine Kinases (PTKs) via membrane rafts,

activating the pathway of mitogen-activated protein Kinase, and involves B- and T- cell apoptosis, development, and cell binding [66, 67].

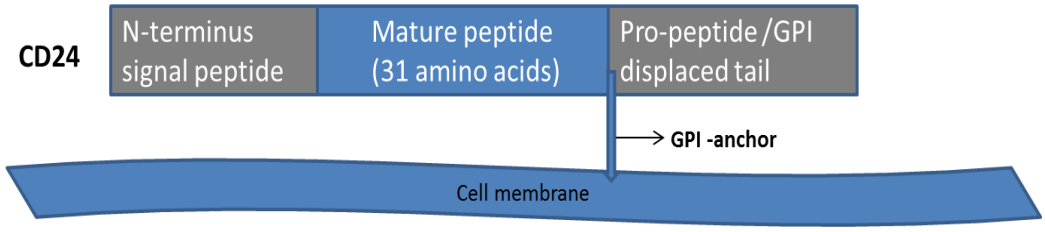


Figure 1-3: a simplified model for the structure of human CD24 protein [68]

1.3.2 Expression of CD24 in normal tissues

In mouse, CD24 is found on haematopoietic cell populations including erythrocytes, thymocytes, neutrophils, B-cells and T-cells. As its expression is developmentally regulated, it was traditionally used as a marker of differentiation for B and T-cells ontogeny [69]. Later it was also found to be expressed during the embryonic stages of other tissues including neuronal tissue and certain epithelia [70]. In humans, CD24 is not expressed on erythrocytes or thymocytes but is highly expressed on progenitor B-cells and remains expressed on mature resting B-cells eventually waning from the plasma cells [71]. Being on activated B-cells it also acts as a co stimulatory molecule for T-cell clonal expansion. On T-cells expression of CD24 varies with different maturation and activation states of T cells [71]. Continued research has shown even broader expression of CD24 on cells and tissues including more hematopoietic cells (eosinophils, neutrophils dendritic cells and macrophages), human neuronal tissue, muscle cells, gastric parietal cells, Pancreatic cells and many stem cells [72]. In addition to its expression in normal tissues, CD24 is shown to be up regulated in a growing list of inflammatory, autoimmune and neoplastic conditions. The list of tumours overexpressing CD24 is still growing and already includes both

solid and haematological malignancies such as B-cell lymphomas, erythroleukemia, gliomas, small cell lung cancer, oesophageal squamous cell carcinoma, hepatocellular carcinoma, cholangiocarcinoma, pancreatic adenocarcinoma, urothelial carcinoma, ovarian cancer, breast cancer, gastric cancer, prostatic carcinoma and colorectal carcinoma[72].

1.3.3 Role of CD24 in autoimmune disease

Autoimmune diseases are thought to be polygenic and multiple genes are being associated with each type of autoimmune disease, however, few are shown to have direct significant impact and CD24 provides one such example. CD24 polymorphism plays an important part in the association and progression of autoimmune disease. CD24 has a SNP (P170) which has neoconservative replacement in the C-terminus of the mature peptide, either Valine (A, $P170^{T}$) or Alanine (A, $P170^{C}$). Zhou *et al*, were the first group who reported that the $CD24^{V/V}$ is associated with risk and progression in multiple sclerosis and also, they found in the peripheral blood T cell, the expression of CD24 was higher in $CD24^{V/V}$ patient than that in $CD24^{A/A}$ patient . Moreover, CD24 is a genetic check point of T-cell homeostatic proliferation in lymphopenic hosts. Through the Lymphopenia, which is the cause of T-cell homeostatic proliferation that consider as a common phenomenon of autoimmune disease, the expression of CD24 on T-cell is essential for T-cell homeostatic proliferation. It has been linked to multiple autoimmune diseases including Systemic lupus erythematosus (SLE), Multiple sclerosis (MS), Autoimmune encephalitis, Rheumatoid arthritis, Crohn's disease and ulcerative colitis to name a few [73].

1.3.4 Role of CD24 in immune system

CD24 is expressed on a variety of haemopoietic and immune cells. As a general rule, it is seen much more abundantly on the progenitor cells and in more metabolically active cells, with a gradual loss from the surface as the cells matures and differentiate. CD24 is considered as a B-cell marker and seen on very early B-cell progenitors and expression varies with stages of differentiation being highly expressed on the progenitor cells to totally absent on the plasma cells [71]. This indicates a role of CD24 in B-cell development and maturation. Several lines of evidence have pointed towards this role of CD24 and studies have also observed that CD24-deficiency resulted in a reduction in late pre-B and immature B-cell populations in the bone marrow. On activated B cells, CD24 functions as a T-cell co-stimulator for $CD4^+$ T-cell clonal expansion. Research has also shown that cross linking of CD24 induces apoptosis in B-cell precursors including pre-B and pro-B ALL(Acute lymphocytic leukemia) cell lines [74]. Quite similar to B-cells, CD24 is highly expressed on immature T cells and expression gets weaker on peripheral T cells, but it is found to be upregulated in activated T cells. Another role of CD24 was shown by by Li *et al* that revealed that a functional CD24 gene is essential for optimal homeostatic proliferation of T cells in a lymphopenic host [75]. Interestingly, on dendritic cells, CD24 is a negative regulator of T-cell homeostatic proliferation and thereby prevents fatal damage associated with the uncontrolled homeostatic proliferation of T-cells in lymphopenic hosts [71].

Another important role has been attributed to CD24 i.e. discriminating between the PAMPs(Pathogen associated molecular patterns) and DAMPs(Damage/Danger associated molecular patterns) responses by the immune cells and it has been shown that the CD24-siglec axis provides the negative feedback mechanism for release of inflammatory cytokines after non-

pathogenic cell injury through repressing the host response to DMAPs [76].

1.3.5 Expression of CD24 in cancer

A great body of literature has shown that expression of CD24 is increased in various types of cancer, from haematological to solid tumours in a variety of body organs. Others have focused on the correlation between CD24 expression in different types of cancer and related clinic-pathological data or patients' prognosis. In haematological malignancies, CD24 has been recognized as a marker that has a major part in the pre-therapeutic prediction of high-risk groups in acute myeloid leukaemia (AML) [77]. In acute lymphoblastic leukaemia, lower CD24/CD45 ratios are associated with a better prognosis [78]. In solid organ cancers, CD24 showed increased expression in different types of tissues. In breast cancer, a strong CD24 cytoplasmic expression is reported in comparison to the rare apical membranous staining in benign ducts
[79]. In another study, the authors propose CD24 as a candidate gene related to oestrogen since CD24 mRNA levels were found to be lower in invasive breast carcinomas positive for oestrogen receptors. Furthermore, it could also be concluded from these findings that CD24 expression is more prevalent in the more aggressive oestrogen negative tumours [80]. An additional study found CD24 expression was connected with shorter disease-free survival time periods and overall survival rates in 201 patients, while membranous CD24 did not show any correlation with survival in a large series of invasive cytoplasmic breast cancers. [81]. However, Al-hajj and colleagues injected immuno-compromised mice with human breast cancer cells and found that even a small number of CD44+CD24-/low cells could form new tumours [82]. These results conflict with the known metastatic capabilities

associated with CD24 expression previously identified in breast cancer studies, and further investigation is warranted.

1.3.6 CD24 as cancer stem cell marker

Because CD24 is expressed in many types of organs and is involved with cell adhesion and metastasis [83], it is considered an important marker for prognosis in tumours. CD24 is identified as an alternate ligand for p selectin and an adhesion receptor on endothelial cells [84]. The association of CD24 with metastasis raises its significance as a new CSC marker [85], [86].

1.3.7 CD24 Glycosylation

Membrane proteins in eukaryotic cells are commonly modified with the addition of complex glycan structures. Three distinct types of modification are seen: N-linked glycosylation of asparagine residues at the consensus sequence Asn-Xaa-Ser/Thr [87], O-linked glycosylation of serine or threonine residues [88], and the glycosylphosphatidylinositol (GPI) anchor which is a glycolipid that can be attached to the C-terminus of a protein during post-translational modification. [89].

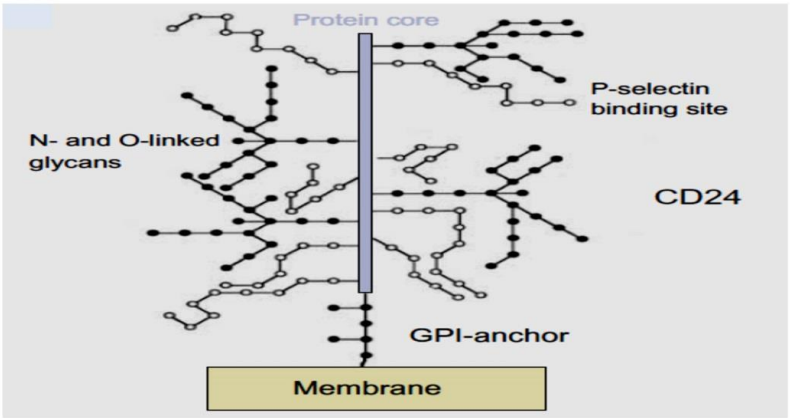


Figure 1-4 : Simplified diagram showing the glycosylation sites of CD24 [90].

1.3.7.1 N-glycosylation

Proteins undergo a wide variety of modifications after their synthesis and that is vital for the immense diversity in their structure and function found in cellular biology. One of the most common modifications is the addition of N-glycan (the sugars, that get attached to the proteins using the Nitrogen atom, present in the amide group of amino acids) to the newly synthesized proteins through a process called N-glycosylation [91]. CD24 contains two asparagine residues located in the potential N-glycosylation target motif Asn-X-Ser/Thr. N-glycosylated residues usually have roles in protein folding and conformation, protein stability, and targeting proteins towards subcellular and extracellular sites, and for functions such as cell-cell and cell matrix interactions. The biosynthesis of N-glycosylation starts in the endoplasmic reticulum (ER) (figure 1-5) by dolichol phosphate-dependent *N*-acetylglucosamine 1-phospho-transferase (GPT) which is encoded by the *DPAGT1.*following that, glycoproteins transit from ER to the Golgi, where N-glycan are modified more, to turn to a mature N-glycosylated protein decorated with oligosaccharides ranging from high mannose/hybrid to complex[92].

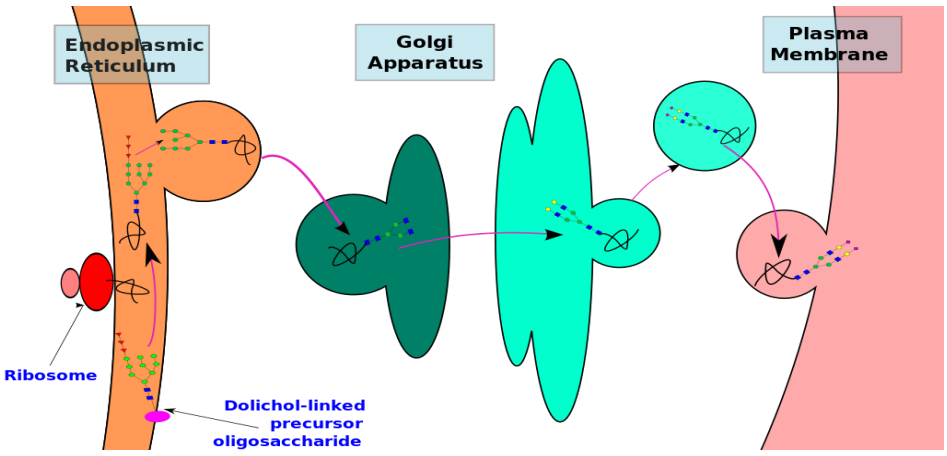


Figure 1-5 : Steps of protein N-glycosylation. (112)
Proteins synthesised in the endoplasmic reticulum are N-glycosylated by attachment of pre-synthesized Dolichol-linked sugar chain. And this chain is further modified and elongated in Golgi apparatus for further maturation.

1.3.7.2 O-glycosylation

Is a process in which the monosaccharides are attached to the Oxygen atom present in the hydroxyl group of serine and threonine residues. It has 12 potential O-glycosylation serine or threonine residue sites scattered along the peptide, although currently there is not an O-linked amino acid consensus sequence.

Protein O-glycosylation started via GalNAc — the first monosaccharide that connects serine or threonine in particular forms of protein *O*-glycosylation (*O*-GalNAc) called mucin-type *O*-glycosylation [93] which then extend3ed into various different structures. There are other types of *O*-glycans as well, such as those attached via *O*-mannose, and the nucleocytoplasmic glycan *O*-linked β-*N*-acetylglucosamine (*O*-GlcNAc) [94].

1.3.7.3 Factors disturbing N-glycosylation

The nitrogen atom of Asparagine amino acid must be existing in a sequon which is a Tri-peptide sequence. The consensus sequence of the N-glycosylation is **Asn-X-S/T** where S represents serine and T represents threonine, whereas the X is any amino acid except proline. Studies have shown the proline is seemed to be an inhibitor of N-glycosylation [95]. Yet another important level of regulation is by the enzymes involved in the glycosylation steps. Glycosyl hydrolases (GHs), glycosyl transferases (GTs) and nucleotide sugar transporters make up the 'hardware' of the pathway. These occur in the Golgi apparatus and are responsible for converting simple glycans like oligomannose, into a hybrid- and complex-type oligosaccharides. These glycan transforming enzymes can fluctuate amid different species, tissues and cell types and produce variable N-glycan structures. This glycosylation is a very dynamic process [96],[97]. These GHs and GTs even have different substrate

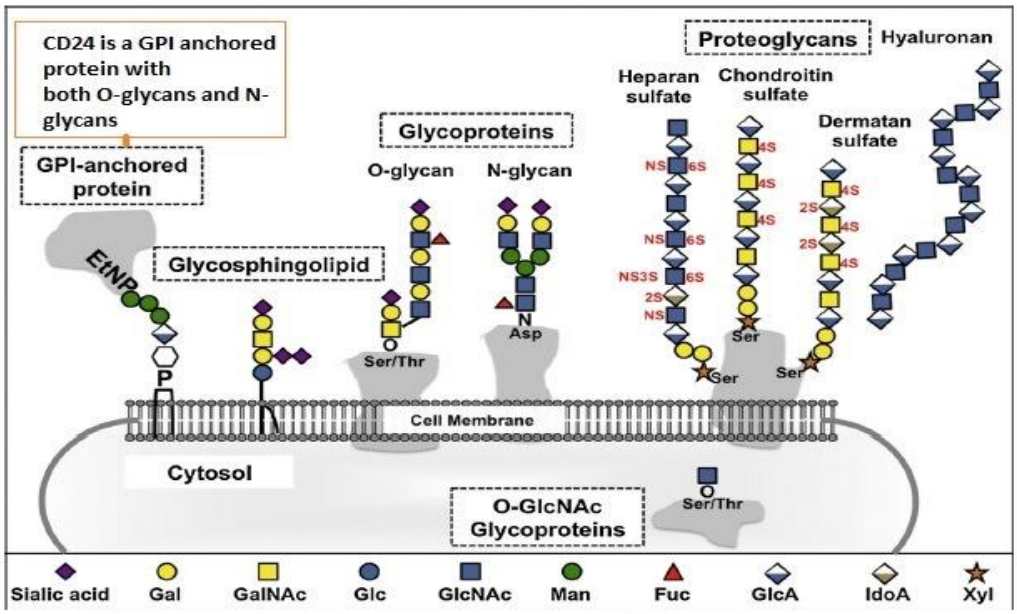
specificities and act sequentially. It is also seen that these enzymes physically compete for the sugar substrate and hence this can be one additional reason of variation in glycosylation of same protein in different tissues [97]. Studies have linked dysregulation of these enzymes to important human diseases including oral cancer [98],[91].

1.3.7.4 Role of glycosylation in cancer

All mammalian cells are decorated with a variety of sugar moieties (Figure 1-6) and it has been observed that changes in the cellular properties also affect these sugars. Neoplastic transformation is also found to alter the glycosylation pattern of tumour cells. Based on these observations certain carbohydrate structures have emerged as helpful tumour markers. Examples include MUC1/2, CEA, Ca19-9 etc. These sugars are also being used as adjuvants in tumour diagnosis and for monitoring prognosis i-e MUC1/2 CEA etc [99], [100]. A recent study by Valeras et al 2014 linked disturbed N-glycosylation of proteins like E-cadherin as a pathogenetic factor of oral cancer [91]. They proposed that dysregulation of DPAGT1 (an enzyme involved in N-glycosylation of proteins including E-cadherin) leads to changes in intercellular interactions and cytoskeletal dynamics.

Another study in 2015 by Sethi et al did a comparison of the N-glycome from colorectal carcinoma tissue and adjacent non tumour tissue and found N-glycoproteins signatures specific to colorectal tumours and also associated with tumour stage [101]. Similarly, Kapiro et al found differences in the N-glycome of colorectal adenomas and carcinomas and even found differences in glycosylation pattern between stage I, II and III tumours [102]. Current research is investigating potential ways of utilising these specific glycomic patterns in designing less invasive diagnostic tools and therapeutic possibilities in tumours expressing them and a few

studies have already shown some promising results [90],[103], [104].



Major glycoconjugate classes on human cells, and location of CD24 .

Figure 1-6 : CD24 and common sugars on the human cell surface [103].

A figure representing major classes of sugars displayed on the cell surface. The CD24 molecule is heavily glycosylated with O and N-sugars and it is attached to the cell membrane via another glycol-conjugate i-e GPI- anchor.

1.3.8 CD24 Post-translation modification

A study by Bleckmann et al, they used ESI (electrospray ionization ion trap) and MALDI (matrix-assisted laser-desorption ionization) analysis of the N-glycan and they spotted heterogeneous glycans with distinct carbohydrate such as sialic acid, blood group H antigen or Le^x repeats and hybrid type species , high-mannose [105]. The same analysis was performed on O-glycan and they found epitopes

such as sialic acid Le^x units. These sugar epitopes have a link to cellular properties such as migration, cell-cell interaction, and adhesion[96],[106]. All these studies indicate glycosylation of CD24 could be an important factor for a variety of function liked to this molecule [105]. For example, the sialyl Le^x carbohydrate is important for CD24-mediated rolling of tumour cells on P-selectin[71],[107]. Likewise, the presence of glycosylation pattern (α- 2,3- linked sialic acid residues) is essential for the interaction of CD24 with L1 [105].

1.3.9 CD24 Ligands

1.3.9.1 P-selectin

P selectin is calcium–dependent transmembrane type-I glycoprotein that interacts with carbohydrate determinants and mucin-like glycoprotein. Three members of selectins have been identified: P-selectin, L-selectin, and E-selectin [108]. Studies have shown that CD24 is a ligand for P-selectin, which is a protein expressed on endothelial cells and on activated platelets. This interaction between CD24/P-selectin is mediated by siaylated carbohydrate or by sialyl-Lex [109]-[110].

1.3.9.2 L1

L1 is one of immunoglobulin super family[111]-[112], its molecular weight 200 kDa, it's expressed on lymphoid cells, and in the central nervous system. Studies have shown that CD24 acts as ligand for L1 [113], and they found that these two co-operate in signal transduction. The binding of CD24 with L1 is totally dependent on the sialic acid present on CD24 [114].

1.4 Downstream targets

1.4.1 Notch1

The first discovery of Notches was in 1917. Later, they found these Notches resulted from the haploinsufficiency of an unknown gene, which in the mid-1980s were cloned and identified as a Drosophila transmembrane receptor Notch. Several studies have shown the association of Notches in diverse types of signalling such as adhesion, differentiation, proliferation, apoptosis, and epithelial-to-mesenchymal transition (EMT) [115].

The human Notch receptor family consists of 4 members: Notch1 to Notch4. Notch1 protein is synthesized inactivated composed of intracellular domains, transmembrane, and extracellular domains. Following transportation to the trans-Golgi network, a Notch is cleaved at a site referred to as the S1 cleavage site and generates two subunits, one with most of the extracellular domain and the other consists of the remaining extracellular domain, complete transmembrane and intracellular domain. The association of these 2 subunits results in the cell-surface expression of a mature heterodimer type I transmembrane receptor.

The ligand of Notch family involves 5 members: Delta-like 1/3/4 (Dll1/3/4) and Jagged 1/2. Notch is expressed on the cell surface as accessible-ligand form (Figure 1-7) of the receptor. The heterodimeric Notch receptor is inactive in the absence of the ligand binding. When Notch receptor binds to Notch ligand on an adjacent cell proteolytic cleavages happens which (stated as S2 and S3 cleavages) leading to releasing of the Notch intracellular domain (NotchIC) which then translocate into the nucleus and binds to CBF1, and nuclear protein MAML, resulting in the formation of a

ternary complex that functions as a transcriptional activator. MAML recruits the histone acetyltransferase protein p300, resulting in histone acetylation and conversion of the local chromatin structure to a form amenable to active transcription, resulting in the transcription of various Notch target genes including those belonging to the HES and HRT (HEY) families . in contrast, the absence of a nuclear NotchIC, the transcription factor CBF1 binds to the DNA sequence 5'-(C/T) GTGGGAA-3' within Notch target gene promoters and represses transcription [116].

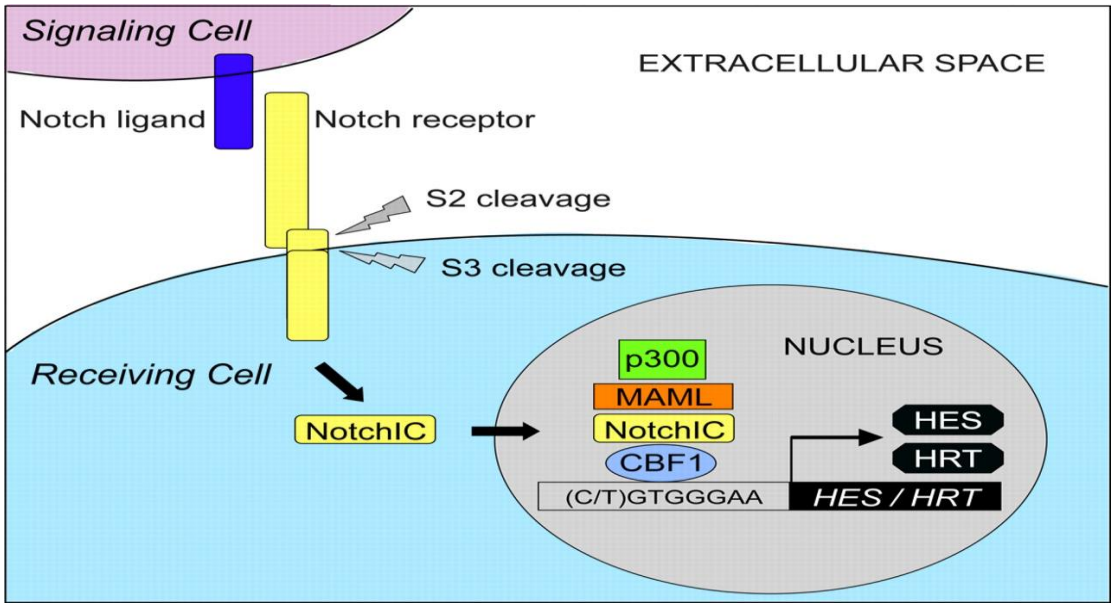


Figure 1-7: Activation of NOTCH signalling.
This figure displays the binding of Notch receptor with Notch ligand in order to activate Notch which then undergoes proteolytic cleavage and end up in the nucleus as NotchIC which then activate the downstream target (*HES, HRT*) [116].

1.4.2 Cten

C-terminal Tensin-like (Cten) is a member of the Tensin gene family but lacks the N-terminus actin-binding domain. Its role in tumours is not very clear as yet and both anti-tumour and pro-tumour roles have been attributed to this molecule and its effects may well be tissue specific [117]. This gene encodes complex protein which has

multiple domains capable of interacting with several molecules which in turn play important roles in cell signalling. Significant domains of Cten include the phospho-tyrosine binding domain (PTB) and the Src homology domain SH2. These domains help Cten bind with the cytoplasmic tails of β integrin at focal adhesions and also with the proteins containing phosphorylated tyrosine residues like focal adhesion kinase (FAK), ILK, p130Cas and P13 kinase [118].

In colorectal cancer (CRC), upregulation of Cten levels has been observed. Our group found that increased expression of Cten results in increased cell migration and also observed that the effect of Cten on cell migration and invasion was via modulation of downstream targets, including down-regulation of E-cadherin and induction of epithelial-mesenchymal transition (EMT) [117].

Little is known about the mechanism and regulation of Cten, and our lab has already proposed EGFR Kras-Cten signalling to be one pathway mediating this molecule. Cten is associated with increased cellular motility, invasiveness, and adhesion.[119] Many of its features indicate a potential link between Cten and CD24. For example, like CD24, Cten is upregulated early in the adenoma carcinoma sequence. Downstream targets for both molecules appear similar. As mentioned above, Altevogt et al. (2012) found that CD24 regulates c-src and FAK as well as STAT3 [120]. Similar effects by CD24 on STAT3 was observed by Lee and colleagues who found STAT3 was activated by CD24 via NANOG [121]. However, Barbieri et al. (2010) proposed that STAT3 upregulates Cten and mediates increased tumour migration and invasiveness.[121, 122].

1.4.3 FAK

FAK (focal adhesion kinase) is a 125 kDa non-receptor and non-membrane associated protein tyrosine kinase (PTK) discovered in the 1990s. It interacts with the cytoplasmic tails of integrins as well as other members of the focal adhesion protein complex such as paxillin [123-125]. It is believed to be involved in many critical cellular events including adhesion, migration, proliferation, and survival. It has been shown that FAK is over-expressed in invasive and metastatic colon tumours at both the protein and the mRNA levels [126]. The expression and phosphorylation of FAK have been shown to correlate with more invasive tumour phenotypes by inducing epithelial mesenchymal transformation. Additionally, some studies have linked FAK and the response of tumour cells to chemotherapy [127]. Studies have also shown regulation of FAK by CD24. Baumann and colleagues have shown very recently (2011) that although the total FAK protein levels remain the same after upregulation of CD24, phospho-FAK is increased along with augmented C-src kinase activity [128].

1.4.4 ILK

Integrin linked kinase (ILK) was discovered in 1996 and as the name suggests it is linked to the cytoplasmic tail of β1 and β3 integrins. Quite similar to FAK, the presence of ILK at focal adhesions allows it to play an essential role in the transduction of many biochemical signals that are triggered by cell-ECM interactions. These signals modulate diverse biological events, including cell survival, differentiation, proliferation, migration, invasion and angiogenesis [129],[130]. It has been found that the C-terminal domain of ILK also interacts with actin-binding adaptor proteins, such as paxillin and parvins, which interact directly with the actin network, allowing ILK to bridge the effects of growth

factors and ECM through growth factor receptors and transmembrane integrins to the actin cytoskeleton and regulate cytoskeletal re-organisation and cell migration processes [131]. It has been found that ILK expression correlates significantly with tumour invasion, grade and stage, in colorectal carcinomas and many other malignancies, suggesting a role in tumour progression. It has also been described that ILK expression correlates with stimulation of the Akt pathway, down-regulation of E-cadherin and activation of β-catenin in human colon cancer[132]. We explored this molecule regarding mediating CD24 associated motility.

1.5 Aims and hypothesis

CD24 has a variety of different functions that are of relevance to carcinogenesis. Glycosylation of CD24 is likely to be important in the activity of CD24 [65]. These project aims were:

a) To investigate the potential functional importance of N-glycosylation in CD24 biology by mutating the N-glycosylation sites of CD24.

b) Mapping the functional sites of CD24 by deleting parts of the mature peptide and to validate the N-glycosylation sites.

c) The signalling pathway by which CD24 is able to promote cell motility is not well defined yet. Similarly, little is known about the mechanism of CD24 regulation, so we looked to investigate the signalling pathway of CD24.

d) Defining the extrinsic signals by which CD24 promotes cell motility.

2. Materials and Methods

2.1 Cell culture

Cell culture was performed to enable the cell lines to proliferate and be maintained for an extended period. The cell lines used were HCT116, and SW620. The cell lines were obtained from the Molecular and Population Genetics Laboratory, London Research Institute, Cancer Research UK, London. All the cell lines were seeded in 75cm2 flasks using Dulbecco's Modified Eagle's Medium (DMEM) containing 10% fetal bovine serum, and 1%L-glutamine (Invitrogen). Serum-free culture medium was prepared from DMEM media supplemented with 1%L- glutamine for use in transfections. Cells were incubated at 37°C and 5% CO_2 and split at 90-100% confluence. For splitting cells medium was removed and culture was washed twice with PBS (phosphate buffered saline). Cells were trypsinised using 2 ml of Trypsin EDTA (0.5% trypsin, 1 mM EDTA, Sigma, USA) and incubated at 37°C for 5 minutes to detach the cells. Cells were suspended in 5ml of DMEM and then plating into new flasks containing 10ml of growing media with 0.1 – 1ml of the cell suspension. The identity of the cell lines were analysed by mutation profile technique. (See appendix 9.3)

Cell line	Age	Sex	Duke stage	Differentiation	Site	Culture condition
HCT116	64	M	D	Well	Colon	adherent
SW620	51	M	C	Moderate	Colon, lymph	adherent

Table 2-1: **Cell lines with their characteristics**

2.1.1 Cell viability maintenance

The cell viability, the degree of confluence, and the absence of fungal or bacterial contaminants were carried out on a daily basis by microscopic examination.

2.1.2 Cell lines sub-culture

The cell lines were sub-cultured once or twice a week, when they reached confluence. The medium were discarded from the flask using 10 ml sterile pipette, then, washed with 5 ml of PBS (Phosphate-buffered Saline, Sigma, USA) to wash away the cellular debris. After PBS was discarded from the flask, 5 ml of Trypsin-EDTA was used to detach the cells then, the flask was incubated at 37^{o}C for roughly 5-10 minutes. 8 ml of fresh Medium was added to the flask to inactivate the trypsin, the mixture was transferred into 20 ml universal tube. Following that, the tube was centrifuged at 1000X (g) for 5 minutes. The supernatant was discarded and new 10 ml of Medium were added to the tube and vortexed for 1-2 minutes. Approximately, 1 ml of the mixture was pipetted into new flask with 10 ml medium.

2.1.3 Cell counting

For specific experimental work, precise cell number was required. Following the vortexing of cells, 20 µl were pipetted into an Eppendorf tube with 20 µl of Trypan blue dye (Sigma Aldrich, USA) and mixed very well. 10 µl of the mixture were loaded into each side of the cell counting slide. Then, the slide was inserted into Automated Cell counter (Bio-rad TC20) for focusing and detection.

2.2 Transfection of cell lines

2.2.1 Gene forced expression

The CD24 expression construct (CD24 - pcDNA3.1) had been previously constructed in our lab and was used to express mutant CD24 in low CD24 expresser cell line HCT116 (see Appendix 9.1). Lipofectamine 2000 (Invitrogen) was used as the transfection reagent. The transfection was performed according to the Lipofectamine 2000 (Invitrogen) instruction“ manual. Briefly, one day before transfection $1.5x10^5$ cells were plated in 2 ml of growth medium (DMEM) with 10 % FBS without antibiotics in 6-well plates (volumes are adjusted according to plate size used). On the second day, cells were transfected when confluence reached between 60 and 90 %. A total of 4 µg of plasmid DNA wild type, plasmid DNA mutant and the control empty vector was diluted in 250 µl of Opti-MEM® I -Serum -reduced medium (Invitrogen) and mixed gently. Lipofectamine™ 2000 (Invitrogen) was gently mixed before use, and then 10 µl was diluted in 250 µl of Opti-MEM® I Medium and incubated for 5 minutes at room temperature. Subsequently, the diluted DNA was combined with the diluted Lipofectamine™ 2000, mixed gently and incubated for 20 minutes at room temperature. The complexes were lastly added to the cells covered by 2 ml of fresh Opti-MEM® I -Serum -reduced medium and plates were incubated at 37ºC in 5% CO_2 incubator. Transfections were performed in duplicate.

2.2.2 Gene Knockdown

Small interfering RNA (siRNA) can be used to inhibit gene expression. siRNA was used for the knockdown of CD24 and Notch1. Briefly, one day before transfection, 500,000 cells were plated in 2 ml of growth medium (DMEM) with 10 % FBS without antibiotics in 6-well plates (volumes are adjusted according to plate

size used). On the second day, cells were transfected when confluence reached between 40-50 %. One hundred picomoles (per well) of the siRNA and 5µl (per well) of the lipofectamine 2000 were diluted in 250 µl of Opti-MEM® I serum-reduced medium (Invitrogen) and mixed gently. Lipofectamine™ 2000 (Invitrogen) was gently mixed before use, and then 10 µl was diluted in 250 µl of Opti-MEM® I medium and incubated for 5 minutes at room temperature. Subsequently, the diluted DNA was combined with the diluted Lipofectamine™ 2000, mixed gently, and incubated for 20 minutes at room temperature. The complexes were lastly added to the cells covered by 2 ml of fresh Opti-MEM® I serum-reduced medium and plates were incubated at 37ºC in a 5% CO2 incubator. The cells grew for 48 hours before further experimentation. Transfections were performed in duplicate.

2.2.3 Co-transfection

Co-transfection was used to assess the downstream partner of CD24 by establishing a system consisting of forced expression of CD24 and a concomitant knockdown of Notch1. Briefly, one day before transfection, 150,000 cells were plated in 2 ml of growth medium (DMEM) with 10 % FBS without antibiotics in 6-well plates (volumes are adjusted according to plate size used). On the second day, cells were transfected when confluence reached 50%. For each co-transfection samples, Lipofectamine® 2000 complexes were prepared as per manufacturer guidelines. One hundred picomoles of siRNA for knock down and 4µg/well pcDNA 3.1 CD24 plasmid were diluted in 250 µl of Opti-MEM® I serum-reduced medium (Invitrogen) and mixed gently. Lipofectamine™ 2000 (Invitrogen) was gently mixed before use, and then 10 µl were diluted in 250 µl of Opti-MEM® I Medium and incubated for 5 minutes at room temperature. Subsequently, the diluted DNA was combined with the

diluted Lipofectamine™ 2000, mixed gently and incubated for 20 minutes at room temperature. The complexes were lastly added to the cells covered by 2 ml of fresh Opti-MEM® I serum-reduced medium and plates were incubated at 37ºC in a 5% CO_2 incubator. After 48 hours, transfected cells were first harvested for protein extraction and then a western blot was used directly for the relevant functional assays. Transfections were performed in duplicate.

Gene	Sequences
CD24 siRNA	ACCCACGCAGAUUUAUUCCAGUGAA
Notch1 siRNA	GCACGCGGAUUAAUUUGCA
Universal non targeting siRNA (Luciferase specific)	CGUACGCGGAAUACUUCGA

Table 2-2 : The sequences of the siRNAs and the reference sequence number (NM) of the genes mRNA.

2.3 Cell Treatment

2.3.1 Cycloheximide

Cycloheximide (CHX) is a means of inhibiting translation of mRNA and can therefore be used to monitor protein degradation. Diluting 0.5 ml of the 10 mg/ml Cycloheximide stock in 50 ml of media results in a final concentration of 100 µg/ml. At 24 hours post-transfection, the media was replaced with fresh media in all wells. Media was replaced with CHX containing media and incubated for 0, 30, 60, and 90 minutes for both CD24 and empty vector transfected cells. Cells were lysed at the same point for all treatment groups using a RIPA buffer as previously described.

2.3.2 Recombinant P-selectin

Cells were treated with recombinant P-selectin to stimulate signalling through the receptor-ligand interaction of CD24 with P-selectin. Cells were seeded and allowed to adhere for 3 hours. Subsequently, the cells were starved in serum free DMEM for 3 hours prior to stimulation. Cells were then treated with 5 µg/ml of recombinant P-selectin for 30 minutes (EMD Millipore Corporation) under normal DMEM. Finally, the cells were lysed and immunoblotted.

2.4 Western Blotting

2.4.1 Protein extraction and quantification

For protein extraction, the tissue culture medium was aspirated and the cells were washed with the ice-cold 1X PBS. Cells were trypsinised and were transferred to a 1.5 ml Eppendorf tube with media containing FBS. Next, the tubes were centrifuged at maximum speed (3000 rpm) at 4 °C for 5 minutes and then washed twice with ice-cold 1X PBS. The cell pellets were afterwards treated with an ice-cold RIPA buffer (Radioimmune-Precipitation Assay, Thermoscientific, UK, Cat. NO. 89901) with a EDTA-free (100X) Halt protease and phosphatase inhibitor cocktail, added at 1:100 concentration (Pierce, UK, Cat. NO.78445). Tubes were incubated for 5 minutes on ice. The Eppendorf tubes were centrifuged at maximum speed (14000 rpm) at 4 °C in a BIOFUGE fresco machine for 20 minutes. The supernatant was collected, aliquoted into 1 ml tubes, and store at -20ºC. Quantification of the proteins was performed by BCA protein assay Kit (Thermo Fisher Scientific Inc., Rockford, USA, Cat. No.23225*)* and by adding protein to the

working solution in a 96 wells plate and reading at absorbance 550nm (See Appendix 9.2)

2.4.2 Neuraminidase digestion

One of the objectives of the project was to remove N-glycosylation sites from CD24. Transfection of modified expression construct would result in a protein which was less glycosylated than the wild type protein. Glycosylation can affect the apparent molecular weight on Western blot and therefore, to assess the transfection efficiency of the constructs, it was necessary to remove the sugars on the amino acid residues. Neuraminidase was used to digest off the sugars. A 30 µl mixture was made; it contained 10 µg of protein lysate, 10 µl of 10x glycoBuffer (NEP, Lot: 0151504), 10 µl of neuraminidase (50,000 U/ml), and 10 µl of nuclease-free water. Next, the reaction was incubated at 37ºC overnight and then the enzyme was deactivated at 68ºC for 10 minutes.

2.4.3 SDS polyacrylamide gel electrophoresis

Using a pre-made Bio-Rad gel system, a 10% Sodium Dodecyl Sulphate Polyacrylamide Gel Electrophoresis (SDS PAGE) running gel was prepared and 30 µg of each protein sample was added to a 4X SDS loading buffer containing 5% β-mercaptoethanol. The samples were boiled at 90ºC for 5 minutes on a hotplate, and samples were subsequently transferred to ice for another 5 minutes after denaturation. After centrifuging for 2 minutes at 13000 rpm, the samples were loaded into the wells and ran for 60 minutes at 60 mA for two gels. A labelled size marker was used to measure the target protein size (Bio-Rad, UK).

2.4.4 Transfer of separated proteins

The gel was equilibrated in a transfer buffer for 5 minutes. A Hybond-P PVDF (Polyvinylidene fluoride) membrane (Amersham Bioscience, Buckinghamshire, UK) was used for protein transfer. Membrane activation with methanol and all equilibrations were conducted according to the manufacturer's instructions. Following the formation of a transfer sandwich, the transfer of proteins was carried out using a semi-dry transfer unit (Bio-Rad, UK) at 0.8mA/cm2 of membranes (64 mA for 2 gels).

2.4.5 Immuno-detection of proteins

After the transfer of protein, the membranes were blocked with 5% non-fat dry milk in PBS containing 0.1% Tween20 for 1 hour at room temperature and then incubated overnight at 4ºC on the roller with the relevant antibody diluted to the optimal concentration in the same solution used for blocking the membranes. For the purpose of loading controls, the monoclonal Anti-β-actin antibody (Sigma Aldrich, UK) was used in a dilution of 1:2000 against the ubiquitous β-actin protein. The blots were washed three times in PBS with 0.1% Tween20 and then incubated for 1 hour at room temperature with a horseradish peroxidase-linked secondary antibody (Sigma Aldrich, UK) either anti-mouse or anti-rabbit (depending on the primary antibody); the secondary antibodies were diluted in the same solution used for blocking. The immuno-reactive proteins were visualized with Enhanced Chemiluminescence detection kit (Super signal West Pico Chemiluminescent Substrate, Thermoscientific, UK) and exposure to C-DiGt Blot Scanner. Primary antibodies and condition are given in table 2-3

No.	Antibody	Species	Source	Primary Ab	Secondary Ab	Size (kDa)
1	CD24 Antibody	Mouse	SWA11 (Gift from Prof.. Altevogt	1:2000	1:5,000	30-70 kDa
2	CD24 SN3 Antibody	Mouse	*Sigma Aldrich, USA*	1:50	1:4,000	35 kDa
3	Cten Antibody	Mouse	*Sigma Aldrich, USA*	1:1000	1:10,000	79 kDa
4	FAK Antibody	Rabbit	Cell singling, UK	1:500	1:5,000	125 kDa
5	ILK Antibody	Rabbit	Abcam, UK	1:500	1:5,000	52 kDa
6	Notch1 Antibody	Rabbit	Abcam, UK	1:500	1:2,000	120 kDa
7	Activated Notch1	Rabbit	Abcam, UK	1:500	1:2000	95 kDa
8	β–Actin Antibody	Mouse	*Sigma Aldrich*, USA	1:2000	1:10,000	42 kDa

Table 2-3: The sources of the antibodies and the working conditions when used in Western Blot.

2.5 Co-immunoprecipitation

Cell lysates were first subjected to a pre-clearing stage to reduce non-specific binding. The protein (1 ml) was incubated with 20 µl of protein G/A agarose beads (Calbiochem IP05) at 4°C with gentle rotation for 30 minutes. The lysate was centrifuged at 4°C at 13,000 rpm for 5 minutes and the supernatant retained. One µg of CD24 SWA 11 (2 µl) antibody was added to 300 µg of the pre-cleared lysate and incubated while rotating overnight at 4°C. Additionally, 300 µg of pre-cleared lysate (without antibody) was also incubated with the pre-cleared beads as a negative control. Following incubation, 30 µl of Protein A/G beads was added to the IP reactions and incubated on a rotator for a further 24 hours at 4°C. The beads were pelleted by centrifugation at 13,000 rpm at 4°C for 5 minutes and washed twice in ice cold PBS. The sample was re-suspended in 10 µl of a 3X NUPAGE loading buffer (Invitrogen NP0007) and heated at 95° for 5 minutes, and then kept on ice for 5 minutes and centrifuged for 2 minutes at 13,000 rpm before it was loaded onto an SDS gel for western blot analysis. Fifty µg of protein was loaded for input.

2.6 Flow cytometry and CD24 expression

Flow cytometry was used to evaluate CD24 expression following plasmid transfection. A single cell suspension of transfected cells was prepared by trypsinising cells using a TE buffer (10 mM Tris-HCl [pH 8], 1 mM EDTA, Sigma, USA) and re-suspending the cells into 1x PBS. Samples were analysed using the EPICS Altra Flow Cytometer (Beckman Coulter, Buckinghamshire, UK) with filters set to detect fluorescence with a wavelength of 530 nm. At least 10,000 events were collected per sample and data analysis was conducted using Weasel software version 2.7 (The Walter and Eliza

Hall Institute of medical research, PV, Australia) and expressed as mean fluorescence intensity (MFI). Dead cells were excluded from analysis according to their forward and side scatter characteristics.

2.7 Total RNA (Ribonucleic acid) extraction

Once cells reached 90% confluence, they were harvested by washing them with PBS, followed by trypsinisation and incubation for 5 minutes at 37°C and 5% CO2 humidity. The cell suspension was centrifuged for 5 minutes at 3000 rpm speed to pellet the cells. The RNA extraction was performed using a RNeasy Mini Kit (Qiagen) following the manufacturer's protocols. Briefly, pellets were re-suspended in 5 mL of the medium, and counted using an automated cell counter (Bio-Rad, TC20™ Automated Cell Counter Model #1450102). The cells were aliquoted to get a maximum of 1 X 10^7 cells per aliquot, washed twice with PBS, re-suspended in 1ml PBS, transferred to a 1.5 ml tube, and then spun for 5 min at 300xg. The supernatant was discarded, and the pellet was lysed with either 350µl or 600µl of a RLT lysis buffer according to the starting number of cells (< 5 X 10^6 cells were lysed in 350 µl, from 5 X 10^6 to 1 X 10^7 were cells lysed in 600 µl).

The cell suspension in the lysis buffer was further homogenized using QIAshredder^{Tm} spin columns (Qiagen, Crawley, UK) placed in a 2 ml collection tube, and centrifuged for 2 min at full speed. The lysate was then mixed with 70% ethanol and placed into a spin column with a silica membrane and centrifuged at >8000xg for 15 sec. On-column DNase digestion was required for the elimination of genomic DNA contamination; to prepare the spin column, 350 µl of the buffer RW1 was added to the RNeasy spin column and centrifuged for 15 seconds at > 8000 xg. To perform DNA digestion, 10 µl of DNase I stock solution was added to 70 µl Buffer RDD, then the DNase I incubation mix (80 µl) was added directly to the

RNeasy spin column membrane and placed on the bench top (20–30°C) for 15 min. The membrane containing the RNA was washed once with 700 µl of a RWI buffer, then twice with 500µl of a RPE buffer (containing ethanol). After the final wash, the column was spun dry at 8000 xg to remove remaining traces of ethanol from the membrane. The RNA was then eluted in 30 µl of RNase free-water.

2.7.1 Assessment of RNA integrity

To check the quantity and quality of the RNA, the spectrophotometer (NanoDropTM 1000 Spectrophotometer, Thermo Scientific) was blanked with RNase free water. The absorbance at 260nm and 280nm was measured. The measure of A260 gave the quantity of total RNA in µg. The ratio A260/A280 gave an estimation of the purity of the RNA (RNeasyt mini Handbook, Qiagen, Crawley, UK). A ratio of ~1.8 is commonly accepted as "pure" for DNA, and the ratio of ~2.0 is generally accepted as "pure" for RNA. If the ratio is noticeably lower, in any case, it may point to the presence of protein, ethanol or other contaminants that absorb strongly at or near 280 nm.

2.8 Complementary DNA (c. DNA) Generation

To generate complementary deoxyribonucleic acid (cDNA), RNA reverse transcription was used. Briefly, 1µg of RNA was prepared in 20µl of water and 1µl of random hexamers (pD [N] 6) and incubated at 70^{o}C for 10 minutes as an initial denaturation step. Samples were placed on ice for 5 minutes and a master mix was prepared by adding 1 µl (200 units) of Moloney Murine Leukaemia Virus Reverse Transcriptase enzyme (M-MLV RT [Invitrogen, UK]), 50mM of dithiothreitol (DTT [Invitrogen, UK]) and 1.5 µl of deoxy ribonucleotide triphosphate (dNTP) mix. In RT negative (RT-)

samples, water was added to replace the enzyme. Master Mix was added to each sample up to a final volume of 50 µl and incubated at 37°C for 1 hour, followed by incubation at 95°C for 10 minutes.

Master Mix	1 reaction (µl)	4 reactions (µl)
5x First-Strand Buffer	10	40
dNTP (10mM)	1.5	6
DTT(0.1M)	5	20
M-MLV-RT (200U/µl) enzyme (Invitrogen)	2	8
dH_2O	10.5	42

Table 2-4 : Master Mix made for the reverse transcription reaction.

Master Mix	1 reaction (µl)	4 reactions (µl)
5x First-Strand Buffer	10	40
dNTP (10mM)	1.5	6
DTT(0.1M)	5	20
dH_2O	12.5	50

Table 2-5 : Master mix made for the RT- negative reactions.

2.9 Real-Time polymerase chain reaction

2.9.1 Primer design

All the primers were designed using a primer design tool (http://frodo.wi.mit.edu/). To ensure specificity, primers were tested by using a blast (http://www.ncbi.nlm.nih.gov/tools/primer-blast/) method against a human genomic database, and it was taken into account that PCR efficiency depends on the quality of the DNA. Since the DNA materials were extracted from FFPE and the process of fixation usually compromises it, primers were designed to amplify 110 to 180 base pairs (bps) as well as flank an exonic region of genes of interest. To reduce interaction between primers, each primer was tested against the others using the UCSC (University of California Santa Cruz) in silico PCR (http://genome.csdb.cn/cgi-bin/hgPcr).

Gene of interest	Primer Sequence	Product size	Annealing temperature
HPRT (NM_000194)	Forward Primer 5'AAATTCTTTGCTGACCTGCTG 3'	122	60˚C
	Reverse Primer 5' TCCCCTGTTGACTGGTCATT 3'		
CD24 (NM_01323 0.2)	Forward Primer 5' ACCCACGCAGATTTATTCCA 3'	110	59˚C
	Reverse Primer 5' CCTTGGTGGTGGCATTAGTT 3'		
Notch1 (NM_032865)	Forward Primer 5' GCGTCTGCTCAGA ATCGAC 3'	110	56˚C
	Reverse primer 5' GATGAGGAAGTGTCGGATGG 3'		

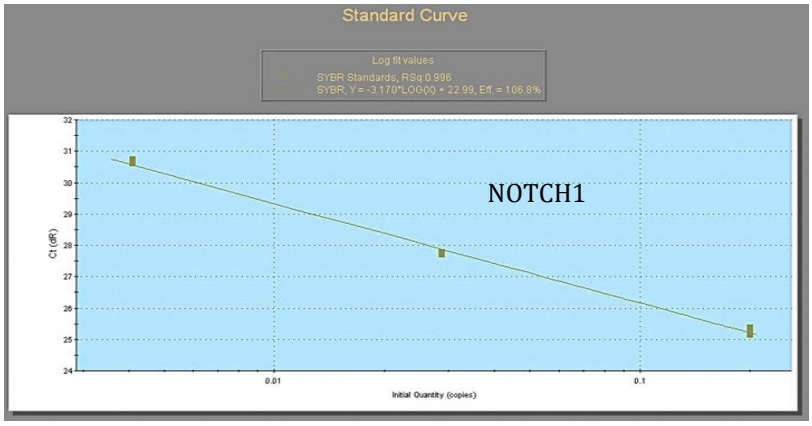
Table 2-6 : RT- PCR Primer sequences.
The table shows the characteristics of the primers used for amplification of HPRT, CD24, and Notch1.

2.9.2 PCR reaction

All experiments were carried out in triplicates and the values of amplification were normalized to the housekeeping gene Homo Sapiens Hypoxanthine phosphoribosyl transferase 1 (HPRT1) (Tables 2-3). The Brilliant SYBR® Green QPCR Master used in this process was purchased from (Stratagen, UK). The final volume of each reaction was 25 µl and contained12.5µl of 1X SYBR Green Master Mix (Stratagen, UK), 1 µl of each primer (final concentration: 250 nM,), and 5 µl of cDNA templates (2 ng/5 µl) (Table 2-4). Cycling conditions for the reactions were 1 cycle of denaturation for 10 minutes at 95ºC followed by 40 cycles of denaturation (30 Seconds at 95ºC), annealing (60 Seconds at a temperature specific for the primer in use) and extension (30 Seconds at 72ºC) in the thermal cycler (Mx3005P™, Stratagene); finally, the reactions were left for 1 cycle of 120 seconds to generate a dissociation curve (divided as 1 minute of denaturation at 95 ºC, 30 seconds at 55 ºC, and 30 seconds at 95ºC). The data for Q-PCR were analysed by the MxPro-QPCR software version 3.20 using the standard curve method. For each QRT-PCR experiment, a standard curve was generated for each target gene. Standard curves were generated using 10-fold serial dilution of image clones of either CD24 or HPRT1. Controls for QPCR experiments were "No template control (NTC)" reactions containing all the reagents excluding the DNA template and a RT- negative control to exclude the possibly of genomic DNA contamination during the step of
c. DNA synthesis.

Components	X1 Reaction(10µl)	X 20 reactions
Master mix	5 µl	100 µl
Forward primer	0.4 µl	8µl
Reverse primer	0.4 µl	8µl
Water (PCR clean)	3.2 µl	64µl
Template	Added separately	1µl each

Table 2-7 : Master mix for qPCR



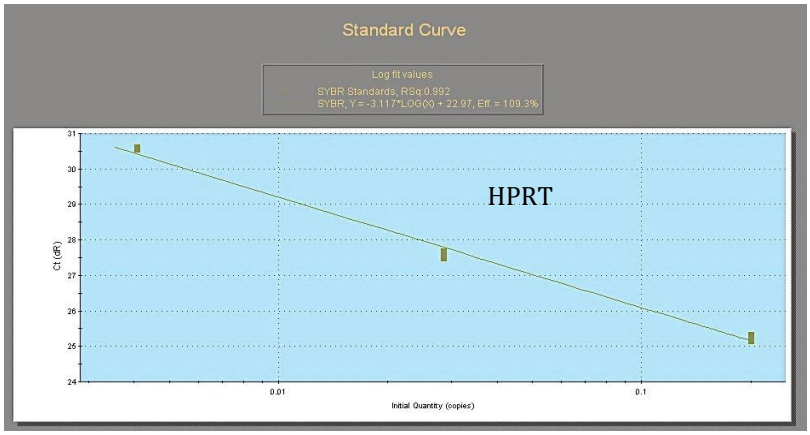


Figure 2-1: A representative example of qPCR.
The qPCR for Notch1 and HPRT were optimised as been described. The standard curve shows exponential amplification with 100% efficiency.

2.10 Site directed mutagenesis and mapping of CD24

Site-directed mutagenesis is a technique that creates a mutation at a defined site. Changes to sequence can be made using PCR by simply including the desired change in the PCR primers. The identification and construction of new commercial polymerases and advances in oligonucleotide synthesis have dramatically increased its efficiency. The protocol is briefly shown in the flow chart Figure 2-2.

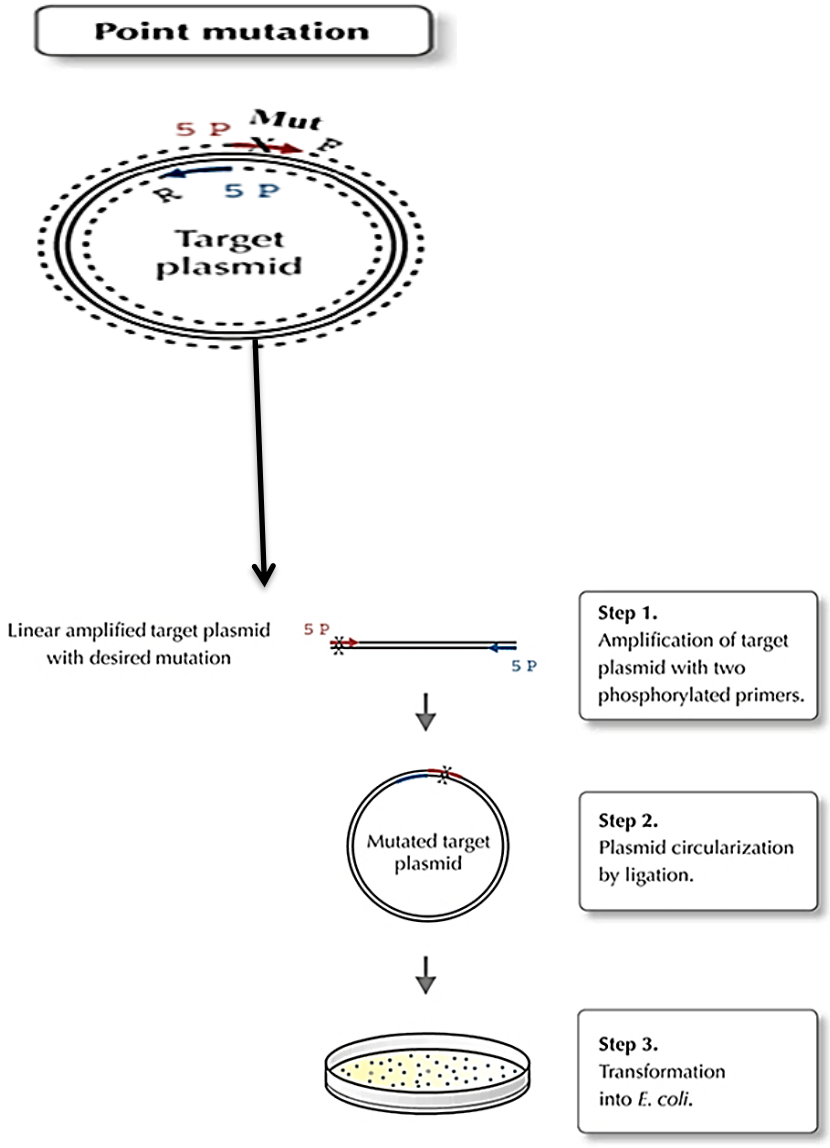


Figure 2-2 : Site directed mutagenesis flow chart.

2.10.1 Primers design

For mutation of the N-glycosylation sites (N36 and N52), missense mutations were introduced to change the asparagine residues to glutamate. For deletion mapping of CD24, small regions were sequentially deleted. Mutation and deletion mapping of CD24 were performed by site-directed mutagenesis. Primers were designed using the Primer x which is available on-line at http://www.bioinformatics.org/primerx/. The selected sequences were further analysed with the Amplifix program available online at http://ifrjr.nord.univ-mrs.fr/ AmplifX-Home-page for additional characteristics: recognition of the primers for the gene of interest, probability of primers forming dimers, or hairpins. Finally, all sequences were submitted to the Blast software, available on the National Centre for Biotechnology Information website www.ncbi.nlm.nih.gov , in order to evaluate gene specificity. Following their design, primers were obtained from (Eurofins MWG Operon) and subsequently diluted to a working concentration of 100 pmol/µl. The sequences were as follows:

a)

Genes	Forward Primer	Reverse Primer
pCCD24^{N36Q}	CAGATACTTCCCAATCTTGGGTTGGCC	GGCCAACCCAGATTGGGAAGTACTCTG
pCCD24^{N52Q}	CCAAATCCAACTCAGGCCACCACCAAG	CTTGGTGGTGGCCTGAGTTGGATTTGG

b)

Genes	Forward Primer	Reverse Primer
pCCD24$^{delta7.1}$	GATTTATTCCAGTAGTAACTCCTCC	GGAGGAGTTACTACTGGAATAAATC
pCCD24$^{delta7.2}$	CTCCCAGAGTACTAATCCAACTAATG	CATTAGTTGGATTAGTACTCTGGGAG
pCCD24$^{delta7.3}$	CTTCCAACTCTAATGCCACCAC	GTGGTGGCATTAGAGTTGGAAG
pCCD24$^{delta7.4}$	CAACTAATGCCACCGGTGGTGCCCTGC	CAGGGCACCACCAGGTGGCATTAGTTG

Table 2-8 : The sequence of the primers, which were produced from Eurofins MWG Operon . a) site directed mutagenesis (change the amino acid Asparagine to Glutamine) and b) mapping the functional sites of CD24 by deleting the mature peptide.

2.10.2 Standard PCR

A standard PCR was performed by using the site one mutant clone of CD24 with the second site primer and the site two mutant clone of CD24 with the first site primer to induce the two mutations into one plasmid (accession number BC064619) in 20 µl of PCR reaction using Pfu DNA polymerase (Agilent Technologies, Cat. No. 600670). The PCR reaction was performed in a Primus advanced 96 machine and allowed to run for 35 cycles with the following cyclic conditions: one cycle of 95ºC for 2 minutes (initial denaturation), followed by 35 cycles of 95ºC for 20 sec (denaturation), and then 52ºC for 30 seconds (annealing) and 72ºC for 15 sec/kb (extension). The final cycle was at 72ºC for 10 minutes (final extension). Finally, PCR products were analysed using gel electrophoresis on a 1% agarose gel to check for a single discrete band.

2.10.3 Agrose gel electrophoresis

One percent agarose gel (w/v) was prepared by mixing 1 gram of agarose (Gibco-BRLife Technologies, USA) with 100 ml of a 1% Tris Borate EDTA (TBE) buffer (Sigma, USA) and heating in a microwave for 1 minute. The gel was cooled to room temperature under running tap water. Ten µl of SYBERSAFE DNA fluorescent dye (1000x) (Sigma, USA) was added and the gel was then transferred into the gel running apparatus and an appropriate size comb was inserted. The gel usually takes about 20 minutes at room temperature to solidify, and during this time, it was covered by foil paper as SYBERSAFE is light sensitive. For testing of PCR products, 12µl of previously prepared DNA samples (formed by 10µl of DNA samples mixed with 2µl loading dye) were loaded into the lanes, and a 100 BP (Base pair) DNA ladder (New England Bio Labs, UK) was loaded to size the samples. Gels were run at 100 volts for 50 minutes using 1X TBE solution as a running buffer. Visualization of the PCR products on the gel was performed using an ultraviolet trans-illuminator (UVP Inc., USA), and photos were captured on a computer and printed.

2.10.4 DNA extraction from agarose gel

Desired bands of DNA with expected molecular sizes were excised from the gel under Ultra Violet (UV) light. The UV exposure time should be as short as possible to avoid DNA damage. The agarose gel slices were transferred into clean Eppendorf tubes and the DNA molecules were purified using a gel band purification kit. Briefly, after the gel slice was weighed, 3 volumes of buffer were added to 1 volume of gel and incubated at 50ºC-60ºC for 10 minutes and mixed every 2-3 minutes until the gel dissolved in the buffer. One volume of isopropanol was added and mixed. The sample was then

transferred into a spin column and centrifuged for 1 minute and the flow-through was discarded. Next, the column was washed with 0.75ml of buffer PE and centrifuged for 1 minute, and the flow-through was discarded. Afterwards, the column was transferred into a clean collection tube (1.5ml), and the DNA was eluted by adding 50µl of buffer EB, incubating for 1minute, and centrifuging for 1 minute to collect the DNA.

2.10.5 Ligation and bacterial transformation

Following PCR, the construct containing the mutation was linear and needed ligation to produce a circular plasmid. For a typical ligation reaction, 5µl of gel-purified DNA was added to a mixture containing 2µl of a 10x ligase buffer (Invitrogen) and 1µl of a ligase enzyme (Invitrogen) in 1.5 ml Eppendorf tubes. The final volume of the reaction was completed to 10µl with Nuclease-free water. The mixture without the ligase enzyme was used as a control and the tubes were incubated at 4°C overnight.

To grow the CD24 expression construct, half of the ligated product (5µl) was transformed into NEP-5 alpha chemically competent E. coli cells (Bio-lab) using the manufacturer's instruction manual. Briefly, 5µl of the ligated reaction were added into a vial of One NEP-5 alpha chemically competent E. coli (50µl) and mixed gently. The reaction was then incubated on ice for 30 minutes, the contents of the vial were heat-shocked for 45 seconds at 42°C without shaking, and then they were immediately transferred to ice for 5 minutes, and 250µl of a room temperature S.O.C. medium (Invitrogen, Catalog No. 15544-034) was added. The tube was tightly closed and shaken horizontally (200 rpm) at 37°C for 1 hour. To ensure that at least one plate would have well-spaced colonies, 60µl from each transformation reaction was spread on a LB (Luria

broth) agar plate containing the appropriate selection of antibiotic to allow propagation of bacteria containing the plasmid (i.e. 50µg/ml ampicillin). The remaining volume (240µl) was spread on another plate. The plates were incubated overnight at 37°C and examined the following morning for the presence of colonies.

2.10.6 DNA isolation and plasmid Mini-prep

Twenty-four hours after incubation of the ligation reaction on the LB agar plates, colonies were picked and cultured overnight in 5 ml of LB containing 50µg/ml ampicillin. The plasmid DNA was isolated from the samples using a GenElute™ Plasmid Mini-Prep kit (Sigma Aldrich). In brief, 5 ml of the culture were pelleted by centrifugation at 13000rpm for 1 minute. The supernatant was discarded, and the pellet was completely re-suspended with 200µl of the re-suspension solution (which is supplied with the kit). The contents were vortexed and pipetted vertically to thoroughly re-suspend the cells until the mixture was homogeneous. To release the DNA, the re-suspended cells were lysed by adding 200µl of the lysis solution, and the contents were immediately mixed by gentle inversion (6–8 times) until it became clear and viscous. A neutralization/binding solution was subsequently added to terminate the lysis reaction and the precipitate, and the cell debris was pelleted by centrifuging at 13000 rpm for 10 minutes. Column preparation solution was then added to each mini-prep column and centrifuged at 13000rpm for 1 minute. The supernatant from the lysis reaction (containing the plasmid) was added to a GenElute Mini-Prep binding column and centrifuged at 13000 rpm for 1 minute. After discarding the flow-through, 750µl of wash solution was added to the column and centrifuged at 13000 rpm for 1 minute. The flow-through was discarded and samples were centrifuged at maximum speed for 2 minutes. Finally, the plasmid DNA was eluted by adding 50µl of DNAase-RNAase-free water to the column and centrifuged at

13000rpm for 1 minute. The quantity and purity of the eluted plasmid were checked using a Nano Drop ND-1000 spectrophotometer. A ratio of 1.8–2.0 was considered an indication of relative purity and gel electrophoresis for checking the size and quality of DNA.

2.10.7 Mutation screening by High resolution melting (HRM)

HRM was performed to screen the plasmids for mutations prior to sequencing. The samples were run in duplicate and a wild-type CD24 was also tested for comparison. A PCR was initially performed on a 50 µl volume reaction containing 5 µl of a 10x reaction buffer, 2 µl of a forward primer at a final concentration of 250nM, 2 µl reverse primer at a final concentration of 250nM, 1 µl dNTPs at a final concentration of 200uM, 9 µl of water, 1 µl of Pfu polymerase (2-3U/ul). The amplification reaction was as follows: initial denaturation was conducted at 95^{O}C for 2 minutes for 1 cycle followed by 35 cycles of denaturation at 95^{O}C for 20 seconds, annealing 52^{O}C for 30 seconds and extension at 72^{O}C for 15 sec/kb. The PCR product was melted using an ABI 7500 Fast System (applied bio system) with a starting temperature of 75^{O}C and a final temperature of 92^{O}C. The difference plot was generated after assigning the wild-type as a control and temperature shifting 4 % difference in fluorescence between test and control was used to separate out the wild-type samples from mutants. The data were analysed using an ABI 7500 Fast system (applied bio system).

2.10.8 Direct sequencing

The direct sequencing was performed in QMC D-96 (Deep sequencing) to confirm the presence of the mutation in the two sites of N-glycosylation of CD24 and deletion mapping of CD24. Combination of T7 forward primer and BGH reverse primer (vector primers) were used to sequence the mutation of CD24. The result of the sequencing were analysed using the *finch TV* software which is freely available at the website http://finchtv.software.informer.com

2.11 Mutation profiling

2.11.1 PCR

Cell line identities were verified by HRM mutation profiling of commonly mutated genes in CRC. Nested PCR was first used to amplify the region around the targeted mutation. An initial multiplex PCR was performed comprising Hotshot Diamond master mix, 188 nM of each outer primer (table 2-6) and 20 ng template in a 20 µl reaction. The reaction was run on the Primus 96 thermocycler with a run cycle comprising a holding step of 95ºC for 5 minutes, 30x (95˚C for 10 seconds/55˚C for 30 seconds/72˚C for 20 seconds). The PCR product was diluted 1:100 with nuclease free H_2O and used as template for the subsequent PCR reaction.

A second PCR reaction was performed using primers internal to the primers from the first reaction. PCR reactions were performed for each inner primer pair with a reaction comprising Hotshot Diamond master mix, 10% Eva Green, 250 nM of forward and reverse primers and 20% template in a volume of 10 µl. The PCR was again performed on the Primus 96 thermocycler with a holding step of 95˚C for 5 minutes followed by 30x (95˚C for 1 second/55˚C for 1 second) with an extension of 72ºC for 2 minutes for *PIK3CA*, TP53, *BRAF* and *PTEN*. The run cycle for *KRAS* comprised a holding step of

95˚C for 5 minutes followed by 30x (95˚C for 1 second/62˚C for 1 second) with an extension of 72ºC for 2 minutes. (See Appendix 2-1)

Gene	Exon	Reaction	Forward Primer	Reverse Primer
KRAS	2	Outer	TGAATATAAACTTGTGGTAGTTGG	GCTGTATCGTCAAGGCACTCT
		Inner	ATATAAACTTGTGGTAGTTGGAG	TATCGTCAAGGCACTCTTGC
PIK3CA	20	Outer	TGAGCAAGAGGCTTTGGAGT	CCTATGCAATCGGTCTTTGC
		Inner	GCAAGAGGCTTTGGAGTATTTC	TTTTCAGTTCAATGCATGCTG
BRAF	11	Outer	TGTTTGGCTTGACTTGACTTT	CTTGTCACAATGTCACCACATTACATA
		Inner	GACGGGACTCGAGTGATGAT	TGTCACAATGTCACCACATTACA
	15	Outer	ATCTACTGTTTTCCTTTACTTACTACAC	CAGCATCTCAGGGCCAA
		Inner	TGTTTTCCTTTACTTACTACACCTCA	CCACAAAATGGATCCAGACA
PTEN	3	Outer	TCATTTTTGTTAATGGTGGCTTT	ACTCTACCTCACTCTAACAAGCAGA
		Inner	GGCTTTTTGTTTGTTTGTTTTG	CCTCACTCTAACAAGCAGATAACTTTC
TP53	6	Outer	AGGCCTCTGATTCCTCACTGAT	ACCCTTAACCCCTCCTCCCA
		Inner	CCTCTGATTCCTCACTGATTGC	CTTAACCCCTCCTCCCAGAG

Table 2-9 : *Mutation profiling primer sequences.*

2.11.2 High resolution melting

PCR products were melted using a light scanner system. Ten µl of the PCR product was added to 10 µl of mineral oil and melted over a range of 68-95ºC (68-98ºC for *TP53*) with a temperature increase of 0.3ºC /second. The melt curves were analysed using a Light Scanner Instrument and Analysis software package (version 2.5.0.3057). A known wild type cell line was used as a reference sample and melt curves displaying >4% change in fluorescence were considered to contain a mutation (see Appendix 9.3).

2.12 Functional studies

2.12.1 Presto blue proliferation assay

A 4-day time course assay for proliferation using presto blue was used. Presto blue is used to measure the metabolic activity of cells in liquid media and was performed after forced expression of the various constructs. Since it is a viable dye, it allows the same cells to be measured repeatedly. Each well of 24 well plates were seeded with $2x10^4$ cells for 24 hours after transfection. On the following day, the media was removed and replaced with 400ul of presto blue reagent and incubated for one hour at 37^oC. Next, 100ul of each well in triplicate were transferred into 96 well plates for measuring the fluorescence of cell viability using BMG FLUOstar Optima Plate reader (495/10, 580/40). The Fluorescence readings were normalised to the 0 hour time point. Assays were performed in triplicate on at least two different occasions.

2.12.2 Cell migration assay

Cell migration was tested using a trans-well migration assay; it uses a Boyden chamber, 24 Trans-well inserts (Costar, Corning, NY,

USA) with 6.5 mm diameter, and a polycarbonate membrane of 8-µm pore size. Six hundred µl of DMEM supplemented with 20% FCS was added in the lower chamber. In the upper chamber, 5 X 10^4 to 2 X 10^5 cells (depending on the cell line type) were suspended in 100µl of DMEM with 10% FBS. Migration was assessed after 24 to 48 hours and single cells, which had migrated through the membrane to the lower chamber, were counted visually by an inverted microscope. Assays were performed in triplicate on at least two different occasions.

2.12.3 Matrigel invasion assay

Cell invasion was measured in the same way as described for cell migration assays in section 2.5.2. However, in the Matrigel invasion assay, the upper chamber was prepared by coating the filter membrane with 100µl of Matrigel (Basement Membrane Matrix, Growth Factor Reduced, BD Biosciences, UK), the stock concentration of Matrigel was 6.9 mg/ml and it was used at 1:3 dilution in serum-free medium. The Matrigel is left to thaw overnight, incubated at 4^{o}C on ice. The pipette tips and tubes used were pre-cooled to prevent Matrigel solidification during the procedure. After coating, the plates were incubated at 37^{o}C in an incubator to allow gelling of the Matrigel for 4 hours. A range of 1 X 10^5 to 2 X 10^5 cells (differs with the cell line type) were suspended in 100µl of DMEM with 10% FBS and added over the Matrigel in the upper chamber. After 24 to 48 hours, the cells at the bottom of the well were counted visually by the microscope, averaged, and compared among several groups. Assays were performed in triplicate and on at least two separate occasions.

2.13 Statistical analysis

In the functional assays, results were displayed as the mean ± standard deviation (SD). Statistical analyses were performed using unpaired two-tailed T-test (Graph Pad software) and a one-way ANOVA test. The differences were defined as significant if the P-values were < 0.05.

3. Investigating the role of N-glycosylation in the regulation of CD24 function

3.1 Introduction

In this chapter, we investigated the functional domains of the CD24 protein. CD24 is heavily glycosylated due to both N- and O-glycosylation. Whilst there are numerous O-glycosylation sites, CD24 contains only two asparagine residues – N36 and N52 – which are located in the potential N-glycosylation target motif of Asn-X-Ser/Thr (N-X-S/T, Figure 3-1).

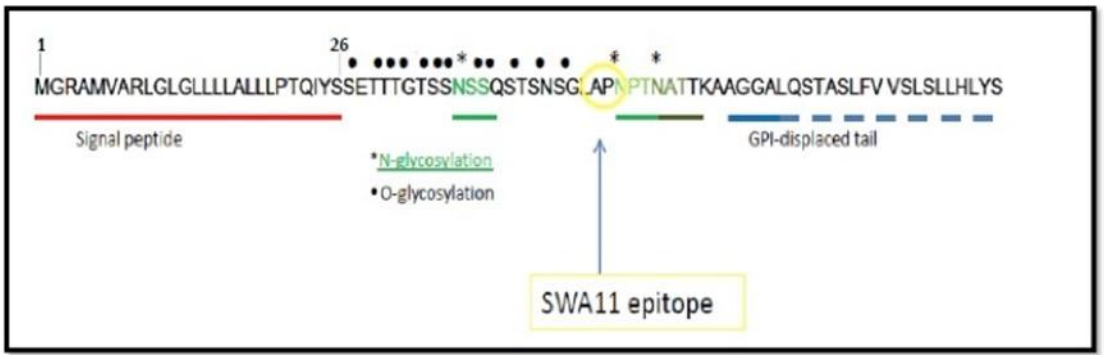


Figure 3-1 : Simplified model structure of CD24 glycosylation [68].
This model structure illustrates the potential site of N-glycosylation with asterisk marks.

In order to investigate the possible role of these residues, mutations were induced in CD24. Site directed mutagenesis (2.10) was used to convert the target asparagine residues (N36 and N52) to glutamate (Q36 and Q52). Each residue was mutated individually to create the constructs pCCD24^{N36Q} and pCCD24^{N52Q} and both residues were mutated together to create the construct pCCD24$^{N36, 52Q}$. These constructs were ectopically expressed in CRC cell line with low/negative CD24 expression (HCT116). The functional activity of these constructs was compared with ectopically expressed wild type CD24 pCCD24^{WT}, and empty vector pCEVC. Assays employed in this chapter were an *in vitro* assessment of cell number by presto blue cell proliferation, migration assay, and Matrigel invasion assay.

Aims of the study:

Mutate the N-glycosylation sites individually and together

3.2 Result

3.2.1 Construction of pCCD24^{N36Q} plasmid

Gradient PCR

In order to create the expression vector pCCD24^{N36Q}, site directed mutagenesis was used. PCR was performed on pCCD24^{WT} using a primer which had been modified to induce this mutation. To make the mutation, the first step was to optimise the primers. This was performed by gradient PCR and confirmed by gel electrophoresis. The tested primers were able to produce specific products over a wide range of temperatures. However, the primer showed the clearest band at 57°C which was used as annealing temperature in the further tests, as shown in Figure 3-2:

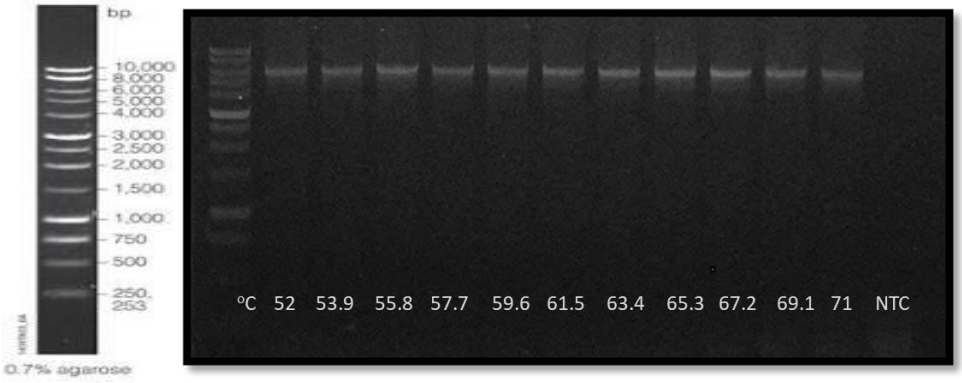


Figure 3-2: PCR optimization of pCCD24^{N36Q} primer.

Gel electrophoresis of PCR product form gradient temperature PCR showed specific single band over a wide range of temperatures range (52°C to 72 °C). However, the annealing temperature of 57 °C was chosen in the further tests. NTC (no template control) showed no amplification.

Following the optimization step, the standard PCR technique was used to amplify a full-length plasmid with CD24 (5.747 kb)

Standard PCR

In order to amplify the desired PCR product the CD24 IMAGE clone (accession number BC064619) was used as a template. After running the PCR, the result showed one discrete band at the size of the plasmid (5.747 kb). The Analysis of PCR product on 1% agrose gel showed a product of the expected size (5.747kb) as shown in Figure 3-3

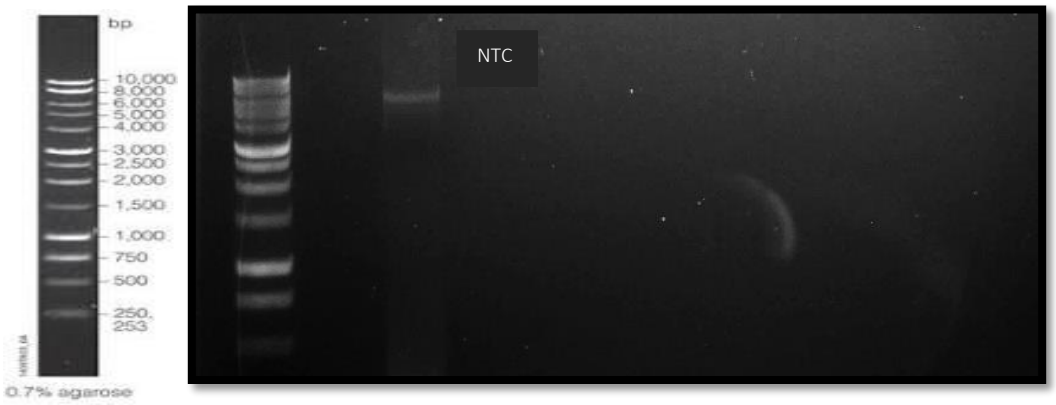


Figure 3-3 : PCR product of primers for creating pCCD24^{N36Q}.

The gel used was 1% agarose gel. The primers were able to produce discrete one clear band. There was no amplification in NTC (no template control).

After visualizing the desired band on the gel, gel extraction of PCR product using a QIAGEN extraction kit was performed as mentioned in the material and Method section (2.10.4). Following the extraction step, the ends of PCR product were ligated with a T4 ligase enzyme, ligase buffer, and nuclease-free water. The ligation product was transformed into NEB 5-alpha Competent *E. coli* (high efficiency) cells. After transformation and then growing colonies on LB agar plates, the resultant colonies were picked and regrown overnight in a LB broth with selective antibiotics and the resultant bacterial growth was used in plasmid mini-prep for purification of Plasmid DNA. To determine the quality and size of the DNA, the plasmids were analysed on 1% agrose gel, as shown in Figure 3-4:

Analysing the extracted plasmid

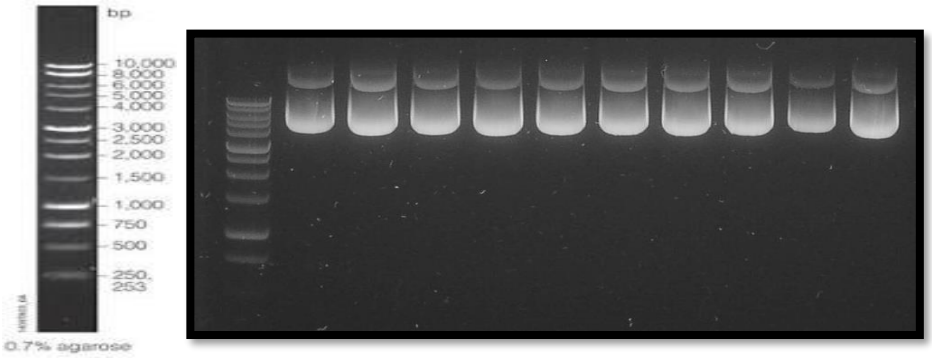


Figure 3-4: Gel electrophoresis of the ten the extracted plasmids.

The 10 plasmids were tested after plasmid Miniprep to check integrity of the plasmids. The ten plasmids showed the right size band (5.747 kb).

Mutation detection by HRM

HRM (High Resolution Melting) was used to screen for the presence of mutation in the plasmids. Primers were designed to amplify the region pCCD24^{N36Q} of the plasmid. The principle of HRM is that different DNA sequences will melt at different temperatures. Thus it should be possible to discriminate wild-type from mutant sequence by the melting pattern of the DNA.

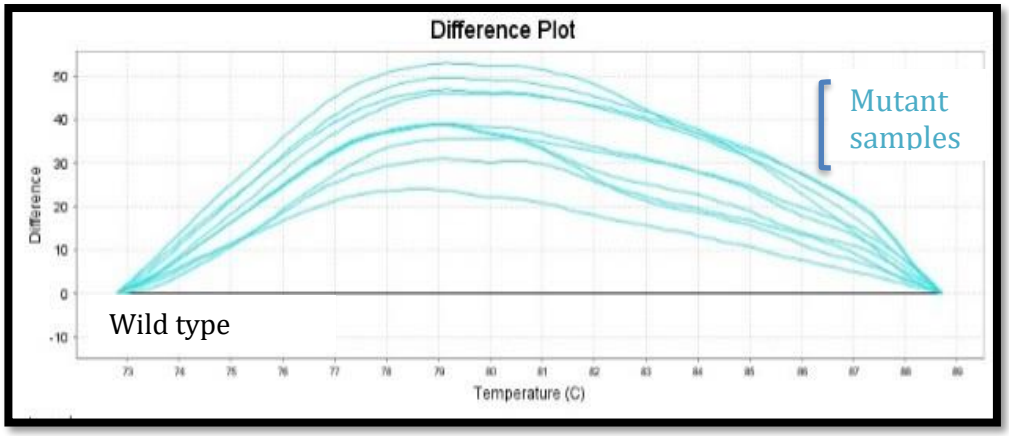


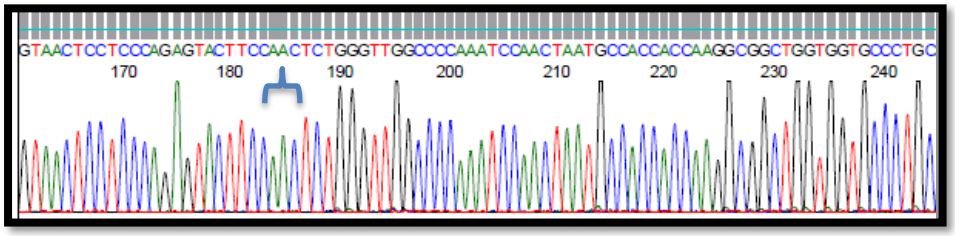
Figure 3-5: The HRM result and the comparison of the wild type and pCCD24^{N36Q} .

Difference plot shows mutant samples (Turquoise) clearly segregated from the wild type reference (Black). Mutant sample carries mismatch makes the DNA molecule less thermodynamically stable and hence melt earlier than the wild type.

Sequencing of pCCD24^{N36Q}

After using the HRM as a screening method to identify mutant plasmids, five plasmids were sequenced to confirm the presence of the mutation. Two sequencing primers were used (i.e. a T7 forward and a BGH reverse primer). Sequencing results were analysed using *finch TV* software, which revealed there is a change of the amino acid Asparagine to Glutamine. As shown in Figure 3-6:

pCCD24^{WT}



pCCD24^{N36Q}

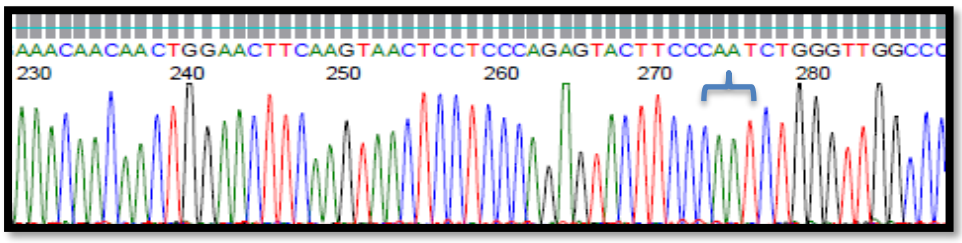


Figure 3-6: Sequencing of pCCD24^{N36Q} .

Sequencing confirmation of changing the amino acid residue Asparagine 36 (AAC) to Glutamine (CAA).

The resultant sequence was aligned with alignment tool by NCBI (https://blast.ncbi.nlm.nih.gov/Blast.cgi) to show the sequence differences, the result showed that, 99% similarity sequence as shown in figure 3-7. This confirmed that no other mutations had been introduced into the coding sequence.

Coding sequence CD24

Identities **Gaps**

245/247(99%) 0/247(0%)

```
Query  1    CACCATGGGCAGAGCAATGGTGGCCAGGCTCGGGCTGGGGCTGCTGCTGCTGGCACTGCT  60
            ||||||||||||||||||||||||||||||||||||||||||||||||||||||||||||
Sbjct  1    CACCATGGGCAGAGCAATGGTGGCCAGGCTCGGGCTGGGGCTGCTGCTGCTGGCACTGCT  60

Query  61   CCTACCCACGCAGATTTATTCCAGTGAAACAACAACTGGAACTTCAAGTAACTCCTCCCA 120
            ||||||||||||||||||||||||||||||||||||||||||||||||||||||||||||
Sbjct  61   CCTACCCACGCAGATTTATTCCAGTGAAACAACAACTGGAACTTCAAGTAACTCCTCCCA 120

Query  121  GAGTACTTCCAACTCTGGGTTGGCCCCAAATCCAACTAATGCCACCACCAAGGCGGCTGG 180
            |||||||||| | ||||||||||||||||||||||||||||||||||||||||||||||
Sbjct  121  GAGTACTTCCCAATCTGGGTTGGCCCCAAATCCAACTCAGGCCACCACCAAGGCGGCTGG 180

Query  181  TGGTGCCCTGCAGTCAACAGCCAGTCTCTTCGTGGTCTCACTCTCTCTTCTGCATCTCTA 240
            ||||||||||||||||||||||||||||||||||||||||||||||||||||||||||||
Sbjct  181  TGGTGCCCTGCAGTCAACAGCCAGTCTCTTCGTGGTCTCACTCTCTCTTCTGCATCTCTA 240

Query  241  CTCTTAA  247
            |||||||
Sbjct  241  CTCTTAA  247
```

Figure 3-7 : Blast 2 analysis of pCCD24^{WT} and pCCD24^{N36Q}.

Blast 2 analysis was used to compare the sequence result of pCCD24^{N36Q} (the query) with pCCD24^{WT}. The result showed 99% similarity when aligned using the NCBI alignment tool.

3.2.2 Construction of pCCD24^{N52Q} plasmid

Gradient PCR

For construction of pCCD24^{N52Q} plasmid, the methodology was repeated as above. The gradient PCR was used to optimise the primer as above. However, the primer showed the clearest band at 59.6°C which were used as annealing temperature in the further tests, as shown in Figure 3-8

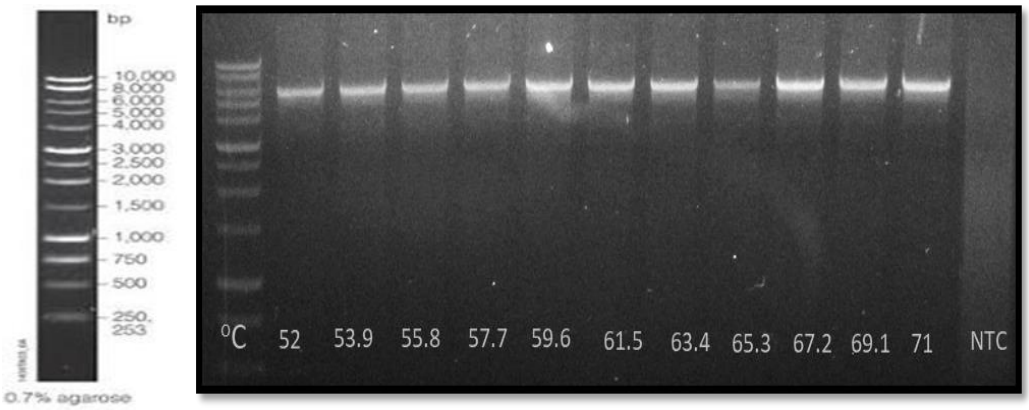


Figure 3-8 : PCR optimization of pCCD24^{N36Q}.
Gel electrophoresis of PCR product form gradient temperature PCR showed specific single band over a wide range of temperatures range (52°C to 72 °C). However, the annealing temperature of 59.6 °C was chosen in the further tests. NTC (no template control) showed no amplification.

Standard PCR

The standard PCR technique was used to amplify a full-length plasmid with CD24 (5.747 kb) as above. Figure 3-9

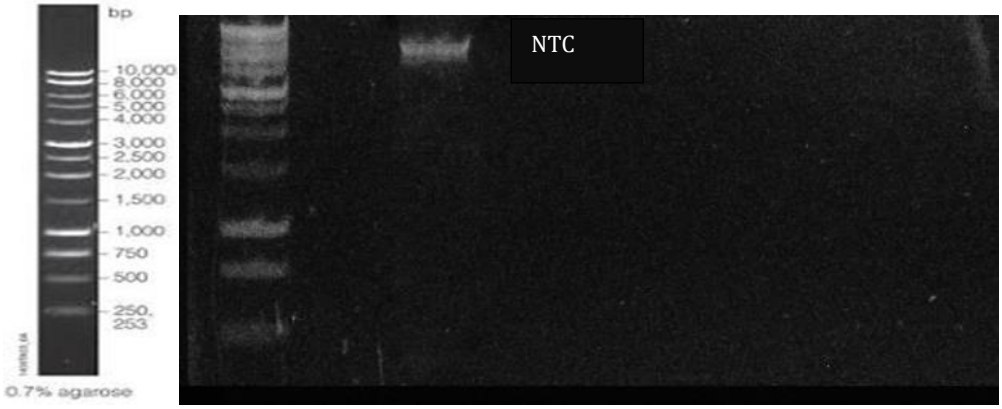


Figure 3-9 : PCR product of primers for creating pCCD24^{N52Q}.

The gel used was 1% agarose gel. The primers were able to produce discrete one clear band. There was no amplification in NTC (no template control).

Analysing the extracted plasmid

The gel was used to check the purity and size of the plasmid as above. Figure 3-10

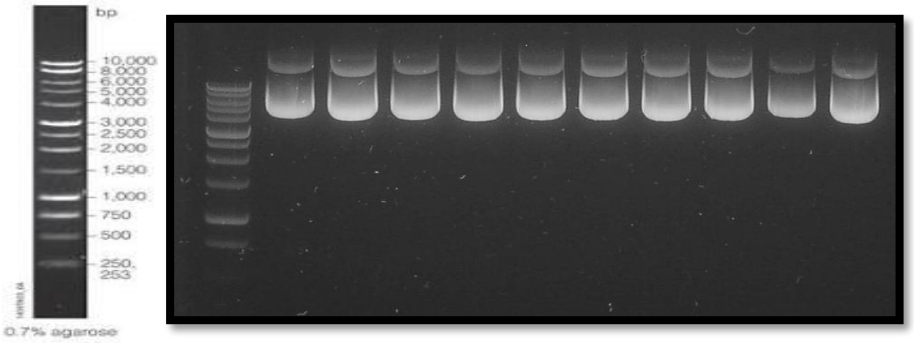


Figure 3-10 : Gel electrophoresis of the ten the extracted plasmids.

The 10 plasmids were tested after plasmid Miniprep to check the integrity of the plasmids . The ten plasmids showed the right size band (5.747 kb).

Mutation detection by HRM

To detect the mutant PCR product as above. Figure 3-11

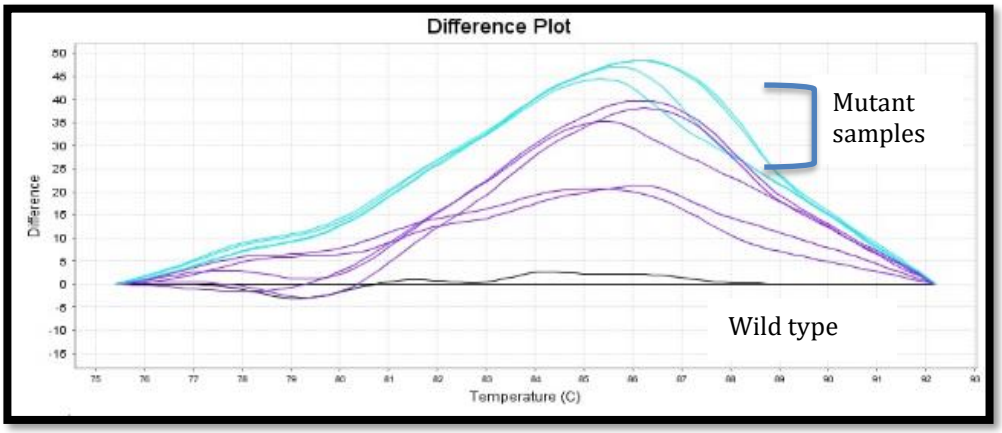


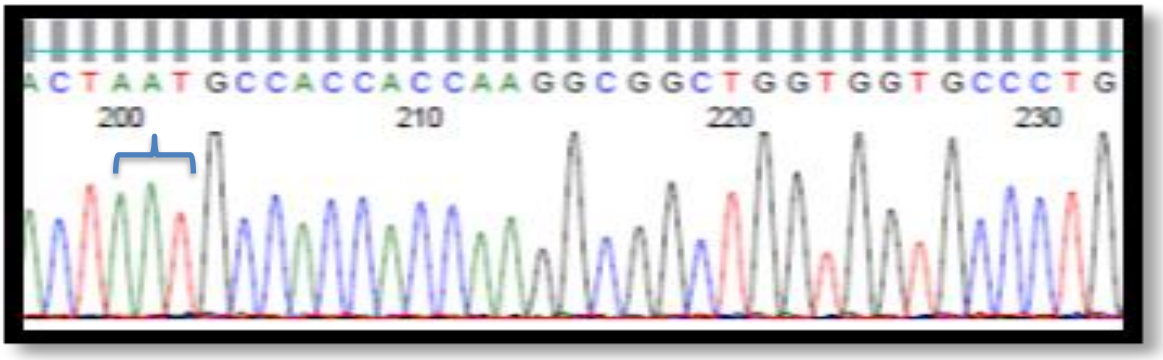
Figure 3-11 : The HRM result and the comparison of the wild type and pCCD24^{N52Q} .

Difference plot shows mutant samples (Turquoise-Purple) clearly segregated from the wild type reference (Black). Mutant sample carries mismatch makes the DNA molecule less thermodynamically stable and hence melt earlier than the wild type.

Sequencing of pCCD24^{N52Q}

For sequencing of pCCD24^{N52Q} plasmid, the methodology were repeated as above. Figure 3-12

pCCD24^{WT}



pCCD24^{N52Q}

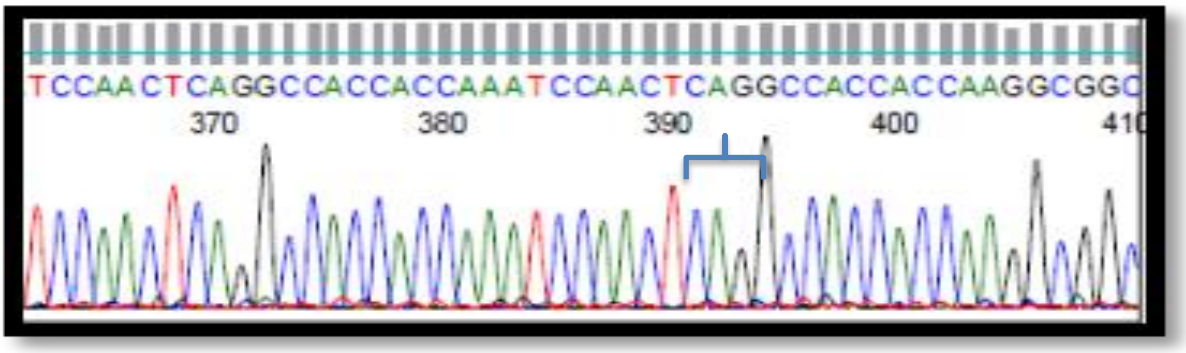


Figure 3-12 : Sequencing of pCCD24^{N52Q} .

Sequencing confirmation of changing the amino acid residue Asparagine 52 (AAT) to Glutamine (CAG).

The resultant sequence was aligned with alignment tool by NCBI (https://blast.ncbi.nlm.nih.gov/Blast.cgi) to show the sequence differences, the result showed that, 99% similarity sequence as shown in figure 3-13. This confirmed that no other mutations had been introduced into the coding sequence.

Coding sequence CD24

Identities **Gaps**

245/247(99%) 0/247(0%)

```
 Query 1    CACCATGGGCAGAGCAATGGTGGCCAGGCTCGGGCTGGGGCTGCTGCTGCTGGCACTGCT  60
            ||||||||||||||||||||||||||||||||||||||||||||||||||||||||||||
Subject  1  CACCATGGGCAGAGCAATGGTGGCCAGGCTCGGGCTGGGGCTGCTGCTGCTGGCACTGCT  60

Query  61   CCTACCCACGCAGATTTATTCCAGTGAAACAACAACTGGAACTTCAAGTAACTCCTCCCA 120
            ||||||||||||||||||||||||||||||||||||||||||||||||||||||||||||
Subject  61 CCTACCCACGCAGATTTATTCCAGTGAAACAACAACTGGAACTTCAAGTAACTCCTCCCA 120

Query  121  GAGTACTTCCAACTCTGGGTTGGCCCCAAATCCAACTAATGCCACCACCAAGGCGGCTGG 180
            |||||||||||||||||||||||||||||||||| | ||||||||||||||||||||
Subject  12 GAGTACTTCCCAATCTGGGTTGGCCCCAAATCCAACTCAGGCCACCACCAAGGCGGCTGG 180

Query  181  TGGTGCCCTGCAGTCAACAGCCAGTCTCTTCGTGGTCTCACTCTCTCTTCTGCATCTCTA 240
            ||||||||||||||||||||||||||||||||||||||||||||||||||||||||||||
Subject  18 TGGTGCCCTGCAGTCAACAGCCAGTCTCTTCGTGGTCTCACTCTCTCTTCTGCATCTCTA 240

Query  241  CTCTTAA  247
            |||||||
Subject241  CTCTTAA  247
```

Figure 3-13 : Blast 2 analysis of pCCD24^{WT} and pCCD24^{N52Q}.

Blast 2 analysis was used to compare the sequence result of pCCD24^{N52Q} (the query) with pCCD24^{WT}. The result showed 99% similarity when aligned using the NCBI alignment tool.

3.2.3 Construction of pCCD24$^{N36, 52Q}$ plasmid

Standard PCR

To mutate both N-glycosylation sites, the pCCD24^{N36Q} expression construct was used as template with the pCCD24^{N52Q} primers. Similarly, the pCCD24^{N52Q} expression construct was used as template with the pCCD24^{N36Q} primers. After running the PCR, the result showed one discrete band at the size of the plasmid (5.747 kb). Analysis of the PCR product on 1% agarose gel showed a product of the expected size (5.747 kb) as shown in Figure 3-14:

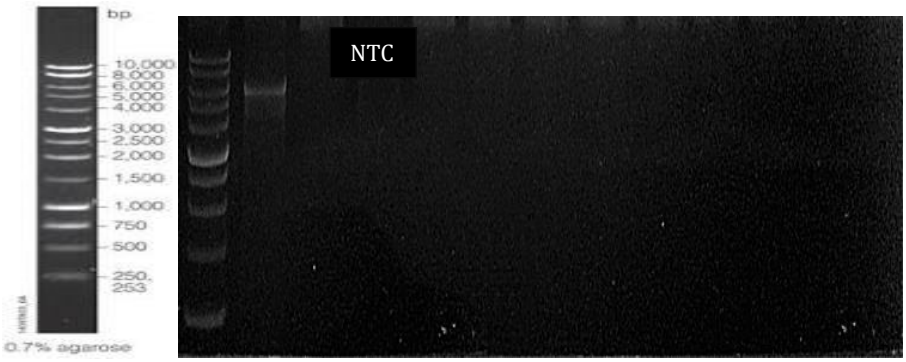


Figure 3-14: PCR product of pCCD24^{N36,52Q} .

1% agarose gel was used. The primers were able to produce a clear band. There was no amplification in NTC (no template control).

To determine the quality and size, the plasmids were analysed on 1% agarose gel, as shown in Figure 3-15:

PCR product

Analysing extracted plasmid

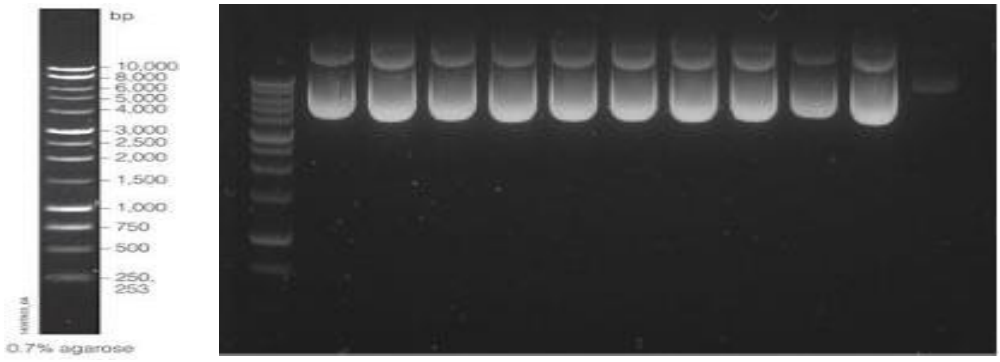


Figure 3-15: Gel electrophoresis of the ten the extracted plasmids.

The 10 plasmids were tested after plasmid Miniprep to check the integrity of the plasmids. The ten plasmids showed the right size band; in lane number 11 is PCR product as control of ligation.

Mutation detection by HRM

To detect the presence of mutant PCR product as above. Figure 3-16

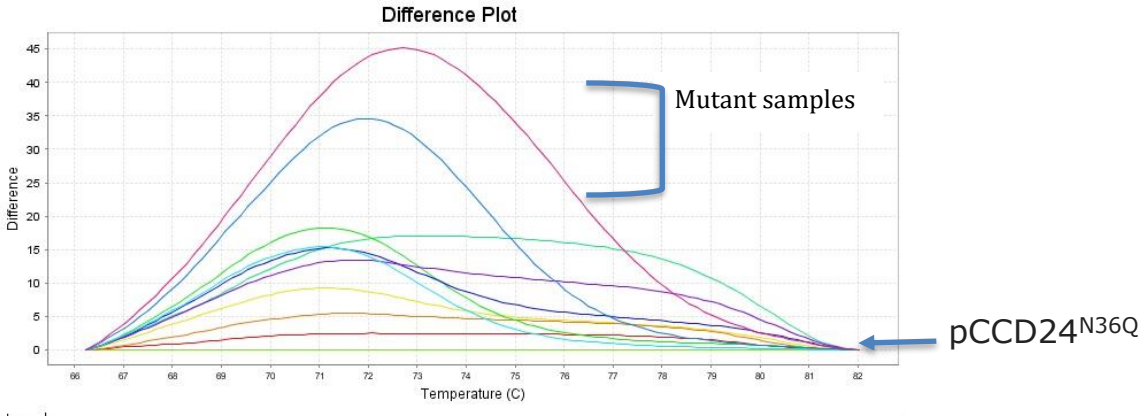


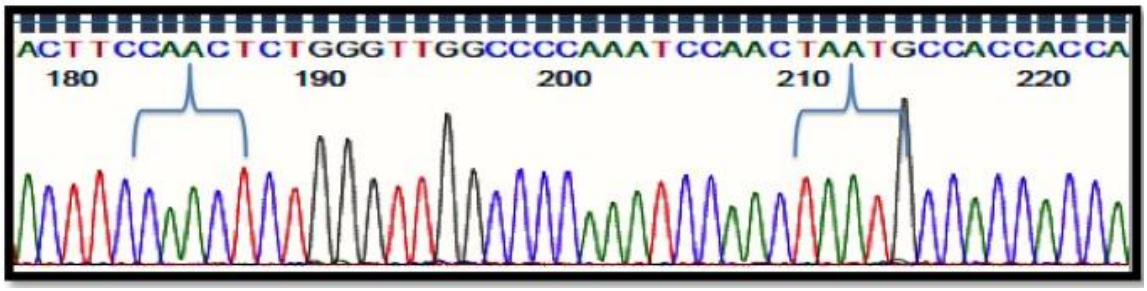
Figure 3-16: The HRM result and the comparison of the wild type and mutant .

Difference plot shows mutant samples from two sites (Purple-blue) clearly segregated from the one site mutant reference (Green). Mutant sample carries mismatch makes the DNA molecule less thermodynamically stable and hence melt earlier than the wild type.

Sequencing of pCCD24$^{N36, 52Q}$

The sequencing was used to confirm the mutation as above. Figure 3-17

pCCD24^{WT}



pCCD24^{N36,52Q}

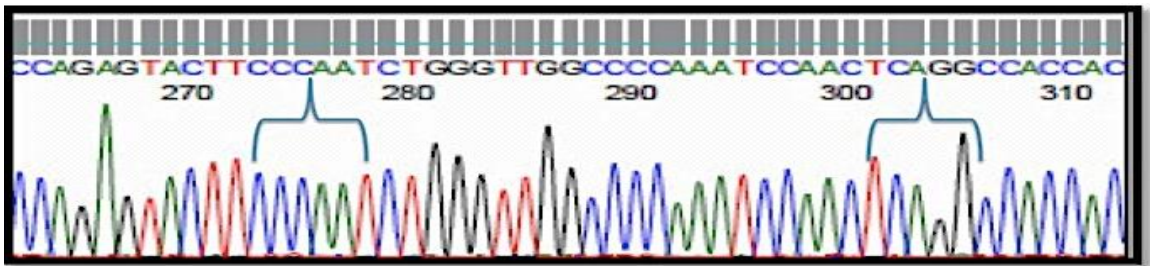


Figure 3-17: Sequencing of pCCD24$^{N36, 52Q}$.

Sequencing confirmation of changing the amino acid Asparagine in N-glycosylation sites N36-N52 (AAC, AAT) to Glutamine (CAA, CAG).

The resultant sequence was aligned with alignment tool by NCBI ((https://blast.ncbi.nlm.nih.gov/Blast.cgi) to show the sequence differences, the result showed that there was 98% similarity sequence as shown in Figure 3-18. This confirmed that no other mutations had been introduced into the coding sequence.

Coding sequence CD24
Length: 247

Identities	**Gaps**
243/247(98%)	0/247(0%)

```
Query  1    CACCATGGGCAGAGCAATGGTGGCCAGGCTCGGGCTGGGGCTGCTGCTGCTGGCACTGCT  60
            ||||||||||||||||||||||||||||||||||||||||||||||||||||||||||||
Subject  1  CACCATGGGCAGAGCAATGGTGGCCAGGCTCGGGCTGGGGCTGCTGCTGCTGGCACTGCT  60

Query  61   CCTACCCACGCAGATTTATTCCAGTGAAACAACAACTGGAACTTCAAGTAACTCCTCCCA 120
            ||||||||||||||||||||||||||||||||||||||||||||||||||||||||||||
Subject  61 CCTACCCACGCAGATTTATTCCAGTGAAACAACAACTGGAACTTCAAGTAACTCCTCCCA 120

Query  121  GAGTACTTCCAACTCTGGGTTGGCCCCAAATCCAACTAATGCCACCACCAAGGCGGCTGG 180
            |||||||||| | ||||||||||||||||||||||| | ||||||||||||||||||||
Subject  12 GAGTACTTCCCAATCTGGGTTGGCCCCAAATCCAACTCAGGCCACCACCAAGGCGGCTGG 180

Query  181  TGGTGCCCTGCAGTCAACAGCCAGTCTCTTCGTGGTCTCACTCTCTCTTCTGCATCTCTA 240
            ||||||||||||||||||||||||||||||||||||||||||||||||||||||||||||
Subject  18 TGGTGCCCTGCAGTCAACAGCCAGTCTCTTCGTGGTCTCACTCTCTCTTCTGCATCTCTA 240

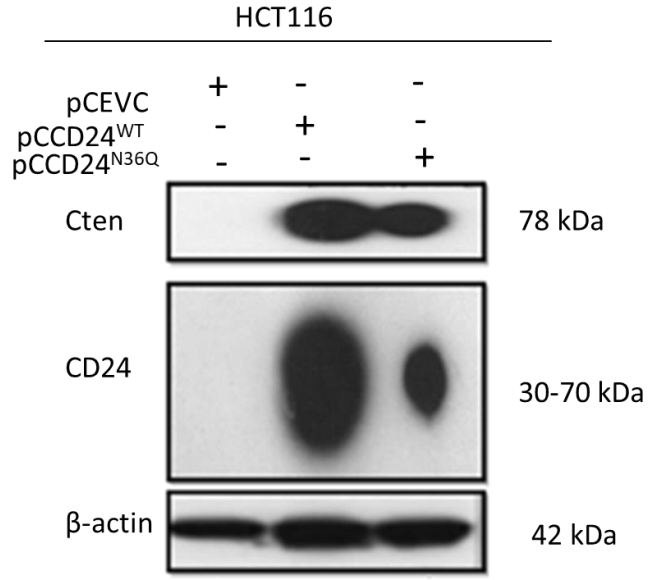
Query  241  CTCTTAA  247
            |||||||
Subject241  CTCTTAA  247
```

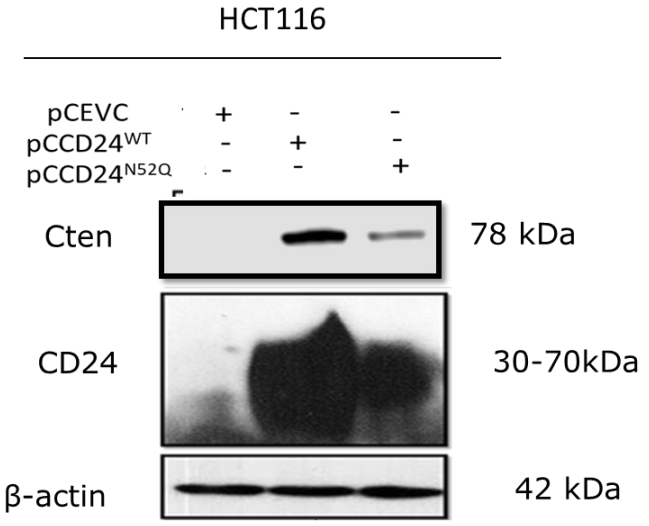
Figure 3-18 : Blast 2 analysis of pCCD24^{WT} and pCCD24^{N36,52Q}.

Blast 2 analysis was used to compare the sequence result of pCCD24^{N36,52Q} (the query) with pCCD24^{WT}. The result showed 98% similarity when aligned using the NCBI alignment tool.

3.2.4 Protein expression of pCCD24^{N36Q,} pCCD24^{N52Q}, and pCCD24$^{N36, 52Q}$

The protein expression of (pCCD24^{WT}, pCCD24^{N36Q}, pCCD24^{N52Q}, pCCD24$^{N36, 52Q}$, and the empty vector (pCEVC) was assessed 48 hours post- transfection of the expression constructs into HCT116 cell by western blot. The expression of pCCD24^{N36Q}, pCCD24^{N52Q}, and pCCD24$^{N36, 52Q}$ was compared to pCCD24^{WT} and an empty vector (pCEVC) to confirm the effect on protein level. The mutation has reduced protein expression of CD24 and Cten. Figure 3-19





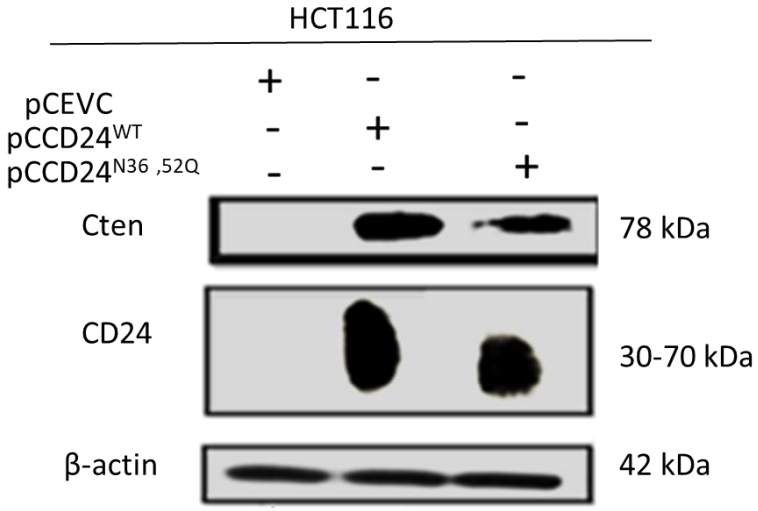
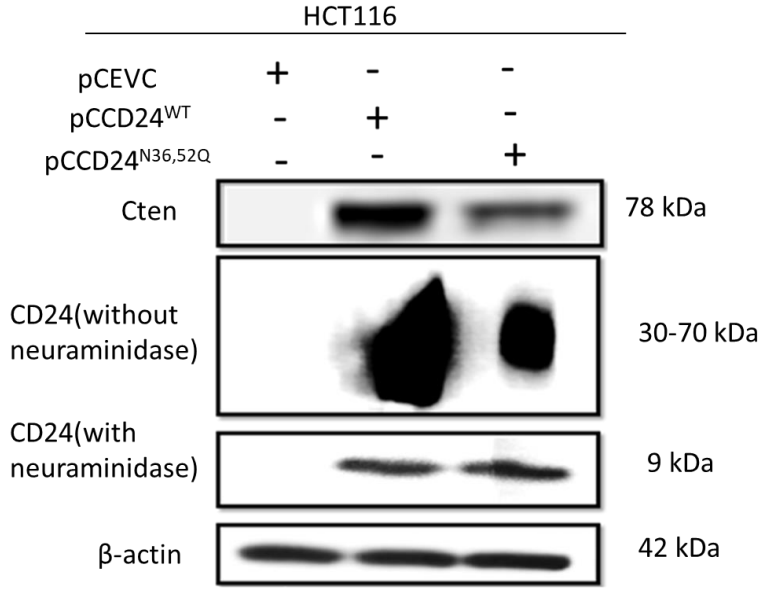


Figure 3-19: The protein expression of pCCD24^{N36,} pCCD24^{N52}, and pCCD24^{N36,52Q}

Forced expression of pCCD24^{N36,} pCCD24^{N52}, and pCCD24$^{N36,\ 52Q}$ in HCT116 to confirm the effect on protein level. The result showed in all the constructs a reduction in the mutant band compared to pCCD24$^{WT.}$

By Western blotting there appeared to be a reduction of the mutant band compared to wild type CD24. It was uncertain whether this was due to reduced transfection efficiency or due to the fact that we had removed the N-glycosylation sites of CD24. Therefore, the expression of the CD24 peptide was tested following removal of all the glycosylation with neuraminidase digestion. Removal of the glycosylation allowed a standard clean band to be visualised rather than the usual smear and showed that there was no difference in the levels of CD24 peptide between the various constructs. Another method used to obtain the transfection efficiency was by flow cytometry and the all constructs had transfection efficiency of around 30 % as shown in figure 3-20

(a)



(b)

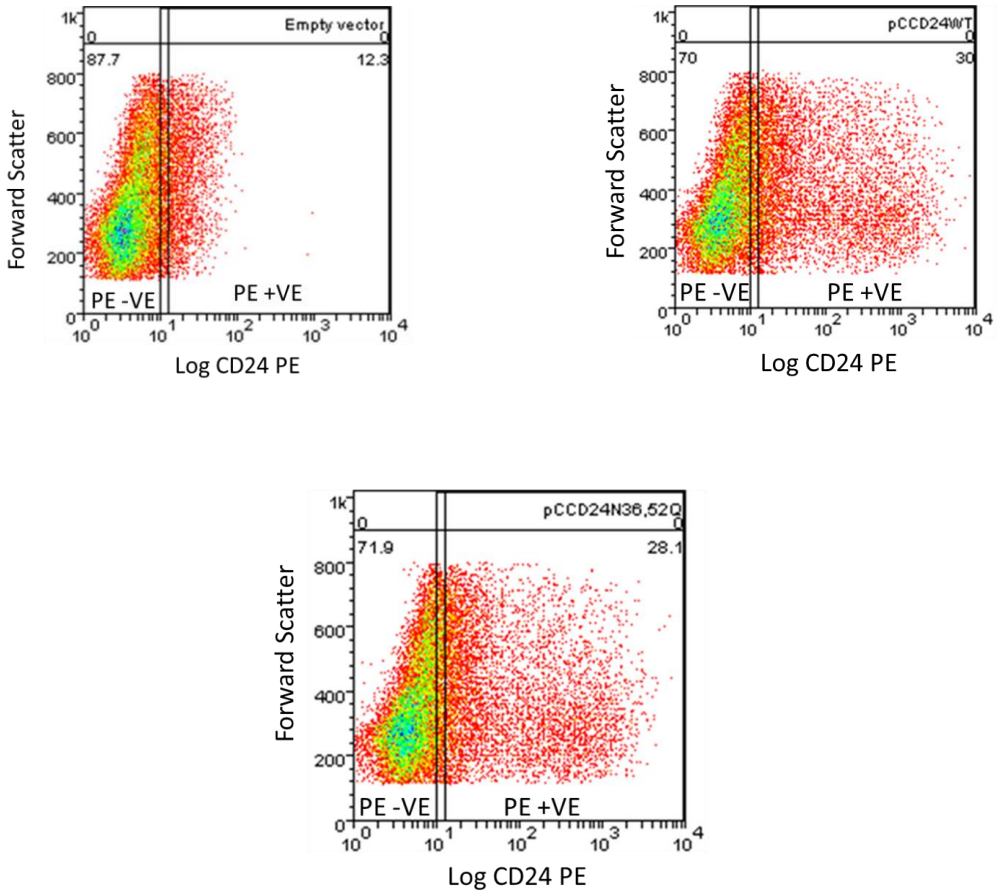


Figure 3-20 : Protein expression following neuraminidase digestion.

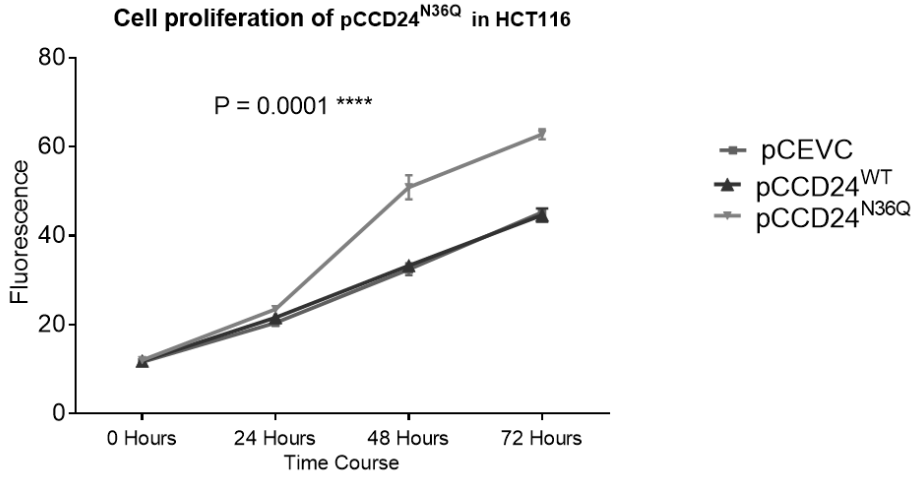
(a)Forced expression of pCCD24$^{N36,\ 52Q}$ in HCT116 followed by neuraminidase digestion to confirm the transfection efficiency. The effect of the mutant was tested on Cten which downstream target of CD24, the result that the mutation has abrogated the induction (b) the histogram from the FACS showing about 30% efficiency of the transfection using CD24-PE. The PE marker was set according to unstained control.

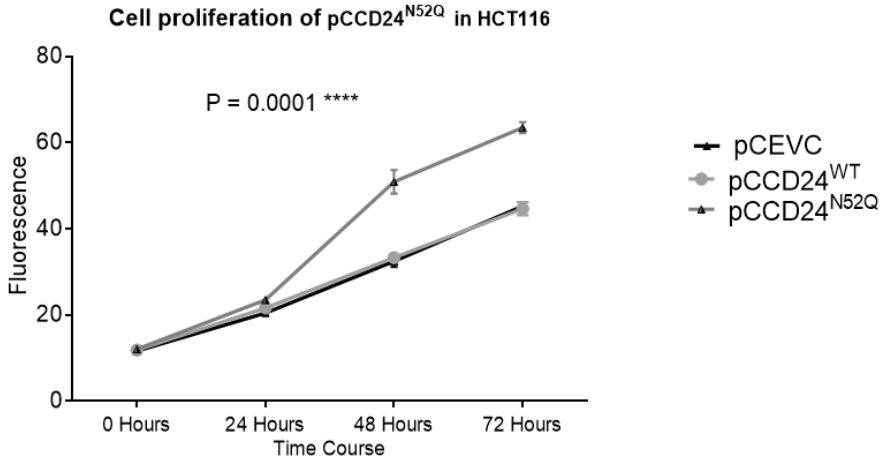
3.2.5 The oncogenic features

3.2.5.1 pCCD24^{N36Q}, pCCD24^{N52Q}, and pCCD24$^{N36,\ 52Q}$ showed highly significant on cell proliferation

We have previously shown that pCCD24^{WT} (wild-type CD24) had no effect on cell proliferation. To evaluate the functional activity of

pCCD24^{N36Q}, pCCD24^{N52Q}, and pCCD24$^{N36, 52Q}$ the effect of over-expression on cell proliferation was assessed using a 4-day time course assay. Adherent cell numbers were measured using presto blue dye fluorescence as measured by spectrophotometer. The number of viable cells in each well was measured and monitored for 4 consecutive days on 0, 24, 48, and 72 h, along with pCCD24^{WT} and empty vector control. When compared with empty vector control pCEVC and pCCD24^{WT}**,** forced expression of pCCD24^{N36Q}, pCCD24^{N52Q}, and pCCD24$^{N36, 52Q}$ in HCT116 caused a highly significant increase in the number of viable cells (P=0.0001). (Figure 3-21).





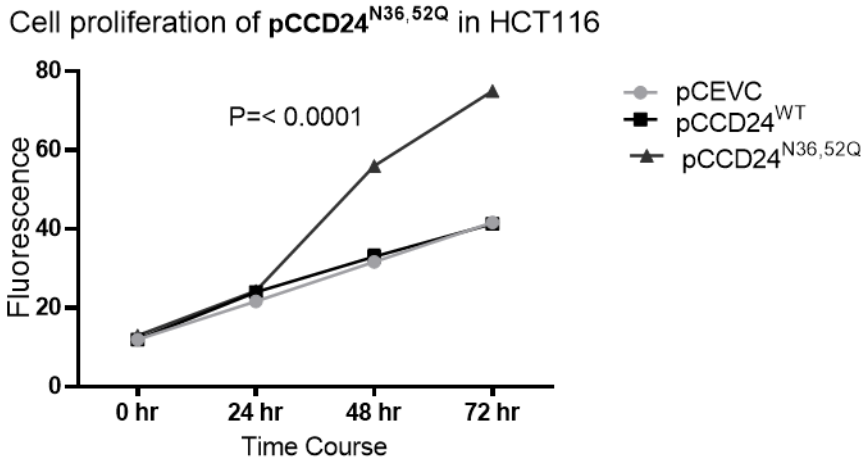


Figure 3-21 : The effect of pCCD24^{N36Q}, pCCD24^{N52Q}, pCCD24^{N36,52Q} on the cell proliferation in HCT116

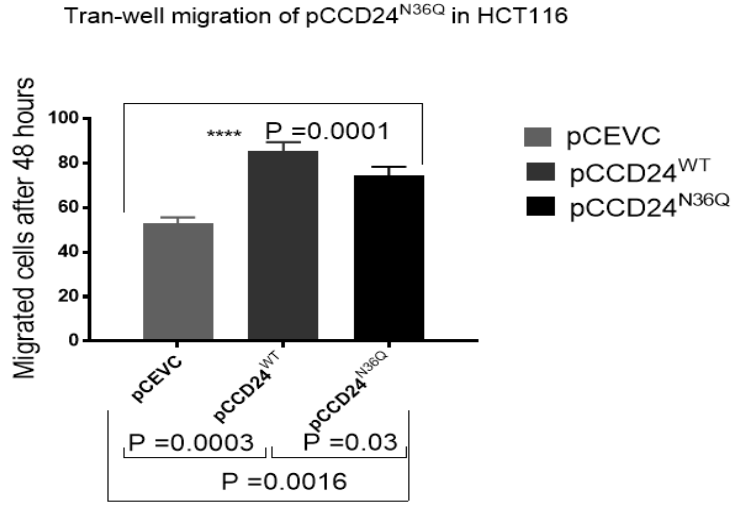
A 4-day time course assay for proliferation using presto blue after forced expression of pCCD24^{N36Q}, pCCD24^{N52Q}, and pCCD24^{N36,52Q} in HCT116 cell line, showed a highly significant effect (P=<0.0001). All values were tested by One-way ANOVA. Each experiment was repeated at least two times.

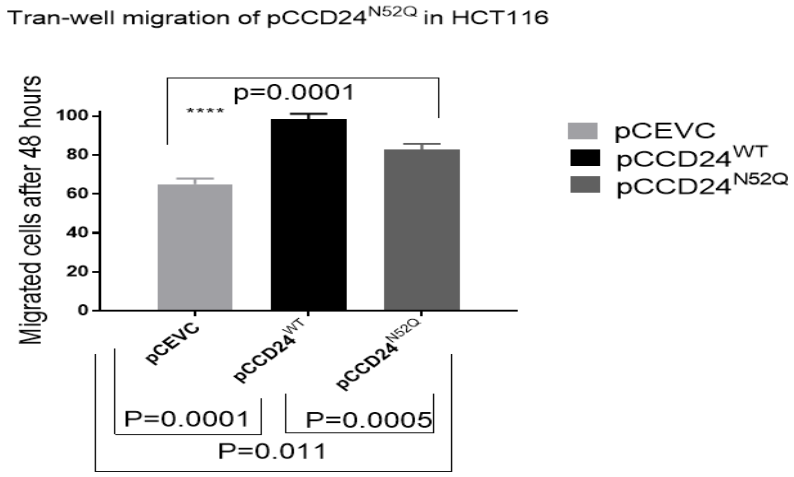
3.2.5.2 The effect of pCCD24^{N36Q}, pCCD24^{N52Q}, and pCCD24$^{N36, 52Q}$ on cell motility

We previously reported that pCCD24^{WT} (wild-type CD24) enhances cell motility. The effect of pCCD24^{N36Q}, pCCD24^{N52Q}, and pCCD24$^{N36, 52Q}$ on cell migration was assessed using trans-well migration in a Boyden chamber across the 8mM pore-size membrane. When pCCD24^{N36Q} was transfected into HCT116, compared to pCEVC, there was a stimulation of migration (p=0.0016). However, when compared with pCCD24^{WT}, the stimulation of migration by pCCD24^{N36Q} was significantly less (p=0.03) thus indicating that the loss of the N36 glycosylation site resulted in a reduction in the motility-inducing activity of CD24.

When pCCD24^{N52Q} was transfected into HCT116, the results were similar. Compared to pCEVC, there was a stimulation of migration (p=0.011). However, when compared with pCCD24^{WT}, the

stimulation of migration by pCCD24^{N52Q} was significantly less (p=0.0005) thus indicating that the loss of the N52 glycosylation site also resulted in a reduction in the motility-inducing activity of CD24. When pCCD24$^{N36,\ 52Q}$ was transfected into HCT116, the results were similar but more marked. Compared to pCEVC, there was no stimulation of migration (p=0.7183). As expected, when compared with pCCD24^{WT}, the stimulation of migration by pCCD24^{N36,52Q} was significantly less (p=0.0003) thus indicating that the loss of the N36 and N52 glycosylation sites, when together, resulted in an abrogation in the motility-inducing activity of CD24. (Figure 3-22).





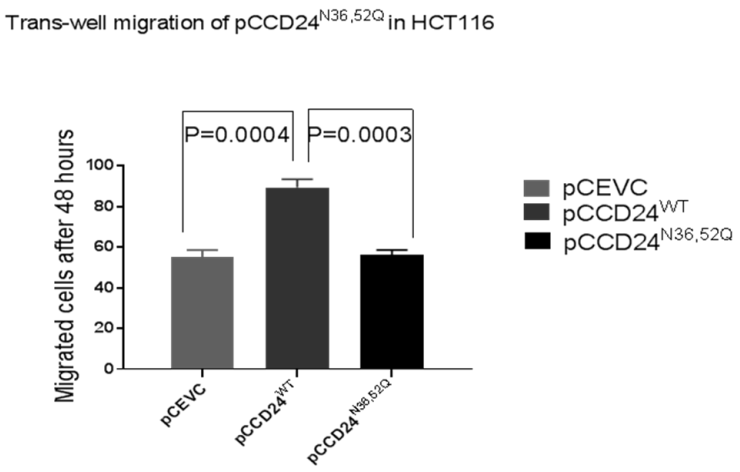


Figure 3-22 : The effect of pCCD24^{N36Q} , pCCD24^{N52Q}, and pCCD24^{N36,52Q} on the cell migration.

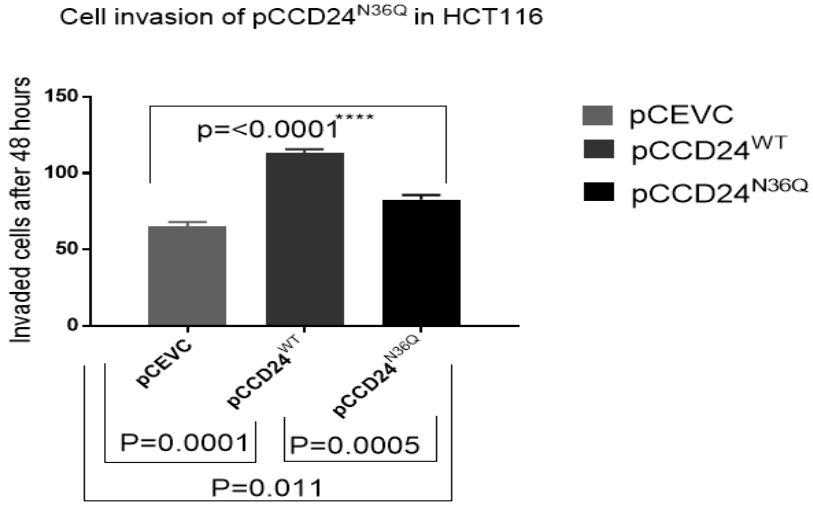
pCCD24^{N36Q,} pCCD24^{N52Q} showed a reduction in the motility inducing activity of CD24. **pCCD24$^{N36,\ 52Q}$** showed a failure to induce the cell motility. All values were tested by t-test. Each experiments was repeated at least two times

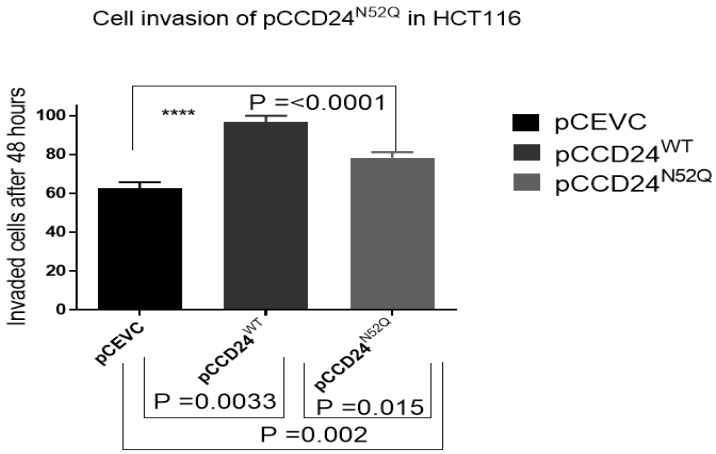
3.2.5.3 The effect of pCCD24^{N36Q}, pCCD24^{N52Q}, and pCCD24$^{N36,\ 52Q}$ on cell invasion

We previously reported that pCCD24^{WT} (wild-type CD24) enhances cell invasion. The effect of pCCD24^{N36Q}, pCCD24^{N52Q}, and pCCD24$^{N36,\ 52Q}$ on cell invasion was assessed using trans-well migration in a Boyden chamber across the 8mM pore-size membrane with a thin layer of Matrigel to the upper side of the filter. When pCCD24^{N36Q} was transfected into HCT116, compared to pCEVC, there was a stimulation of invasion (p=0.011). However, when compared with pCCD24^{WT}, the stimulation of invasion by pCCD24^{N36Q} was significantly less (p=0.0005) thus indicating that the loss of the N36 glycosylation site resulted in a reduction in the invasion activity of CD24.

When pCCD24^{N52Q} was transfected into HCT116, the results were similar. Compared to pCEVC, there was a stimulation of invasion (p=0.002). However, when compared with pCCD24^{WT}, the

stimulation of invasion by pCCD24^{N52Q} was significantly less (p=0.015) thus indicating that the loss of the N52 glycosylation site also resulted in a reduction in the invasion activity of CD24. When pCCD24$^{N36,\ 52Q}$ was transfected into HCT116, the results were similar but more marked. Compared to pCEVC, there was no stimulation of invasion (p=0.9106). As expected, when compared with pCCD24^{WT}, the stimulation of invasion by pCCD24^{N36,52Q} was significantly less (p=<0.0001) thus indicating that the loss of the N36 and N52 glycosylation sites, when together, resulted in an abrogation in the invasion activity of CD24. Figure 3-23.





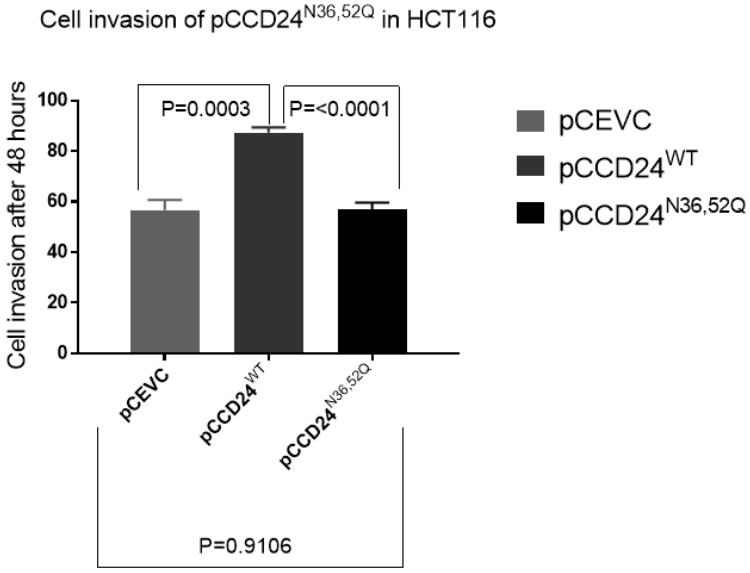


Figure 3-23 : The effect of pCCD24^{N36Q}, pCCD24^{N52Q} ,and pCCD24^{N36,52Q} on the cell invasion.

Forced expression of pCCD24^{N36Q} and pCCD24^{N52Q} **in** HCT116 showed a reduction compared to pCCD24^{WT} and empty vector pCEVC (0.005). While in pCCD24$^{N36, 52Q}$ showed a failure to induce the cells (p=0.0001). All values were tested by t-test. Each experiment was repeated at least two times.

3.3 Discussion:

The aim of this current study was to investigate the importance of the two N-glycosylation sites to CD24 function. This has been achieved through site-directed mutagenesis followed by functional assays to explore the differences between the pCCD24^{WT}, pCCD24^{N36Q}, and pCCD24^{N52Q} individually as well as pCCD24$^{N36,\ 52Q}$ combined. The mutations we induced were point mutations, which substituted one amino acid with another amino acid. The consensus sequence of N-glycosylation sites of CD24 is Asn-Xaa-Ser/Thr [133], and we changed the amino acid Asparagine to Glutamine. However, O-glycosylation sites will not be affected by these mutations as Glutamine does not bind to O-glycans [95] . According to a previous study (Mohamed Abdel Hamid, 2011) the cell lines HCT116 has no or very low CD24 expression, therefore this was chosen for transfecting the CD24 expression constructs. The functional studies included the effect of the constructs on cell proliferation, cell motility, and cell invasion.

The various constructs were created by site-directed mutagenesis, screened for mutation by HRM and mutations confirmed by sequencing. However, the band in pCCD24^{N36Q}, pCCD24^{N52}, and pCCD24$^{N36,\ 52Q}$ combined did appear to be smaller than in the pCCD24^{WT} raising the possibility of variation in transfection efficiency of the constructs and which could then confound the experiments.
However, 80% of CD24's weight is actually because of its glycosylation which causes the "smeared" effect of the protein bands and which makes notoriously difficult on the western blots.

The constructs bearing the mutated glycosylation sites showed smaller bands although it could not be ascertained whether this was due to lower levels of expression or due to lower levels of glycosylation. To test the efficiency of the transfection, we digested the protein with a neuraminidase enzyme to remove the sugar, and the results showed a band with a similar size as seen in pCCD24^{WT}, pCCD24^{N36Q}, ^{N52Q}, which confirmed the transfection's efficiency.
As a second measure, the cells transfected with the various constructs were tested by flow cytometry and all had a transfection efficiency of around 30%. This allowed us to be confident that our observations were not artefacts of transfection efficiency

Data from our lab have previously shown that pCCD24^{WT}, when transfected in CD24 negative cell lines, had no effect on cell proliferation. Similarly, in the experiments performed here, transfection of pCCD24^{WT} had no effect on cell proliferation. However, forced expression of the CD24 which had lost one or both N-glycosylation sites (pCCD24^{N36Q}, pCCD24^{N52Q} and pCCD24$^{N36, 52Q}$) in HCT116 was shown to have a significant increase in cell number compared to expression of wild type CD24 or transfection of empty vector (pCEVC). This effect was consistent in repeated experiments. The effect of the mutations to confer a proliferation inducing activity into CD24 was totally unexpected. At this stage, we do not know why this is the case and we can only guess that loss of the glycosylated residues must result in either escape from an inhibitor or, perhaps more likely, binding to a new molecule or ligand.

Cell motility (both migration and invasion) is a key feature in tumors cells' metastasis process [134]. Therefore, we investigated

the potential role of the N-glycosylation sites in the motility inducing activity of CD24. The data for both invasion and migration were similar. Ectopic expression of wild type CD24 in HCT116 was associated with an increase in cell motility when compared to the empty vector controls (pCEVC). When constructs pCCD24^{N36Q}, and pCCD24^{N52Q} were transfected into HCT116 in order to express CD24 protein which had lost one of the N-glycosylation sites, each of the constructs induced motility compared to the empty vector controls. However the level of motility induction was significantly less than that induced by wild type CD24. When HCT116 was transfected with pCCD24$^{N36,\ 52Q}$ expressing CD24 with two mutated N-glycosylation sites, the level of motility was no different to that seen in the cells transfected with the empty vector controls.

Complementing our observations with cell motility were our observations of Cten levels in HCT116. Our lab has identified Cten as a downstream motility inducing target of CD24 (unpublished data). We measured the level of Cten induction by western blot analysis and found that the mutations of the N-glycosylation sites reduced the Cten inducing activity of CD24. However, even with both sites mutated, there was not a complete abrogation. The features were reproducible over many experiments and seen with both mutations individually and combined.

It is generally considered that O-glycosylation is relevant for structural proteins whilst N-glycosylation is relevant for proteins with functional activity. Our observations are that the two N-glycosylation sites are important for CD24 function – they stimulate cell proliferation and they inhibit cell motility. At this stage we can only conjecture on the mechanism of activity. We would assume that the mutations result is loss of a ligand/receptor binding site

although the nature of the ligands/receptors is not known. P-Selectin been proposed as one possibility and this is explored in a subsequent chapter of this thesis.

So, we conclude, based on these findings that, the N-glycosylation sites are key for CD24's functions; mutation of these sites results in loss of the ability to induce the motility and invasion of cells although proliferation appears to be increased.

4. Mapping the functional sites in the regulation of CD24

4.1 Introduction

In this chapter we sought to identify other functionally important sites of CD24 within the protein in addition to the N-glycosylation sites. We therefore performed deletion mapping along the length of the CD24 protein. The mature peptide of CD24 was divided, from N-terminus to C-terminus into three segments of 7 amino acids and one segment of 4 amino acids (at the end of the mature peptide to not disturbing the GPI sequence). There were deleted using site directed mutagenesis on pCCD24^{WT} template. We created pCCD24$^{\Delta 7.1}$, pCCD24$^{\Delta 7.2}$, pCCD24$^{\Delta 7.3}$, pCCD24$^{\Delta 4.4}$ (Figure 4-1).The pCCD24$^{\Delta 7.1}$, pCCD24$^{\Delta 7.2}$, pCCD24$^{\Delta 7.3}$, pCCD24$^{\Delta 4.4}$ constructs were ectopically expressed in CRC cell lines with low/negative CD24 expression (HCT116) and compared with ectopically expressed pCCD24^{WT} and empty vector pCEVC to investigate whether any the deleted sites resulted in loss of function. The assays employed in this chapter were *in vitro* assessments of cell proliferation by presto blue and cell migration assay.

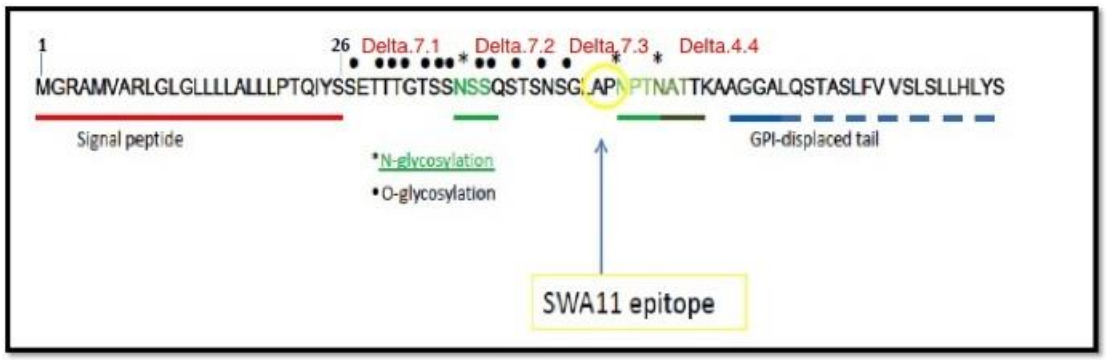


Figure 4-1: Model structure of CD24 glycosylation [68].

This model structure illustrated the mature peptide with circle above the amino acid.

Aims of the study:

Mapping the functional sites in the regulation of CD24.

4.2 Result

4.2.1 Construction of pCCD24$^{\Delta 7.1}$ plasmid.

Gradient PCR

The sequences of the primers used for site directed mutagenesis are given in the material and methods section (2.10.1). A gradient PCR was performed to optimise each of the primer pairs and to define the optimal annealing temperature. PCR products were analysed with gel electrophoresis. However, the primer showed a clearest band at 59.6°C which were used as annealing temperature in the further tests as shown in Figure 4-2.

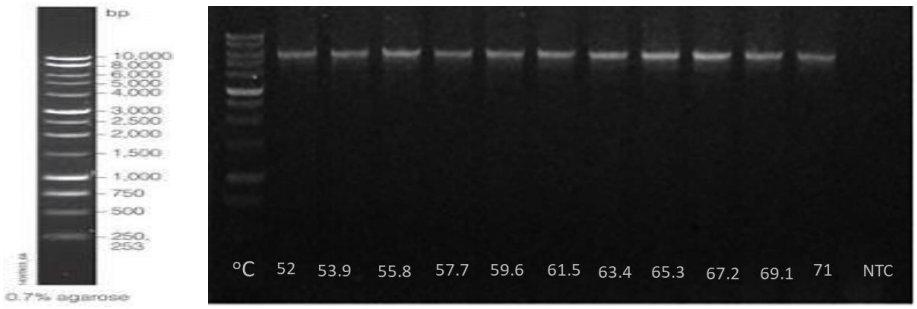


Figure 4-2: Primer optimization of pCCD24$^{\Delta 7.1}$.

Gel electrophoresis of PCR product form gradient temperature PCR showed specific single band over a wide range of temperatures range (52°C to 72 °C). However, the annealing temperature of 59.6°C was chosen in the further tests. NTC (no template control) showed no amplification.

Following visualizing the desired band on the gel, gel extraction of the PCR product was performed by using QIAGEN extraction kit as mentioned in the material and methods (2.10.4). Following the extraction step, the ends product was ligated with a T4 ligase enzyme, ligase buffer, and nuclease-free water. Afterwards, bacterial transformation and plasmid mini-prep were performed as mentioned in the material and methods (2.10.6). To determine the quality and size of plasmid, the plasmids were analysed on 1% agrose gel, as shown in Figure 4-3.

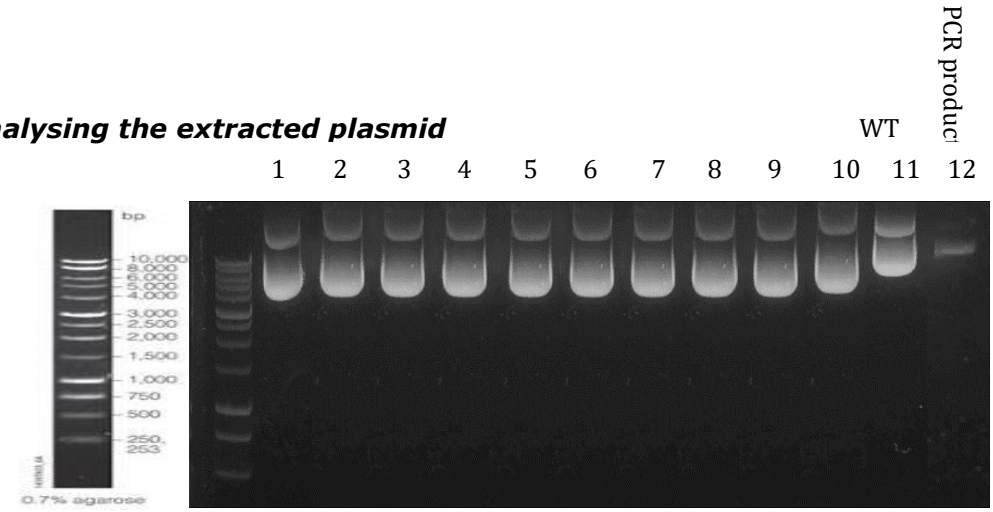


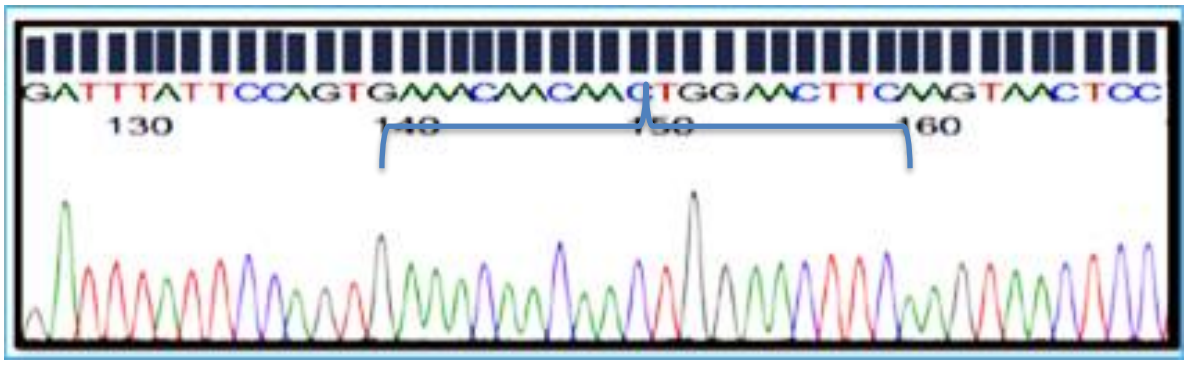
Figure 4-3: Gel electrophoresis of the ten the extracted plasmids.

The 10 plasmids were tested after plasmid Miniprep. The ten plasmids showed the right size band. Along with it wild type plasmid in lane 11 was as control of deleted plasmid and PCR product in lane 12 as control for ligation.

Sequencing of pCCD24$^{\Delta 7.1}$

Sequencing of the samples was performed to confirm the presence of the deleted amino acid of the mature peptide of CD24. Two sequencing primers were used (i.e. a T7 forward and a BGH reverse primer). Sequencing results were analysed using *finch TV* software, which revealed a deletion of seven amino acids of the mature peptide, as shown in Figure 4-4

pCCD24^{WT}



pCCD24$^{\Delta 7.1}$

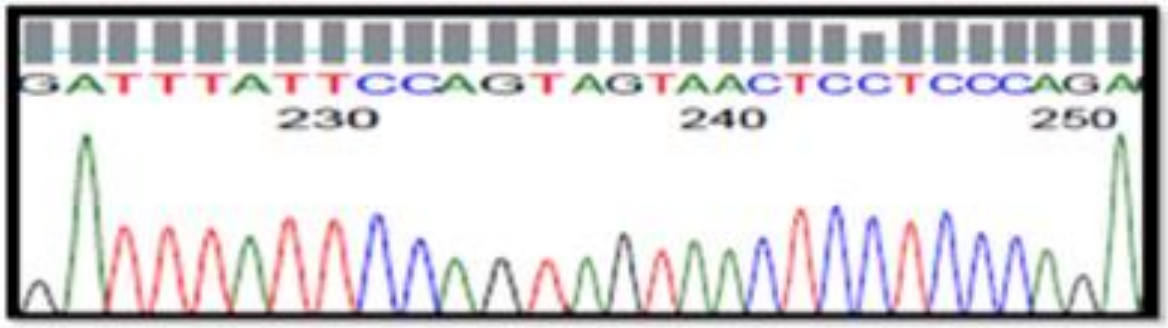
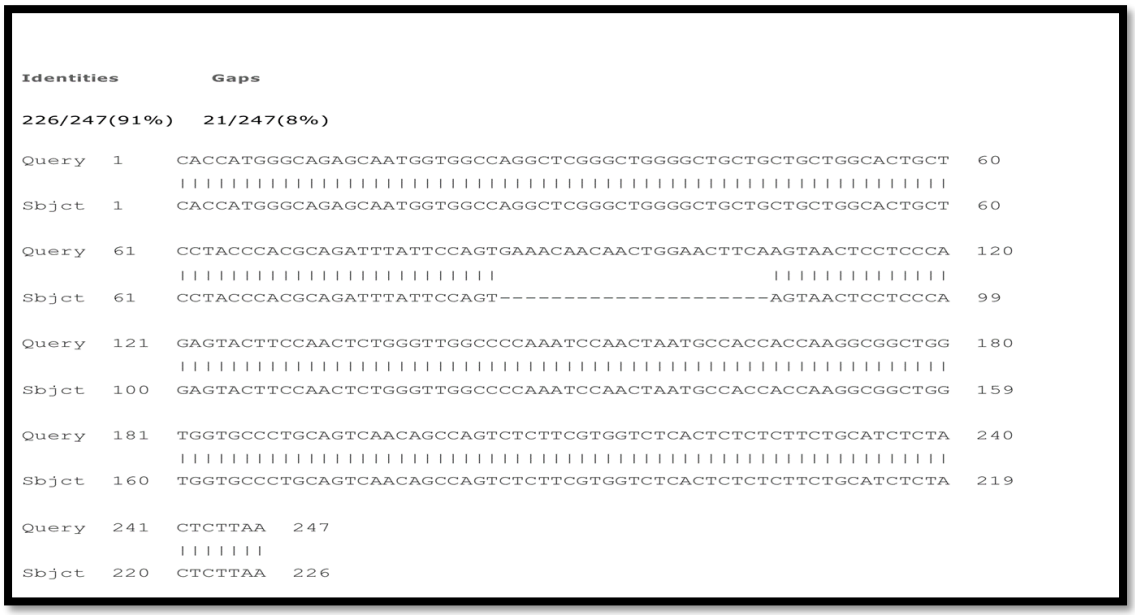


Figure 4-4 : Sequencing of pCCD24$^{\Delta 7.1}$

Sequencing confirmation of deleting seven amino acid (21 bp) as illustrated by brace.

The resultant sequence was aligned with alignment tool by NCBI https://blast.ncbi.nlm.nih.gov/Blast.cgi) to show the sequence differences, the result showed that, 91% similarity sequence. As shown in figure 4-5. This confirmed that no other mutations had been introduced into the coding sequence.

Coding sequence CD24



```
Identities        Gaps

226/247(91%)   21/247(8%)

Query  1     CACCATGGGCAGAGCAATGGTGGCCAGGCTCGGGCTGGGGCTGCTGCTGCTGGCACTGCT  60
              ||||||||||||||||||||||||||||||||||||||||||||||||||||||||||||
Sbjct  1     CACCATGGGCAGAGCAATGGTGGCCAGGCTCGGGCTGGGGCTGCTGCTGCTGGCACTGCT  60

Query  61    CCTACCCACGCAGATTTATTCCAGTGAAACAACAACTGGAACTTCAAGTAACTCCTCCCA  120
              ||||||||||||||||||||||||                      ||||||||||||||
Sbjct  61    CCTACCCACGCAGATTTATTCCAGT----------------------AGTAACTCCTCCCA  99

Query  121   GAGTACTTCCAACTCTGGGTTGGCCCCAAATCCAACTAATGCCACCACCAAGGCGGCTGG  180
              ||||||||||||||||||||||||||||||||||||||||||||||||||||||||||||
Sbjct  100   GAGTACTTCCAACTCTGGGTTGGCCCCAAATCCAACTAATGCCACCACCAAGGCGGCTGG  159

Query  181   TGGTGCCCTGCAGTCAACAGCCAGTCTCTTCGTGGTCTCACTCTCTCTTCTGCATCTCTA  240
              ||||||||||||||||||||||||||||||||||||||||||||||||||||||||||||
Sbjct  160   TGGTGCCCTGCAGTCAACAGCCAGTCTCTTCGTGGTCTCACTCTCTCTTCTGCATCTCTA  219

Query  241   CTCTTAA  247
              |||||||
Sbjct  220   CTCTTAA  226
```

Figure 4-5 : Blast 2 analysis of pCCD24^{WT} and pCCD24$^{\Delta 7.1}$.

Blast 2 analysis was used to compare the sequence result of pCCD24$^{\Delta 7.1}$ with pCCD24^{WT}. The result showed 91% similarity when aligned using the NCBI alignment tool.

4.2.2 Construction of pCCD24$^{\Delta 7.2}$ plasmid.

Gradient PCR

Gradient PCR was used to optimise the primer as described above. The primer showed the clearest band at 61.5°C which were used as annealing temperature in the further tests as shown in Figure 4-6

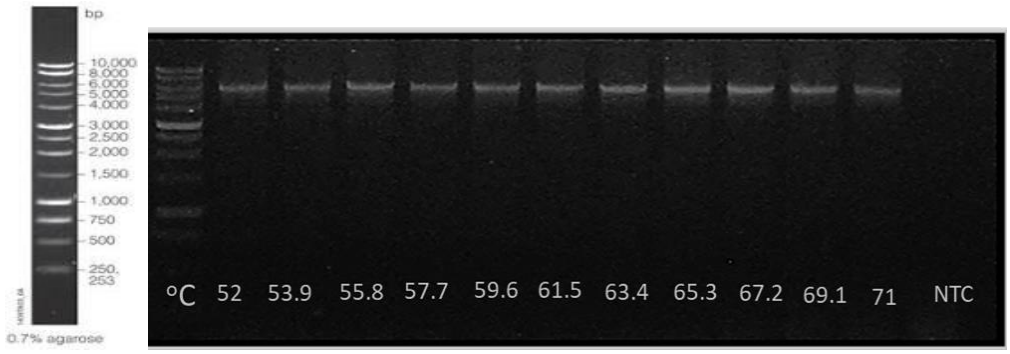


Figure 4-6 : Primer optimization of pCCD24$^{\Delta 7.2}$.

Gel electrophoresis of PCR product form gradient temperature PCR showed specific single band over a wide range of temperatures range (52˚C to 72 ˚C). However, the annealing temperature of 61.5°C was chosen in the further tests. NTC (no template control) showed no amplification.

To determine the quality and size as described above the plasmids were analysed on 1% agrose gel, as shown in Figure 4-7.

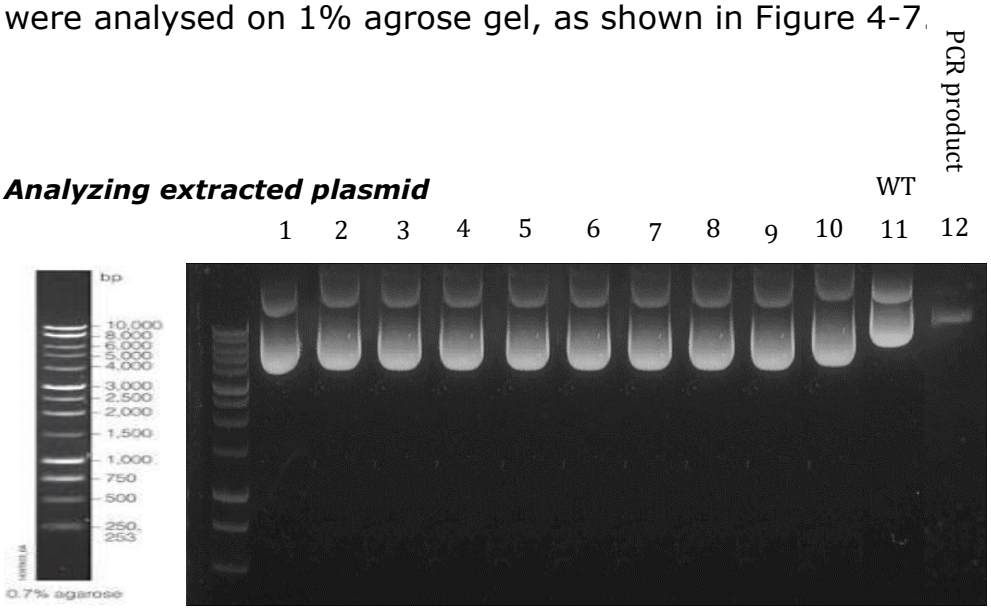


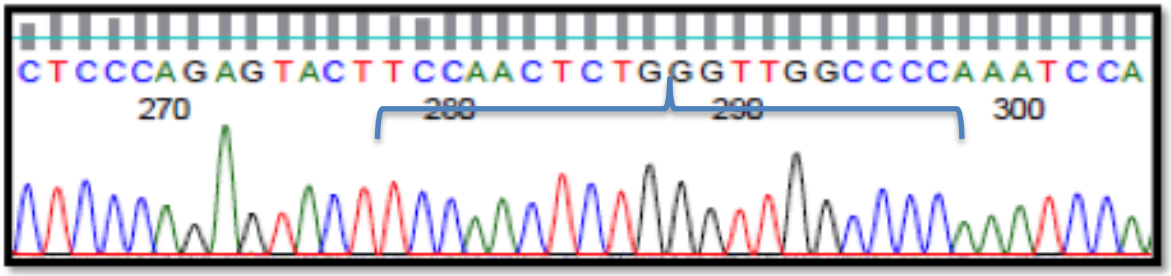
Figure 4-7 : Gel electrophoresis of the ten the extracted plasmids.

The 10 plasmids were tested after plasmid Miniprep. The ten plasmids showed the right size band. Along with it wild type plasmid in lane 11 was as control of deleted plasmid and PCR product in lane 12 as control for ligation.

Sequencing of pCCD24$^{\Delta 7.2}$

Sequencing of the samples was performed to confirm the presence of the deleting amino acid of the mature peptide of CD24 as described above. Figure 4-8

pCCD24^{WT}



pCCD24$^{\Delta 7.2}$

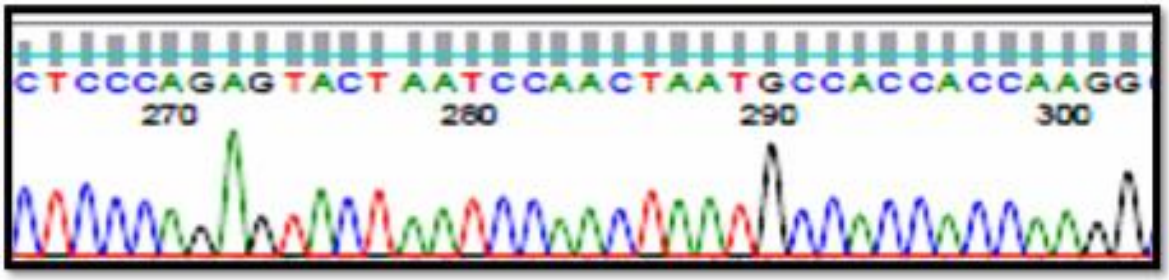


Figure 4-8 : Sequencing of pCCD24$^{\Delta 7.2}$

Sequencing confirmation of deleting seven amino acid (21 bp) as illustrated by brace.

The resultant sequence was aligned with alignment tool by NCBI (https://blast.ncbi.nlm.nih.gov/Blast.cgi) to show the sequence differences, the result showed that, 91% similarity sequence. As shown in figure 4-9. This confirmed that no other mutations had been introduced into the coding sequence

Coding sequence CD24



```
 Identities                              Gaps

 226/247(91%)                            21/247(8%)

Query  1    CACCATGGGCAGAGCAATGGTGGCCAGGCTCGGGCTGGGGCTGCTGCTGCTGGCACTGCT  60
            ||||||||||||||||||||||||||||||||||||||||||||||||||||||||||||
Sbjct  1    CACCATGGGCAGAGCAATGGTGGCCAGGCTCGGGCTGGGGCTGCTGCTGCTGGCACTGCT  60

Query  61   CCTACCCACGCAGATTTATTCCAGTGAAACAACAACTGGAACTTCAAGTAACTCCTCCCA  120
            ||||||||||||||||||||||||||||||||||||||||||||||||||||||||||||
Sbjct  61   CCTACCCACGCAGATTTATTCCAGTGAAACAACAACTGGAACTTCAAGTAACTCCTCCCA  120

Query  121  GAGTACTTCCAACTCTGGGTTGGCCCCAAATCCAACTAATGCCACCACCAAGGCGGCTGG  180
            |||||||                      ||||||||||||||||||||||||||||||||
Sbjct  121  GAGTACT----------------------AATCCAACTAATGCCACCACCAAGGCGGCTGG  159

Query  181  TGGTGCCCTGCAGTCAACAGCCAGTCTCTTCGTGGTCTCACTCTCTCTTCTGCATCTCTA  240
            ||||||||||||||||||||||||||||||||||||||||||||||||||||||||||||
Sbjct  160  TGGTGCCCTGCAGTCAACAGCCAGTCTCTTCGTGGTCTCACTCTCTCTTCTGCATCTCTA  219

Query  241  CTCTTAA  247
            |||||||
Sbjct  220  CTCTTAA  226
```

Figure 4-9 : Blast 2 analysis of pCCD24^{WT} and pCCD24$^{\Delta 7.2}$.

Blast 2 analysis was used to compare the sequence result of pCCD24$^{\Delta 7.2}$ with pCCD24^{WT}. The result showed 91% similarity when aligned using the NCBI alignment tool.

4.2.3 Construction of pCCD24$^{\Delta 7.3}$ plasmid

Gradient PCR

Was used to optimise the primer as above. Figure 4-10

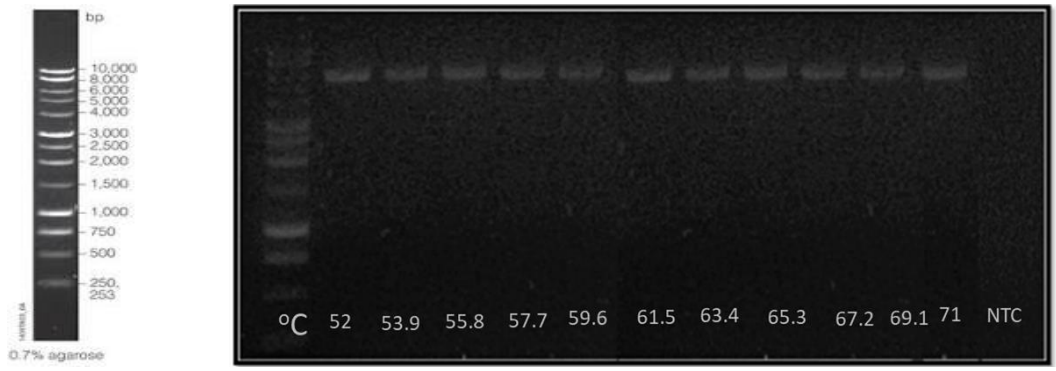


Figure 4-10 : Primer optimization of pCCD24$^{\Delta 7.3}$.

Gel electrophoresis of PCR product form gradient temperature PCR showed specific single band over a wide range of temperatures range (52°C to 72 °C). However, the annealing temperature of 61.5°C was chosen in the further tests. NTC (no template control) showed no amplification.

To determine the quality and size of the plasmids as described above, the plasmids were analysed on 1% agrose gel, as shown in Figure 4-11.

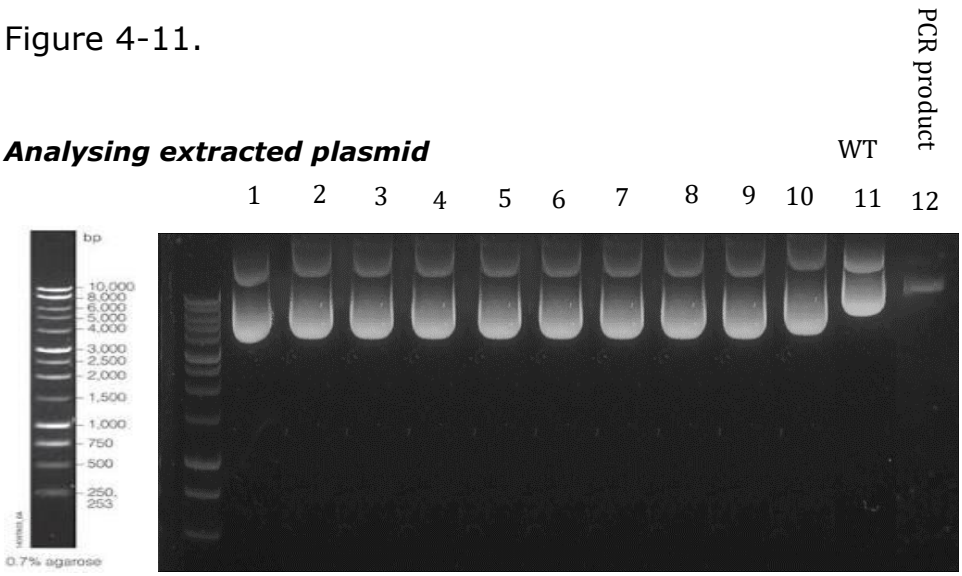


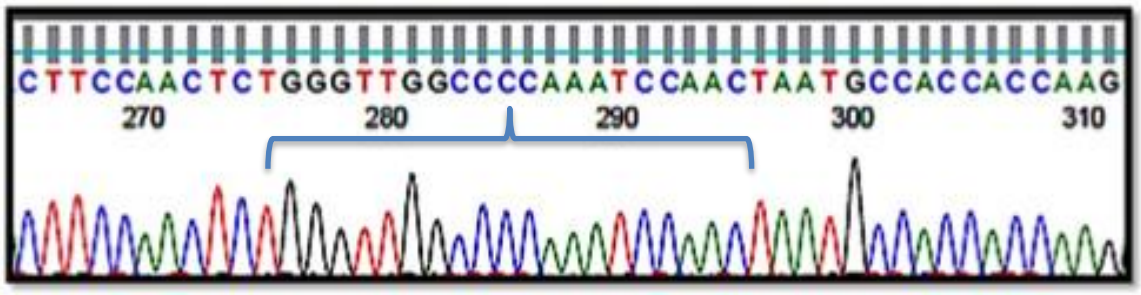
Figure 4-11 : Gel electrophoresis of the ten the extracted plasmids.

The 10 plasmids were tested after plasmid Miniprep. The ten plasmids showed the right size band. Along with it wild type plasmid in lane 11 as control of deleted plasmid and PCR product in lane 12 as control for ligation.

Sequencing of pCCD24$^{\Delta 7.3}$

Sequencing of the samples was performed to confirm the presence of the deleting amino acid of the mature peptide of CD24 as shown above. Figure 4-12

pCCD24^{WT}



pCCD24$^{\Delta 7.3}$

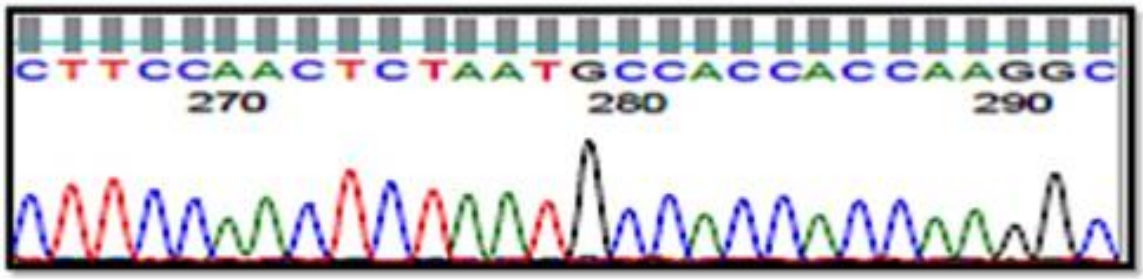


Figure 4-12 : Sequencing of pCCD24$^{\Delta 7.3}$

Sequencing confirmation of deleting seven amino acid (21 bp) as illustrated by brace.

The resultant sequence was aligned with alignment tool by NCBI (https://blast.ncbi.nlm.nih.gov/Blast.cgi) to show the sequence differences, the result showed that, 91% similarity sequence. As shown in figure 4-13. This confirmed that no other mutations had been introduced into the coding sequence.

Coding sequence CD24

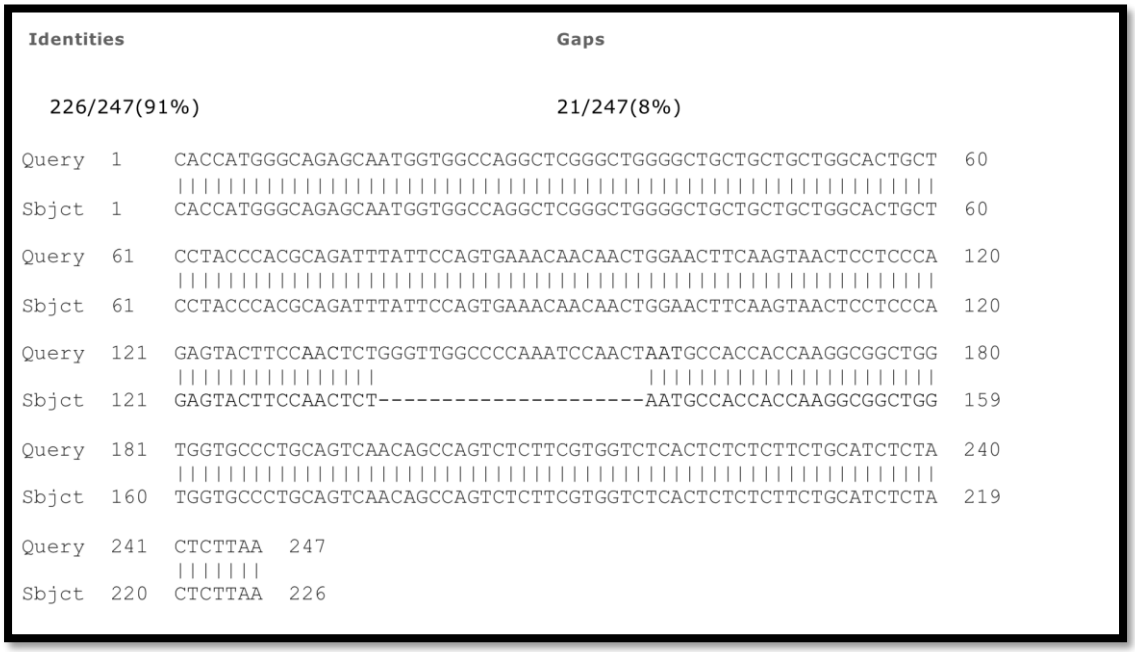


Figure 4-13 : Blast 2 analysis of pCCD24^{WT} and pCCD24$^{\Delta 7.3}$.

Blast 2 analysis was used to compare the sequence result of pCCD24$^{\Delta 7.3}$ with pCCD24^{WT}. The result showed 91% similarity when aligned using the NCBI alignment tool.

4.2.4 Construction of pCCD24$^{\Delta 4.4}$

Gradient PCR

Gradient PCR was used as described previously to optimise the primer. The primer showed the clearest band at 59.6°C which were used as annealing temperature in the further tests as shown in Figure 4-14

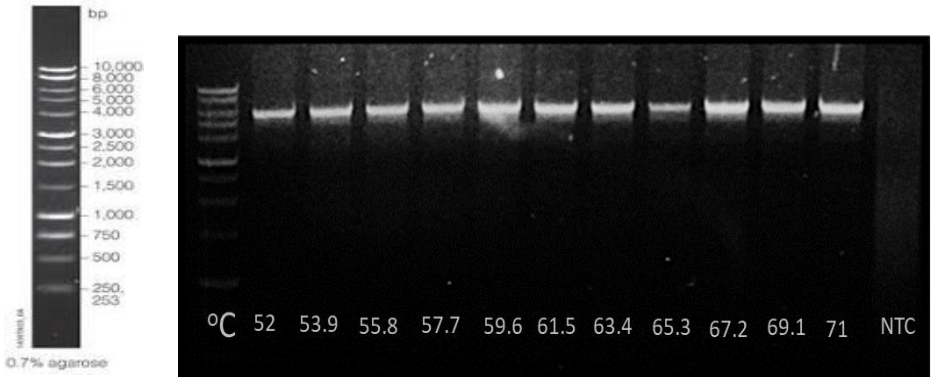


Figure 4-14 : Primer optimization of pCCD24$^{\Delta 4.4}$.

Gel electrophoresis of PCR product form gradient temperature PCR showed specific single band over a wide range of temperatures range (52°C to 72 °C). However, the annealing temperature of 59.6°C was chosen in the further tests. NTC (no template control) showed no amplification.

To determine the quality and size plasmids were analysed on 1% agrose gel, as shown in Figure 4-15.

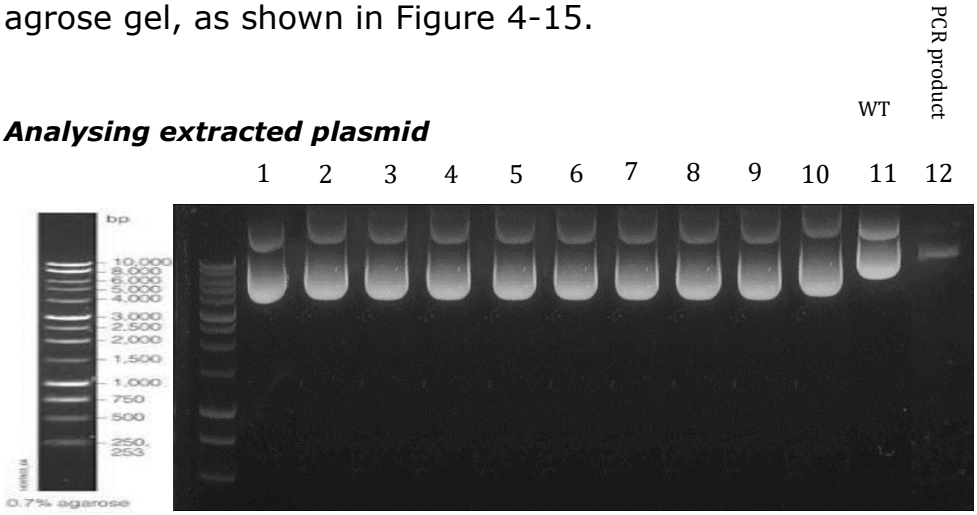


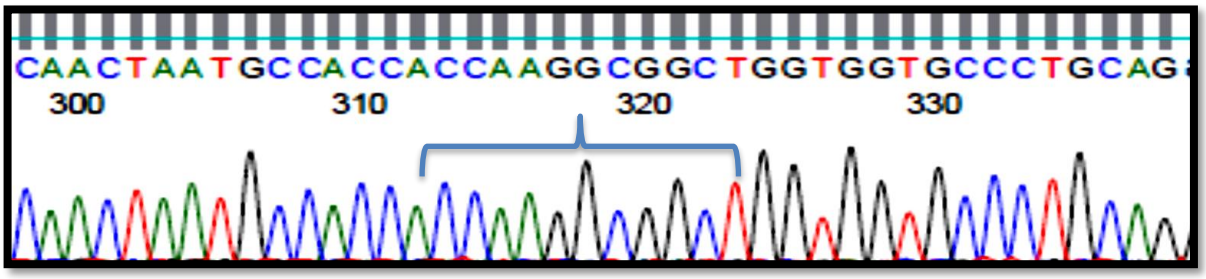
Figure 4-15 : Gel electrophoresis of the ten the extracted plasmids.

The 10 plasmids were tested after plasmid Miniprep. The ten samples showed the right size band. Along with it wild type plasmid in lane 11 as control of deleted plasmid and PCR product in lane 12 as control for ligation.

Sequencing of pCCD24$^{\Delta 4.4}$

The sequencing was performed to confirm the presence of the deleting amino acid of the mature peptide of CD24 as above. Figure 4-16

pCCD24^{WT}



pCCD24$^{\Delta 4.4}$

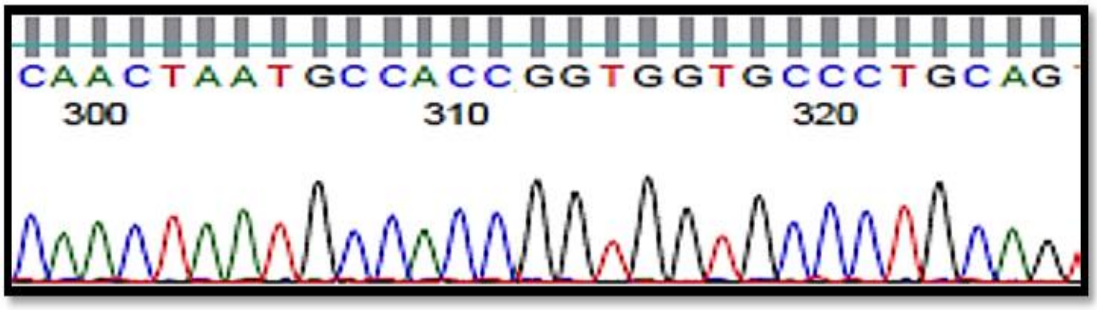


Figure 4-16 : Sequencing of pCCD24$^{\Delta 4.4}$

Sequencing confirmation of deleting four amino acid (12 bp) as illustrated by brace.

The resultant sequence was aligned with alignment tool by NCBI https://blast.ncbi.nlm.nih.gov/Blast.cgi to show the sequence differences, the result showed that, 91% similarity sequence. As shown in figure 4-17. This confirmed that no other mutations had been introduced into the coding sequence.

Coding sequence CD24

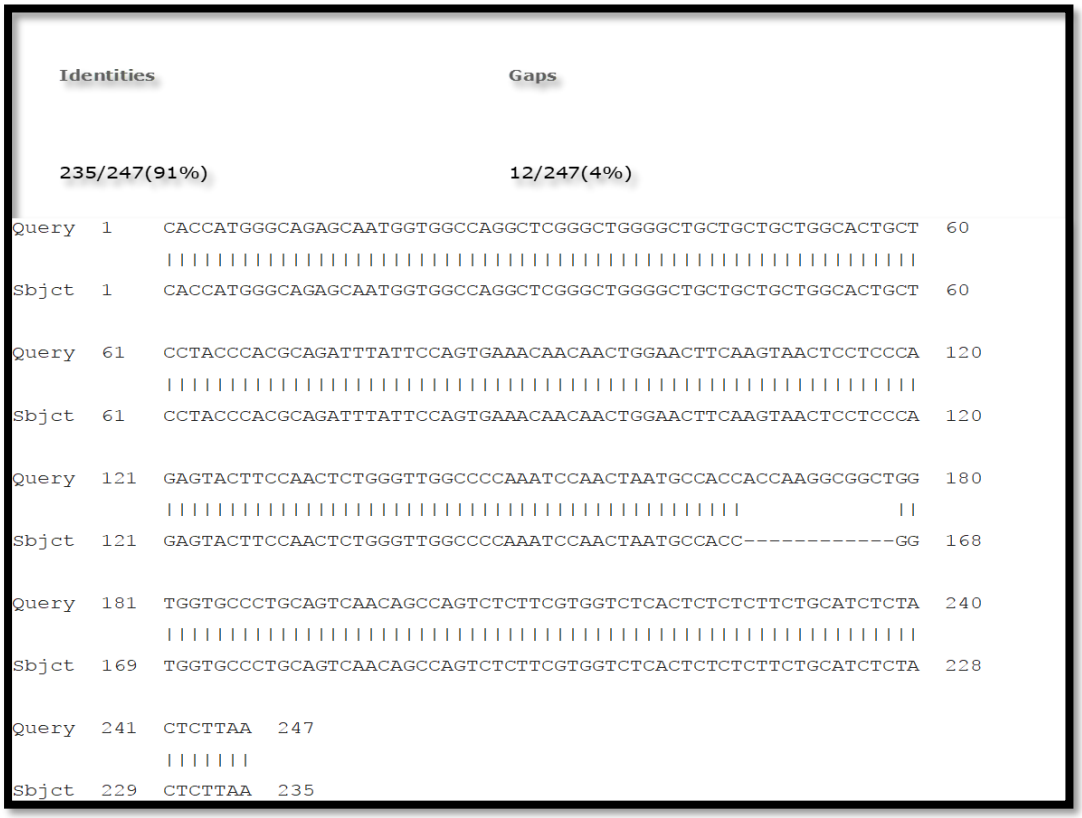
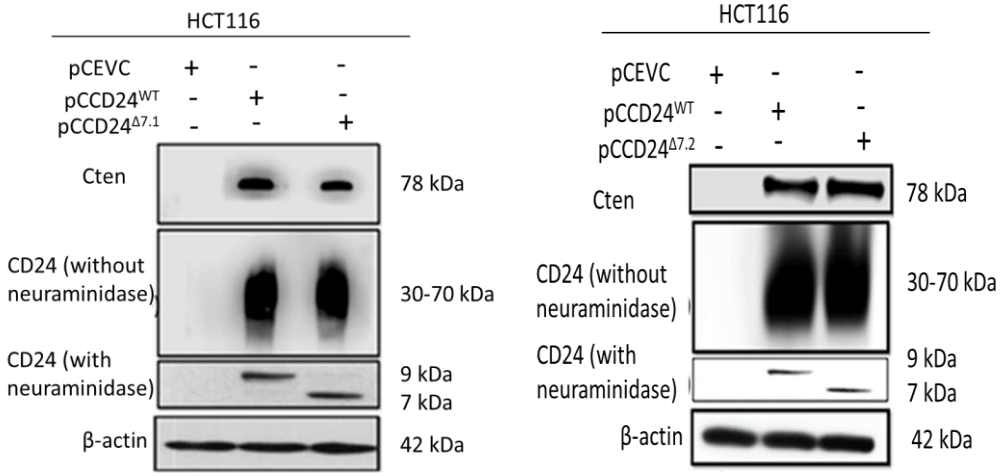


Figure 4-17 : Blast 2 analysis of pCCD24^{WT} and pCCD24$^{\Delta 4.4}$.

Blast 2 analysis was used to compare the sequence result of pCCD24$^{\Delta 4.4}$ with pCCD24^{WT}. The result showed 91% similarity when aligned using the NCBI alignment tool.

4.2.5 Protein expression of pCCD24$^{\Delta 7.1}$, pCCD24$^{\Delta 7.2}$, pCCD24$^{\Delta 7.3}$, and pCCD24$^{\Delta 4.4}$

To determine the protein expression of pCCD24$^{\Delta 7.1}$, pCCD24$^{\Delta 7.2}$, pCCD24$^{\Delta 7.3}$, pCCD24$^{\Delta 4.4}$, pCCD24^{WT} and an empty vector pCEVC was assessed using western blot, 24-48 hours post-transfection into the HCT116 cell line. The expression of pCCD24$^{\Delta 7.1}$, pCCD24$^{\Delta 7.2}$, pCCD24$^{\Delta 7.3}$, pCCD24$^{\Delta 4.4}$ pCEVC was compared to pCCD24^{WT} and an empty vector pCEVC. It showed similar appearances in all the constructs compared to pCCD24^{WT}. However, following treatment with neuraminidase, pCCD24$^{\Delta 7.1}$, pCCD24$^{\Delta 7.2}$, and pCCD24$^{\Delta 4.4}$ showed a shifted band compared to pCCD24^{WT}, which indicate the deleted amino acids, thereby confirming the deletion. However, because the epitope of SWA11 antibody was deleted in pCCD24$^{\Delta 7.3}$, we used instead a SN3 antibody, which detects the glycan structure shown in Figure 4-18.



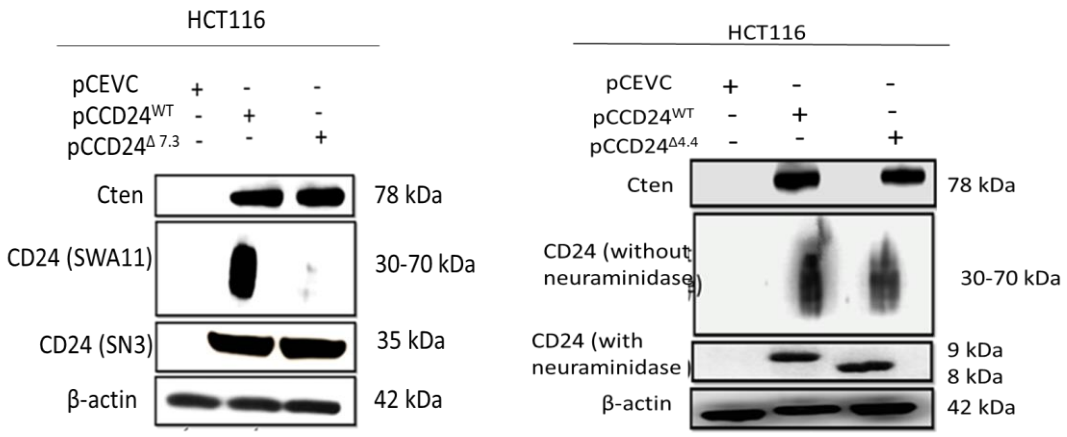


Figure 4-18 : The protein expression of pCCD24$^{\Delta 7.1}$, pCCD24$^{\Delta 7.2}$, pCCD24$^{\Delta 7.3}$, and pCCD24$^{\Delta 4.4}$.

Forced expression of pCCD24$^{\Delta 7.1}$, pCCD24$^{\Delta 7.2}$, pCCD24$^{\Delta 7.3}$, pCCD24$^{\Delta 4.4}$ in HCT116 to confirm the effect on protein level compared to pCCD24^{WT} and empty vector pCEVC.

4.2.6 The oncogenic features

4.2.6.1 pCCD24$^{\Delta 7.1}$, pCCD24$^{\Delta 7.2}$, pCCD24$^{\Delta 7.3}$, and pCCD24$^{\Delta 4.4}$ had no effect on cell proliferation

To evaluate functional activity, the effect of pCCD24$^{\Delta 7.1}$, pCCD24$^{\Delta 7.2,}$ pCCD24$^{\Delta 7.3}$, and pCCD24$^{\Delta 4.4}$ over-expression on cell proliferation was assessed using a 4-day time course assay. Adherent cell numbers were measured using presto blue dye fluorescence as measured by a spectrophotometer. The number of viable cells in each well was measured and monitored for 4 consecutive days on 0 hour, 24, 48, and 72, along with pCCD24^{WT} and an empty vector control (pCEVC). When compared with the empty vector control (pCEVC) and pCCD24^{WT}, forced expression of pCCD24$^{\Delta 7.1}$, pCCD24$^{\Delta 7.2}$, pCCD24$^{\Delta 7.3}$, and pCCD24$^{\Delta 4.4}$ in HCT116 showed no effect on the number of viable cells
(p = 0.9992)(p=0.9996)(p=0.9994)(p=0.9998), figure 4-19.

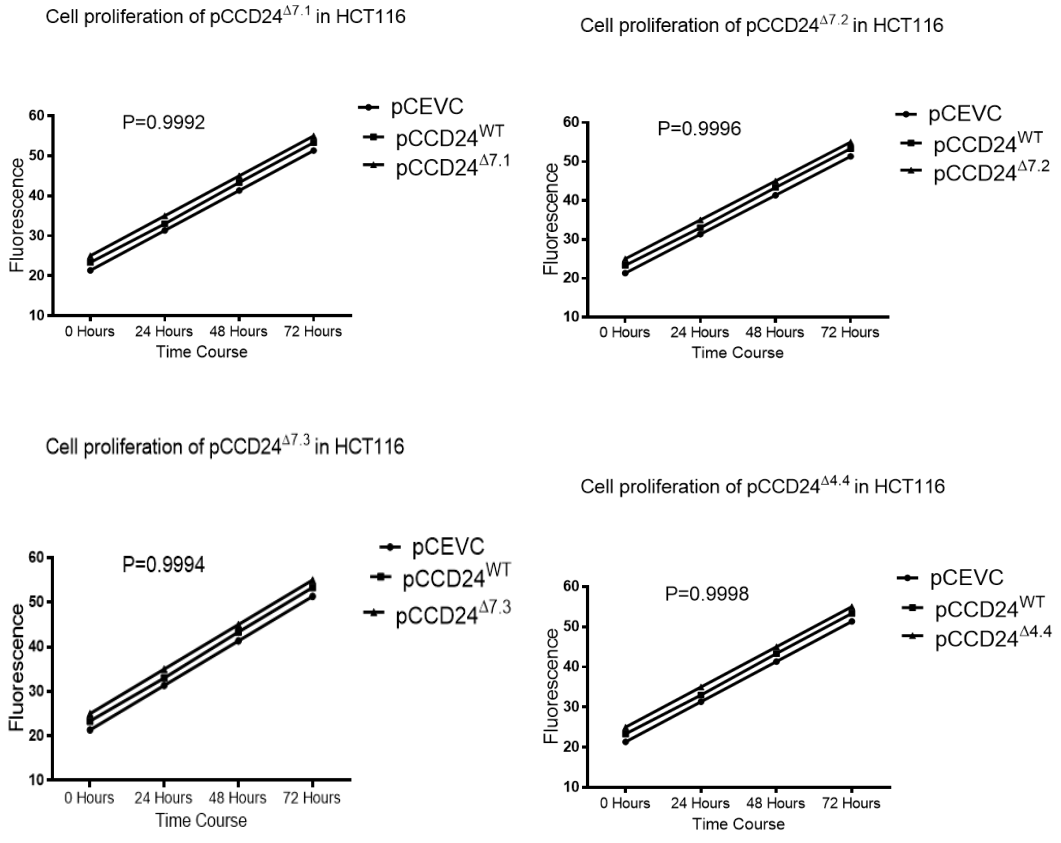
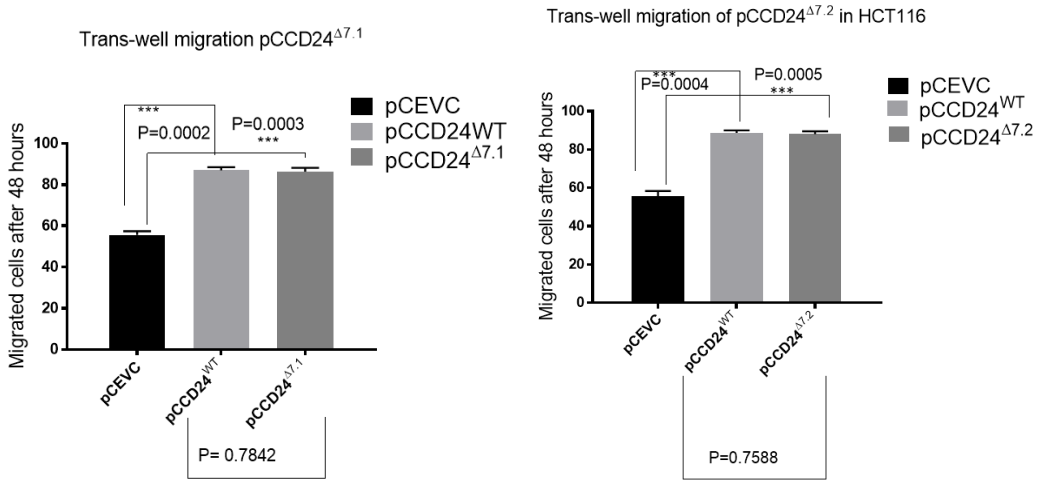


Figure 4-19 : The effect of pCCD24$^{\Delta 7.1}$, pCCD24$^{\Delta 7.2}$, pCCD24$^{\Delta 7.3}$, and pCCD24$^{\Delta 4.4}$ on the cell proliferation in HCT116.

A 4-day time course assay for proliferation using presto blue after forced expression of pCCD24$^{\Delta 7.1}$, pCCD24$^{\Delta 7.2}$, pCCD24$^{\Delta 7.3}$, and pCCD24$^{\Delta 4.4}$ in HCT116 cell line, showed an insignificant effect (P=0.9992) (p=0.9996) (p=0.9994) (p=0.9998). One-way ANOVA tested all values**.** Each experiment was repeated at least two times.

4.2.6.2 pCCD24$^{\Delta 7.1}$, pCCD24$^{\Delta 7.2}$, pCCD24$^{\Delta 7.3}$, and pCCD24$^{\Delta 4.4}$ showed no effect on cell motility

We previously reported that pCCD24^{WT} (wild-type CD24) enhances cell motility. The effect of pCCD24$^{\Delta 7.1}$, pCCD24$^{\Delta 7.2}$, pCCD24$^{\Delta 7.3}$, and pCCD24$^{\Delta 7.4}$ on cell migration was assessed using trans-well migration in a Boyden chamber across the 8mM pore-size membrane. When pCCD24$^{\Delta 7.1}$ was transfected into HCT116, compared to pCEVC, there was a stimulation of migration (p=0.0003).When pCCD24$^{\Delta 7.2}$ was transfected into HCT116, the results were similar. Compared to pCEVC, there was a stimulation of migration (p=0.0005). When pCCD24$^{\Delta 7.3}$ was transfected into HCT116, the results were similar compared to pCEVC, there was stimulation of migration (p=0.0002). As well as when pCCD24$^{\Delta 4.4}$ was transfected in HCT116, compared to pCEVC, there was a stimulation of migration (p=<0.0001) (see Figure 4-20).



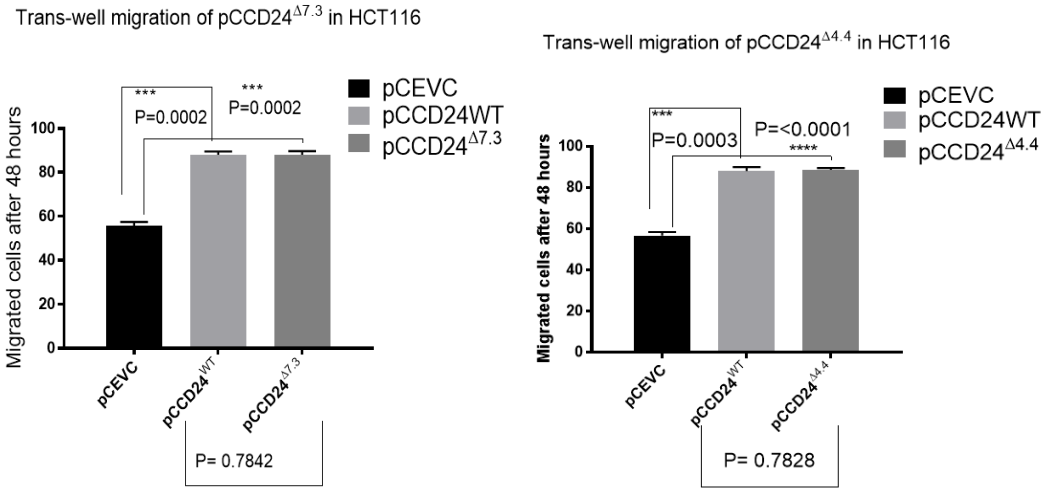


Figure 4-20: The effect of pCCD24$^{\Delta 7.1}$, pCCD24$^{\Delta 7.2}$, pCCD24$^{\Delta 7.3}$, and pCCD24$^{\Delta 4.4}$ on the cell motility.

pCCD24$^{\Delta 7.1}$, pCCD24$^{\Delta 7.2}$, pCCD24$^{\Delta 7.3}$, and pCCD24$^{\Delta 4.4}$ enhances the cell motility with significantly increased in the number of cells (P=0.0003) (p=0.0005) (p=0.0002) (p=<0.0001). All values were tested by t-test. Each experiment was repeated at least two times.

4.3 Discussion:

In the previous chapter we found the N-glycosylation sites of CD24 are responsible of the activity of CD24, because when we removed the N-glycosylation sites CD24 lost its functionality. Based on these result we validated the N-glycosylation sites. This was achieved by deleting seven parts of a CD24 mature peptide without deleting the N-glycosylation sites, followed by functional assays to study the effect on each site. The cell line used for this study was HCT116 which is a low expressor of CD24. Functional studies included the effect of the constructs on cell proliferation and motility. As mentioned previously, in our lab, $pCCD24^{WT}$ had no effect on cell proliferation despite a significant increase in cell motility. $pCCD24^{\Delta 7.1}$, $pCCD24^{\Delta 7.2}$, $pCCD24^{\Delta 7.3}$, $pCCD24^{\Delta 4.4}$, and $pCCD24^{WT}$ were forcibly expressed in HCT116 and compared with an empty vector pCEVC. On cell proliferation measures, $pCCD24^{WT}$ showed no effect, which is consistent with our previous data; $pCCD24^{\Delta 7.1,}$ $pCCD24^{\Delta 7.2}$, $pCCD24^{\Delta 7.3}$, and $pCCD24^{\Delta 4.4}$ also showed no effect on cell proliferation when compared with $pCCD24^{WT}$ and an empty vector pCEVC. However, this effect was consistent on repeat experiments.

Regarding cell migration, which is a key feature of tumour cells' metastasis [134]. We investigated the effect of $pCCD24^{\Delta 7.1}$, $pCCD24^{\Delta 7.2}$, $pCCD24^{\Delta 7.3}$, and $pCCD24^{\Delta 4.4}$ on cell motility. $pCCD24^{WT}$ showed a significant increased effect on cell motility compared with an empty vector pCEVC. We tested the expression level of $pCCD24^{\Delta 7.1}$, $pCCD24^{\Delta 7.2}$, $pCCD24^{\Delta 7.3}$, $pCCD24^{\Delta 4.4}$, $pCCD24^{WT}$, and empty vector pCEVC by western blot, and it showed the same smearing band even though we only removed seven amino acids from the mature peptide. We sought to show the effect of deleting parts of the mature peptide, so neuraminidase digestion was used

to remove the sugar attached to the core protein of CD24; results showed a shifted band in $pCCD24^{\Delta 7.1}$, $pCCD24^{\Delta 7.2}$, $pCCD24^{\Delta 4.4}$ compared to $pCCD24^{WT}$, which confirmed the effect. In $pCCD24^{\Delta.7.3}$, we used the SN3 antibody which detects the glycan structure instead of SWA11 which detects the core protein as we deleted the epitope of the SWA11 antibody.

It is highly conceivable to conclude from our results that N-glycosylation sites are responsible for the functionality of CD24 where with the deleting parts of the O-glycosylation the function of CD24 has not affected at this stage we do not know why but, the only explanation is since the potential sites of O-glycosylation are serine and threonine, deleting these sites by site directed mutagenesis it may showed an affect.

5. Signalling pathway of CD24

5.1 Introduction

Although there has recently been much discovery of the functions of CD24, there is still relatively little understanding of the signalling mechanism or molecules through which the functions are achieved. CD24 is small, heavily glycosylated molecule GPI anchored molecule which does not have a cytoplasmic domain through which to transmit extracellular signals. One study, based on results from a MDA-MB-231 breast carcinoma cell line found that CD24 is a key regulator of signalling through lipid rafts and that the chemokine receptor CXCR4 was driven out of the lipid rafts. This disrupts binding with the ligand SDF-1α (stromal cell-derived factor) and leads to an abrogation in the downstream target signalling that inhibits cell motility and invasion [135]. Another study described CD24 may have an essential role in activating signalling of the β1 integrin subunit by driving it from the outside to inside of the lipid rafts. Once inside the lipid rafts, it gets activated and leads to enhancement of cell motility and cell invasion [136].

Research in our lab has previously shown that CD24 regulates Cten (unpublished data), which is a downstream motility-inducing target. When we mutated the N-glycosylation sites of CD24, as shown in the previouse chapters, there is a failure to induce motility. We found that the mutations also reduced Cten induction.
A recent study [115] reported that, in the MCF-7 breast carcinoma cell line, CD24 knockdown results in decreased expression of Notch1 and that CD24-mediated cell migration and invasion was regulated by Notch1 [115]. This led us to investigate whether CD24 was signalling through Notch1 in CRC and whether there was any relationship with activation of Cten.

Aim of this study:

Investigate the signalling pathway of CD24- in particular the interactions of CD24, Notch1 and Cten.

5.2 Result:

5.2.1 CD24 regulates Notch1

To test whether CD24 regulates Notch1, we modulated the expression of CD24 – through either ectopic expression or RNA interference – and examined the effect of this modulation on Notch1 expression. The CD24 wild-type expression construct pCCD24^{WT} was transiently transfected into the CRC cell line HCT116 and compared with empty vector control (pCEVC). HCT116 is a low CD24 expressing cell line and the levels of Notch1 and the levels of its intracellular domain NICD (indicating activated Notch1) were investigated by western blot. The protein levels were compared 48 hours after transfection. We found that, compared to pCEVC, the levels of both Notch-1 and NICD were increased as we forcibly expressed CD24 (Figure 5-1A). This indicates that CD24 is positively inducing Notch1 expression.

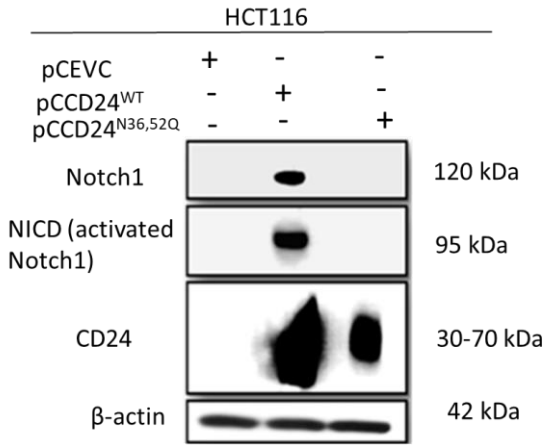
We had the constructs to express CD24 with loss of the N-glycosylation sites. These were also transfected into HCT116 and, compared to wild type CD24, the induction of Notch1 and NICD by the mutated CD24 was abrogated (Fig 5-1A). This suggests that activation of Notch1 signalling by CD24 is dependent on N-glycosylation.

To validate this finding, we used an alternative method to alter CD24 expression. The CRC cell line SW620 has high expression of CD24 and we used specific siRNA to knock down CD24 and compared this with transfection of siRNAs targeted to Luciferase as a negative control. The protein levels were compared after 48 hours

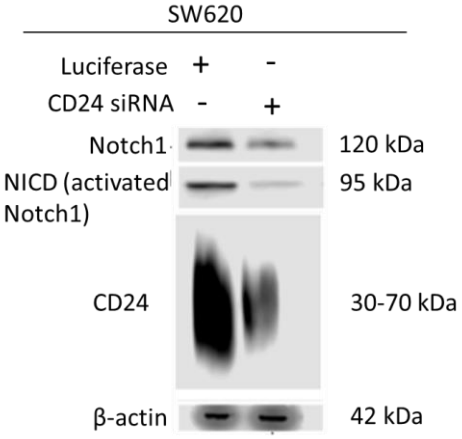
of transfection. Reduction in the levels of CD24 resulted in a reduction in the levels of both Notch1 and NICD (Figure 5-1B). These results validated the data suggesting that CD24 is a regulator of Notch1 signalling.

In order to ascertain whether our observations were specific to CRC or they represented a general interaction between CD24 and Notch1, the experiments were repeated in a non-small cell lung cancer cell lines, A549, which shows high expression of CD24. In agreement with the data from SW620, as the CD24 expression level decreased, the level of Notch1 also decreased (Figure 5-1C).

(a)



(b)



(c)

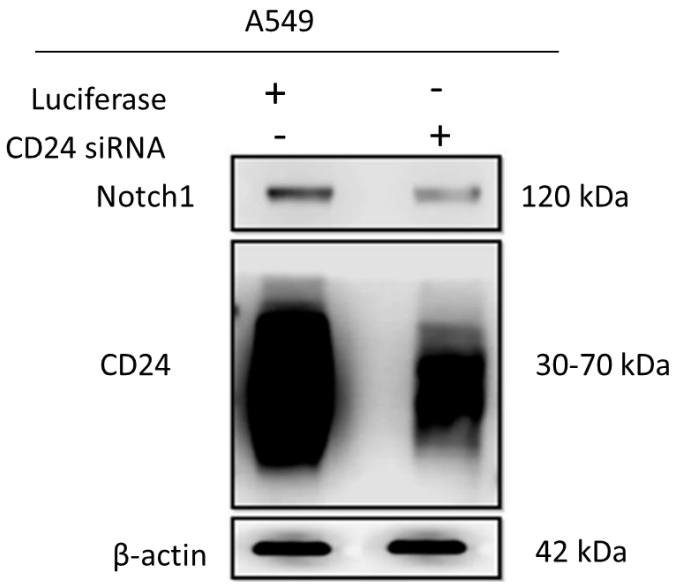


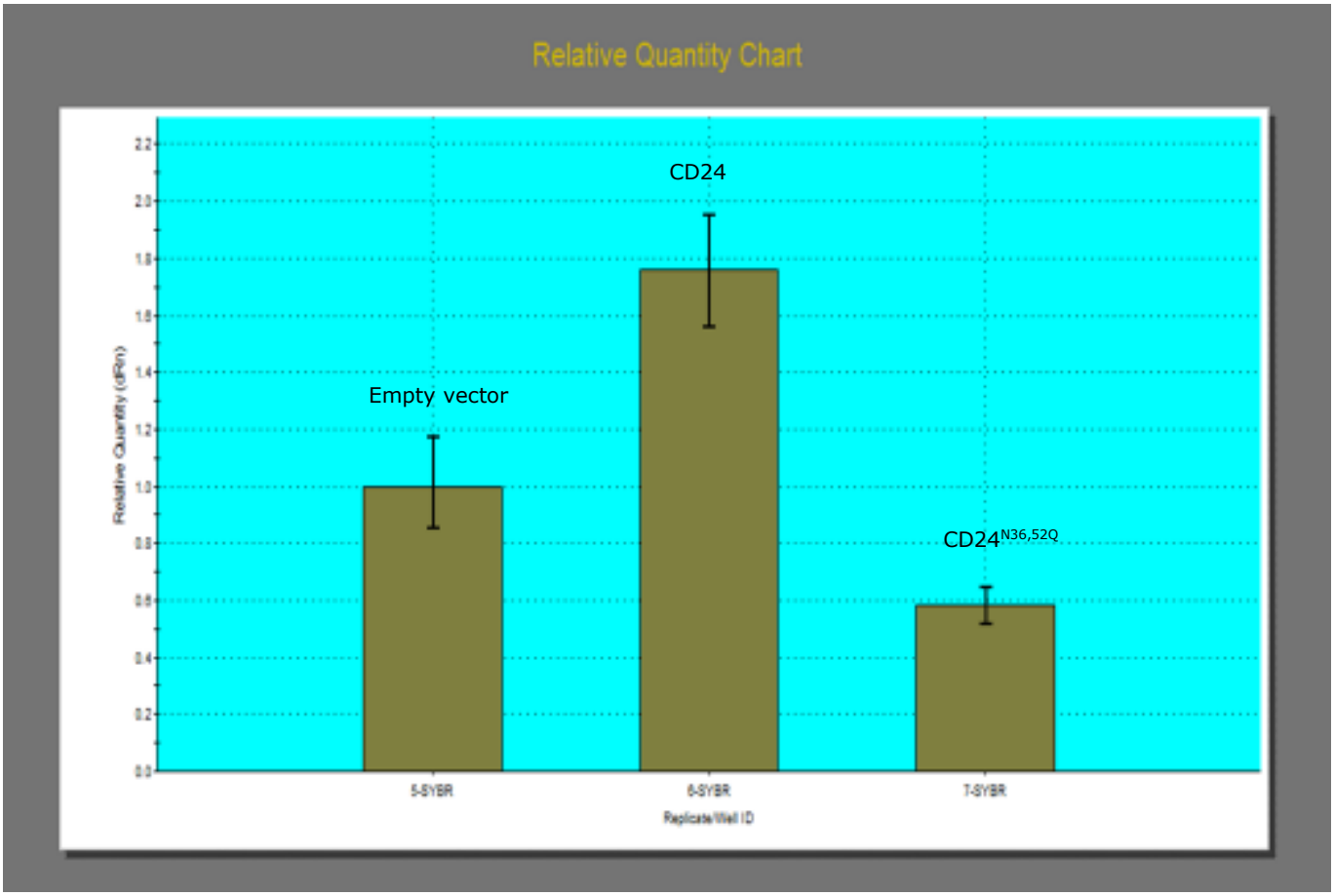
Figure 5-1: CD24 and regulation of Notch1

(a) Forced expression of CD24 in HCT116 resulted in up regulation of Notch1, while forced expression of pCCD24$^{N36, 52Q}$ resulted in abrogate of Notch1. β-actin was used as protein loading control. (b) Knockdown of CD24 in SW620 resulted in down regulation of Notch1. β-actin was used as protein loading control. (c) Knockdown of CD24 in A549 showed a decreased in the expression of Notch1.

5.2.2 CD24 regulates Notch1 at transcriptional level

Our data showed that CD24_regulates Notch1 though it was unclear whether it does so through direct up-regulation of transcription or whether it was through post-transcriptional regulation. To test this further, the mRNA level of Notch1 was measured by quantitative RT-PCR following forced expression of wild type CD24 and mutant ($CD24^{N36, 52Q)}$. There was an increase in Notch 1 mRNA level induced by CD24, whereas, with the mutant CD24, there was a failure to induce Notch 1 (Figure 5-2 A), suggesting there was transcriptional regulation. To further validate this, the Notch1 mRNA level was measured by quantitative RT-PCR following CD24 knockdown. This showed there was reduction in Notch1 mRNA levels when CD24 was knocked down (Figure 5-2 B).

(a)



(b)

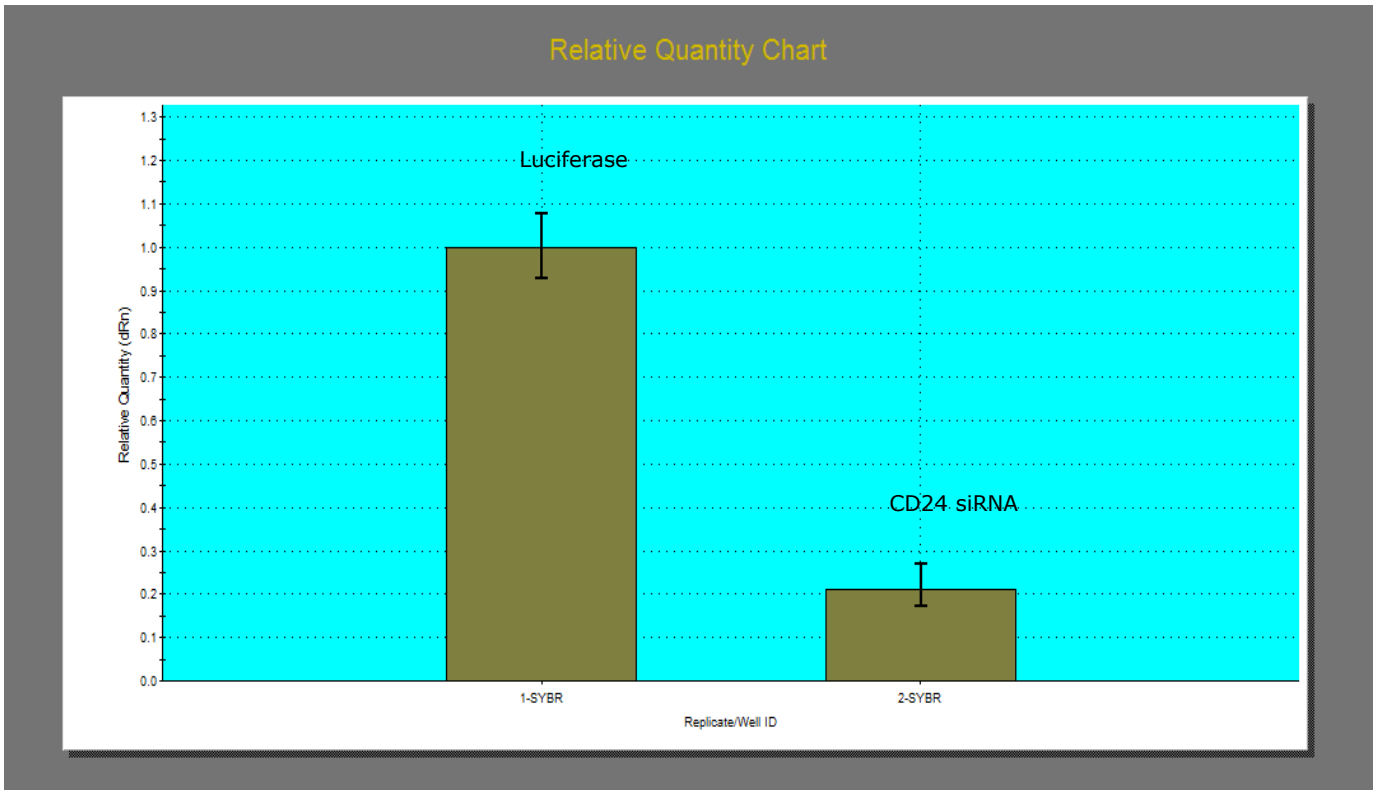


Figure 5-2: CD24 regulates Notch1 at transcriptional level.

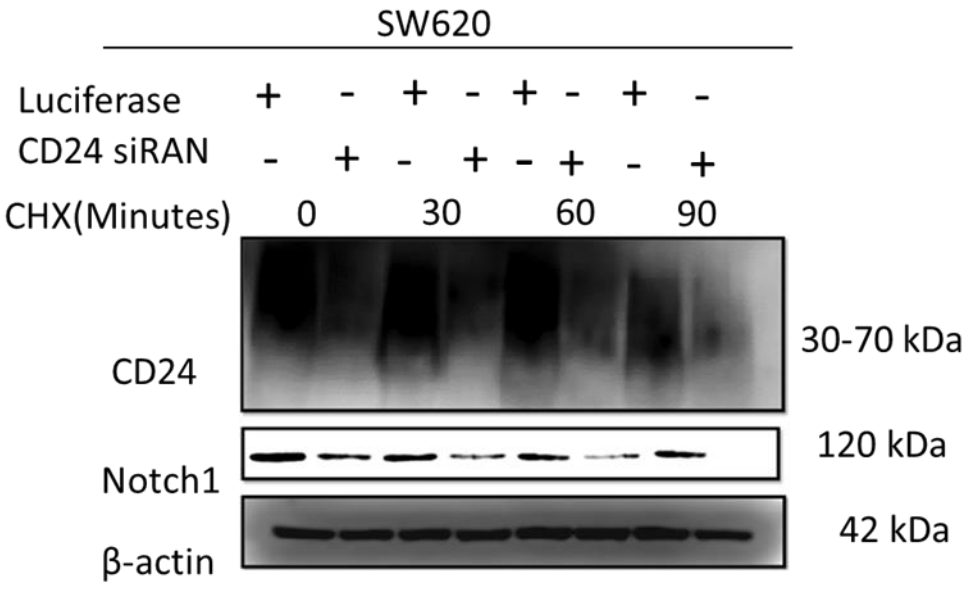
(a) Following forced expression of CD24 and CD24 mutant ($CD24^{N36,52Q}$) in HCT116, mRNA level of Notch1 were quantified and normalised to the housekeeping gene HPRT, the result showed that there was an increase in mRNA level induced by CD24 and failure to induce by CD24 mutant (data shown from replicates). (b) To support this, CD24 knocked down in SW620 and mRNA level were quantified and normalised to the housekeeping gene HPRT, there were reduction in mRNA levels.

5.2.3 CD24 stabilises Notch1

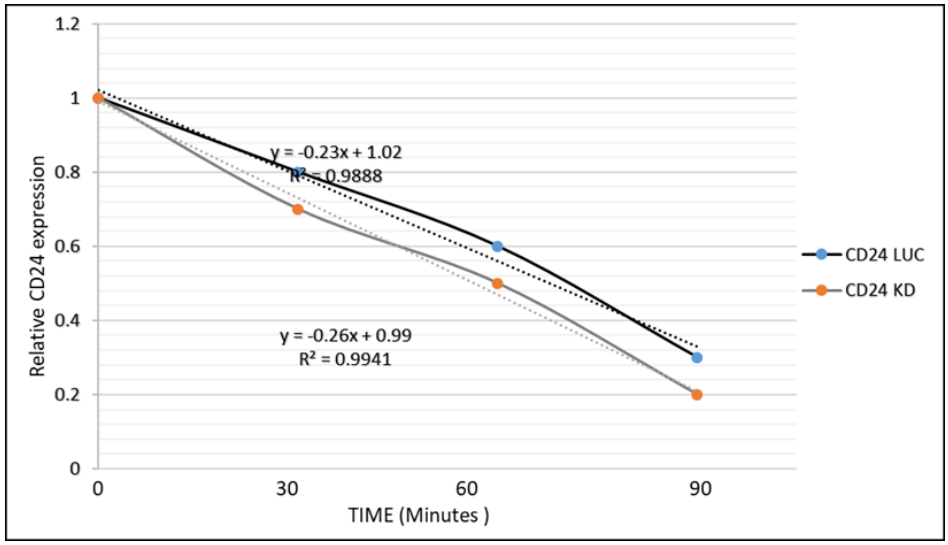
It has been demonstrated that CD24 regulates Notch1 at a transcriptional level but, it is possible that, CD24 regulates Notch1 protein at the post-transcriptional level as well. To investigate this, we used cycloheximide (CHX) protein degradation assay. CHX is a protein synthesis inhibitor which stops the elongation of peptides during protein translation. Thus, at the point that CHX is administered, new protein synthesis stops and this allows us to track the protein degradation. CHX was added to SW620 following CD24 siRNA transfection and control luciferase to investigate the changes of Notch1 protein expression (Figure 5-3) in the presence and in the absence of CD24 protein. In the luciferase control SW620 cells, both CD24 and Notch1 protein were expressed and, although there was degradation, they were still detectable at 90 minutes. Following CD24 knock-down in SW620, both CD24 and Notch1 protein were detectable but at a lower level. This is not surprising since, as shown above, Notch1 is a target of CD24. However, CD24 was still visible at 90 minutes whilst Notch1 protein had been degraded after 60 minutes. Given the differences in starting levels of the CD24 and Notch1 protein in the two conditions of CD24 knockdown and luciferase controls, assessment of degradation was difficult. Therefore the rate of degradation of each of the proteins was quantified by densitometry using the C-DiGt Blot Scanner software. The CD24 and Notch1 were normalised to β-actin and the value at time 0 was set to 1. The values at each of the time points were plotted as a ratio of the value at time 0 and the slope which would give the rate of protein degradation - was calculated.
The data showed that in each condition the rate of CD24 degradation was similar. However, the rate of degradation of Notch1 was almost 2 fold greater in the CD24 knockdown condition. This suggests that CD24 may stabilise Notch1 protein therefore

providing post-transcriptional regulation as well as transcriptional regulation.

(a)



(b)



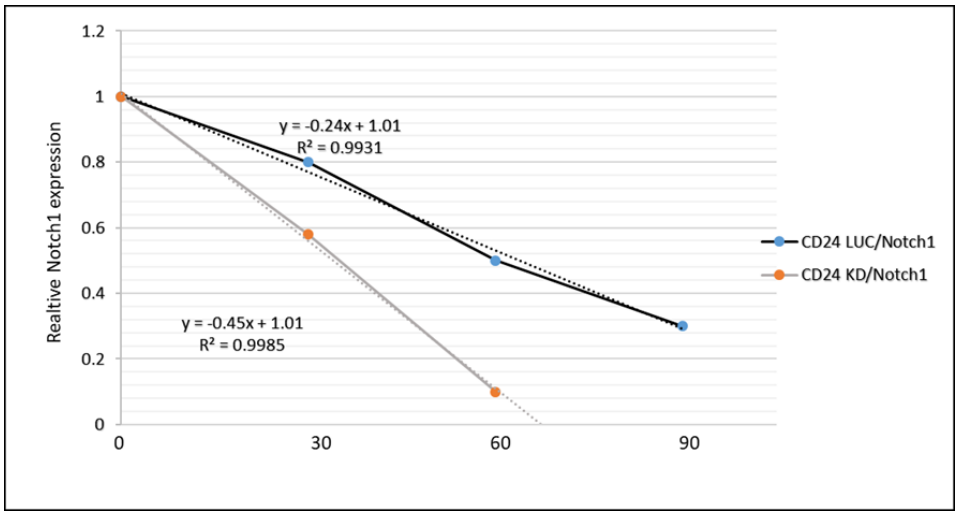


Figure 5-3: CD24 stabilises Notch1.

(a) Notch1 protein was stabilised for longer in SW620 expressing CD24 following treatment with CHX compared to SW620 cells with CD24 knocked down. (b) The CD24 and Notch1 decay curve following treatment with CHX. CD24 and Notch1 proteins were normalised to β-actin and then normalised to the 0 hour time point.

5.2.1 CD24 physically interacts with Notch1

The stabilisation of Notch1 protein by CD24 raises an important question of whether CD24 physically interacts with Notch1 especially since both are located on the cell membrane. To answer this question, a co-immunoprecipitation technique was used in SW620. Immunoprecipitation was performed using the anti-CD24 antibody SWA11 to pull down CD24 and Western blot was performed using the antibody to Notch1. The input lane was Notch1 which was the lysate alone (positive control) for Notch1. The IP CD24 was the lysate with beads and CD24 Ab to pull out CD24 and its attached proteins. The negative control lane was beads containing only lysate were used to test the non-specific binding of CD24 to the beads. The presence of Notch1 input indicates the presence of Notch1 in lysates and the size of the band (120 kDa). In CD24 IP, the band indicates the physical interaction between CD24 and Notch1. The absence of a band in the negative control excludes nonspecific binding by the beads and antibodies, the other way round which is IP with Notch1 could not be done as the Notch1 antibody used was only suitable for western blot and not with CO-IP. Figure5-4.

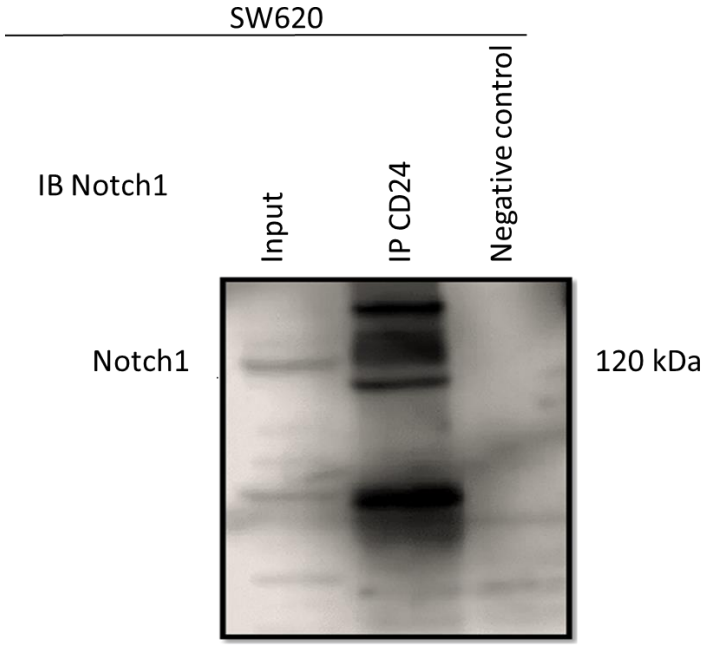


Figure 5-4: The physical interaction between CD24 and Notch1.

Co-immunoprecipitation was performed for CD24 and Notch1 from SW620 protein lysate. Notch1 input was the lysate alone. CD24 IP was the lysate with the beads and CD24 SWA11 Ab to pull out CD24. Beads with lysate only were used as negative control.

5.2.1 Nuclear/ cytoplasmic localisation of CD24 and Notch1

The localisation of protein plays an important role in characterising cellular function [137]. In order to investigate the regulation of CD24 to Notch1 protein in the cytoplasm and/or nucleus, following transfection of CD24 and empty vector in HCT116, total protein lysates underwent fractionation to separate nuclear and cytoplasmic proteins (as described in Chapter 2). Cytoplasmic and nuclear fractions were separated and a western blot was used to detect the protein. Lamin b1 was used as a nucleus marker, and alpha-tubulin was used as a cytoplasm marker. The result revealed that CD24 and Notch1 localise to both cytoplasm and nucleus and therefore CD24 may regulate Notch1 both in the cytoplasm and nucleus (Figure 5-5).

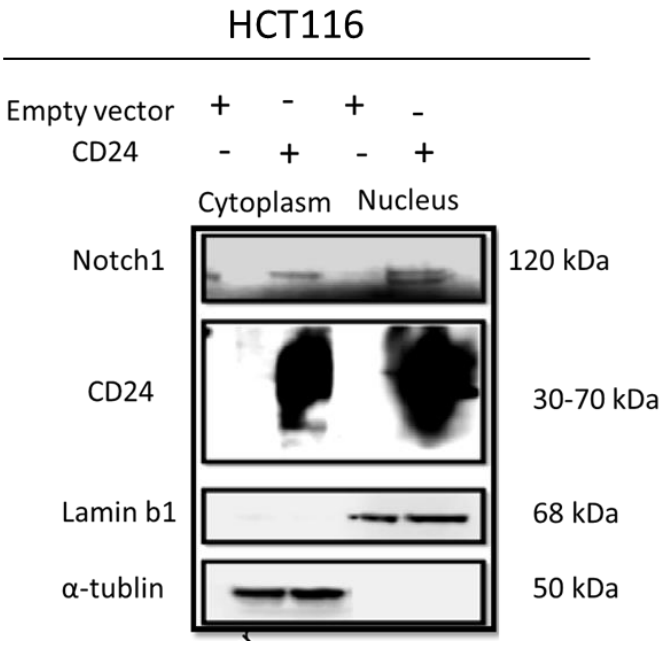


Figure 5-5: Nuclear and cytoplasmic fractionation.

The data showing that CD24 and Notch1 are expressed in both cytoplasmic and nuclear fraction.

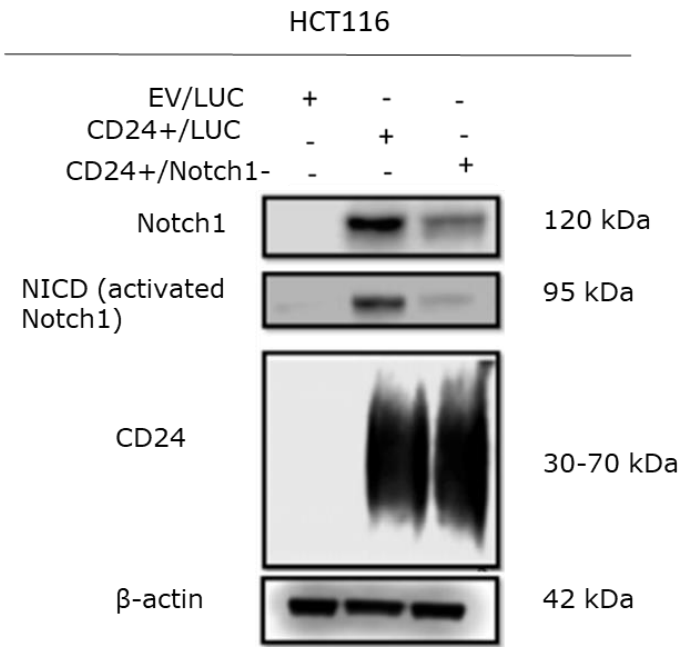
5.2.2 Functional interaction between CD24 and Notch1

CD24 was shown to positively regulate Notch1 through both gene knockdown and ectopic expression. To test whether the hypothesised CD24-Notch1 pathway has any functional relevance, we compared the conditions of forcibly expressed CD24 with CD24 forced expression and concomitant of Notch1 knockdown. If the Notch1 knockdown resulted in a failure of CD24 to induce its usual effects, it would suggest that there was functional relevance.

The HCT116 cell line was transfected with a construct causing ectopic expression of CD24 ($HCT116^{CD24+}$) and co-transfected with Notch1-specific siRNA ($HCT116^{CD24+/NOTCH1-}$) and with luciferase control ($HCT116^{CD24+/LUC)}$. The experimental control was cells co-transfected with luciferase siRNA and an empty vector ($HCT116^{EV/LUC}$), creating a condition in which neither Notch1 nor CD24 were altered as shown in Figure 5-3.

The ectopic expression of CD24 ($HCT116^{CD24+/LUC}$) showed a significant effect on cell motility in trans-well migration assay compared to the control ($HCT116^{EV/LUC}$) ($p= 0.0001$). The co-transfection with Notch1-specfic siRNA ($HCT116^{CD24+/NOTCH1-}$) showed a failure to induce motility compared to the control ($HCT116^{EV/LUC}$) ($p= 0.0018$). Thus, these data showed the effect of Notch1 knockdown causing an abrogation of the motility-inducing activity of CD24, which demonstrated that CD24 signals through Notch1 to induce its functional activity.

(a)


HCT116
EV/LUC + - -
CD24+/LUC - + -
CD24+/Notch1- - - +
Notch1
120 kDa
NICD (activated Notch1)
95 kDa
CD24
30-70 kDa
β-actin
42 kDa

(b)

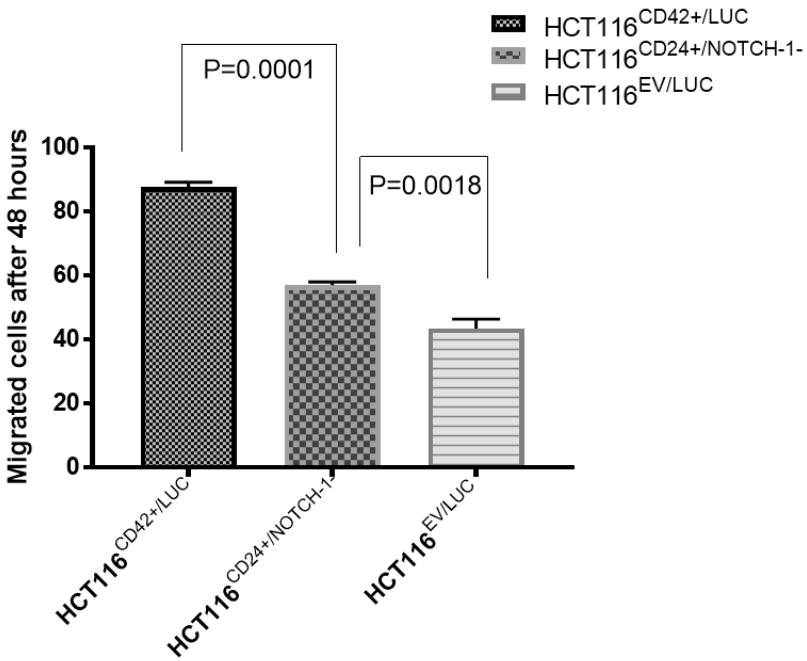

HCT116CD42+/LUC
HCT116CD24+/NOTCH-1-
HCT116EV/LUC
P=0.0001
P=0.0018
Migrated cells after 48 hours
100
80
60
40
20
0
HCT116CD42+/LUC
HCT116CD24+/NOTCH-1-
HCT116EV/LUC

Figure 5-6: the relationship between CD24 and Notch1.

(a) HCT116 cells were transfected with construct causing up regulation of CD24-empty vector and cells co-transfected with Notch1-specific siRNA and Luciferase control to test the induction of the motility caused by CD24. Controls were co-transfected with Luciferase controls siRNA and empty vector. (b) Trans-well migration assay with $HCT116^{CD24/LUC}$ showed an increase in the cell motility, while, with $HCT116^{CD24+/Notch1-}$ there was a failure to induce the cell motility compared to control $HCT116^{EV/LUC}$. All values were tested by t-test. Each experiment was repeated at least two times.

5.2.3 Notch1 regulates Cten

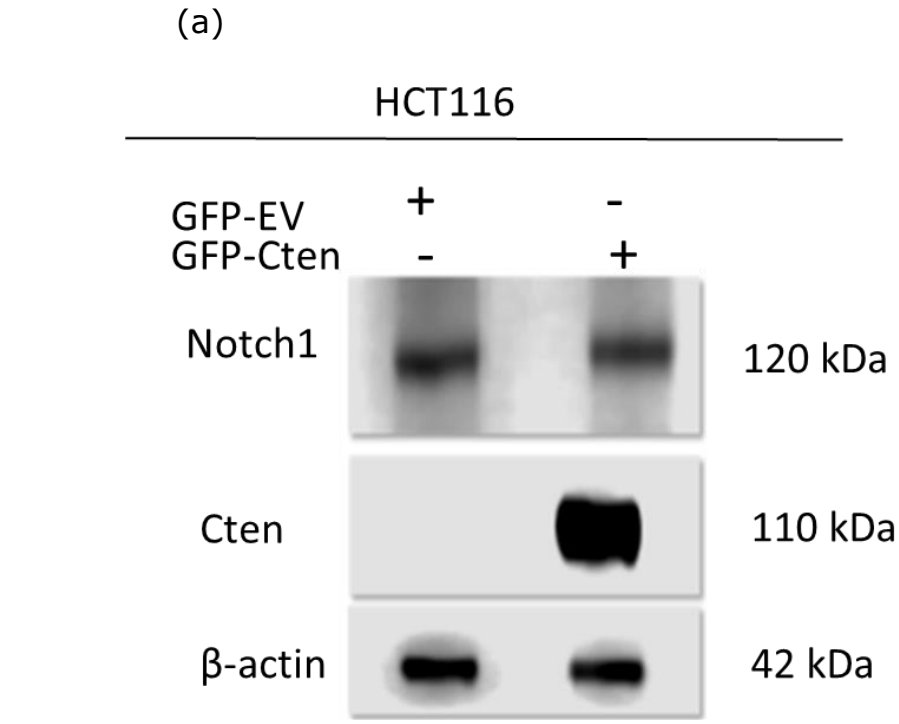
Our data showed that CD24 is a positive regulator of Notch1. We have previously shown that it is also a positive regulator of Cten. This prompted us to wonder whether Notch1 and Cten represent independent targets or whether there is a linear relationship which could form a signalling pathway.

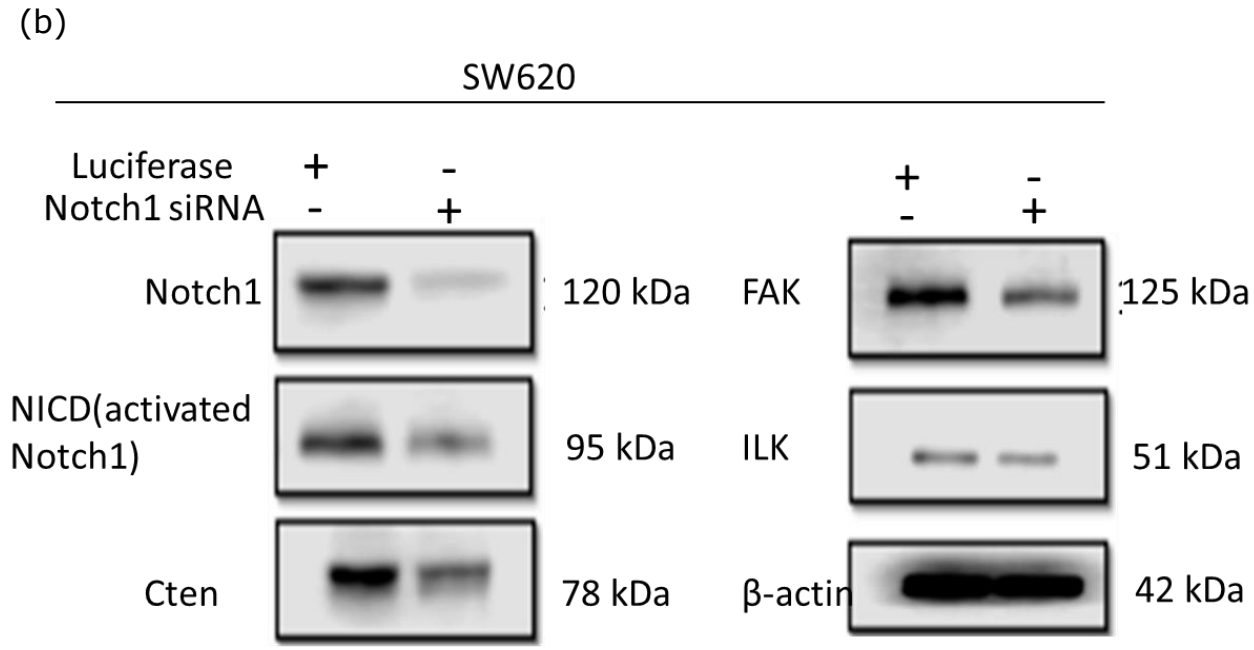
Initially, we investigated whether GFP-Cten could influence expression of Notch1. The cell line HCT116 is a low expresser of Cten and thus GFP-Cten was ectopically expressed in this cell line. The expression level of Notch1 after transient transfection of GFP-Cten and GFP-EV for Cten was investigated by western blot; its expression level did not change indicating that Cten was unlikely to be a regulator of Notch1 (Figure 5-7A).

Next we investigated whether Cten could be a downstream target of Notch1 and regulated by Notch1. The CRC cell line SW620 expresses high levels of both Notch1 and Cten. We used specific siRNA to knock down Notch1 and tested the level of Cten expression by Western blotting. We found that, with the knockdown of Notch1, there was as expected a reduction in the level of NICD. We also found that, with the knockdown of Notch1, the expression level of Cten was decreased.

We have previously described ILK and FAK as downstream targets of Cten [138].If the effect of Notch1 knockdown on Cten was functionally important, a secondary effect would also be expected

on FAK and ILK. As shown in (Figure 5-7B) there was a decrease in expression of both of these proteins.





(c)

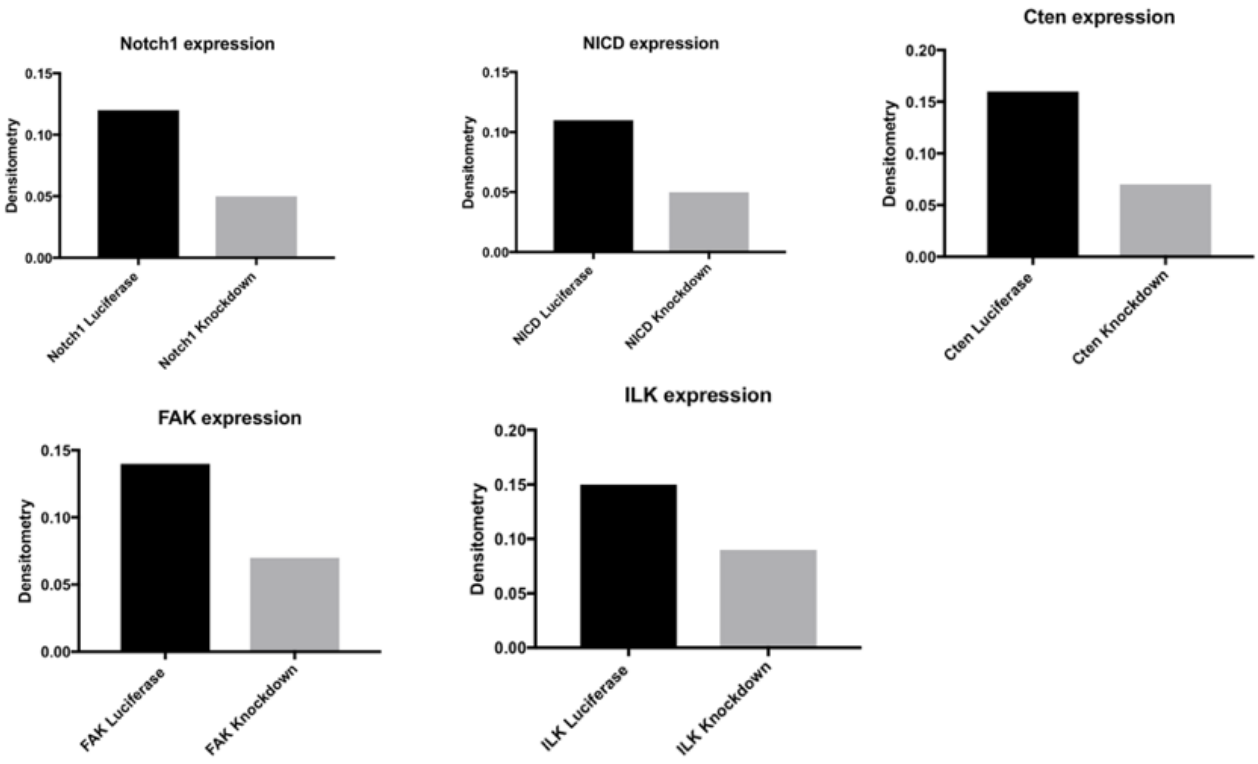


Figure 5-7: Notch1 and regulation of Cten

(a) Forced expression of GFP-Cten and GFP-EV in HCT116 showed no effect on Notch1. β-actin was used as protein loading control. (b) Knockdown of Notch1 in SW620 resulted in down regulation of Cten and other down streams target of Cten, FAK, and ILK, which showed that Cten is down-streams target of Notch1. β-actin was used as protein loading control. (c) Densitometry of expression following knockdown Notch1. Proteins were normalised to β-actin.

5.2.4 The CD24-Notch1-Cten pathway

We found that CD24 is a positive regulator of both Notch1 and Cten. Furthermore we demonstrated that Notch1 is a positive regulator of Cten. This led us to hypothesise that CD24 could regulate Cten through Notch1 i.e. there may be a linear CD24-Notch1-Cten pathway. In order to investigate this, we compared a condition of forcibly expressing CD24 and concomitant Notch1 knockdown in HCT116. The HCT116 cell line was transfected with a construct causing ectopic expression of CD24 and co-transfected with Notch1-specific siRNA and Luciferase control. The experimental control was cells co-transfected with Luciferase control and an empty vector, and an empty vector co-transfected with Notch1 specific siRNA.

Thus we would expect the level of Notch1 and Cten to increase with the ectopic expression of CD24. If Notch1 was a direct regulator of Cten, then knockdown of Notch1 would resulted in a failure to induce CD24 despite the high levels of CD24.
Figure 5-8 shows that, when the empty vector and the siRNA for luciferase were co-transfected into HCT116, there was no CD24, Cten or Notch1 (lane 1). When CD24 and the siRNA for luciferase were co-transfected, there was expression of CD24, Cten and Notch1 (lane 2). When CD24 and the siRNA for Notch1 were co-transfected, there was expression of CD24 and a reduction in expression of Notch1. In this experiment, there was also a reduction in the level of Cten even though the level of CD24 expression was the same in lane 2. (See Figure 5-8).

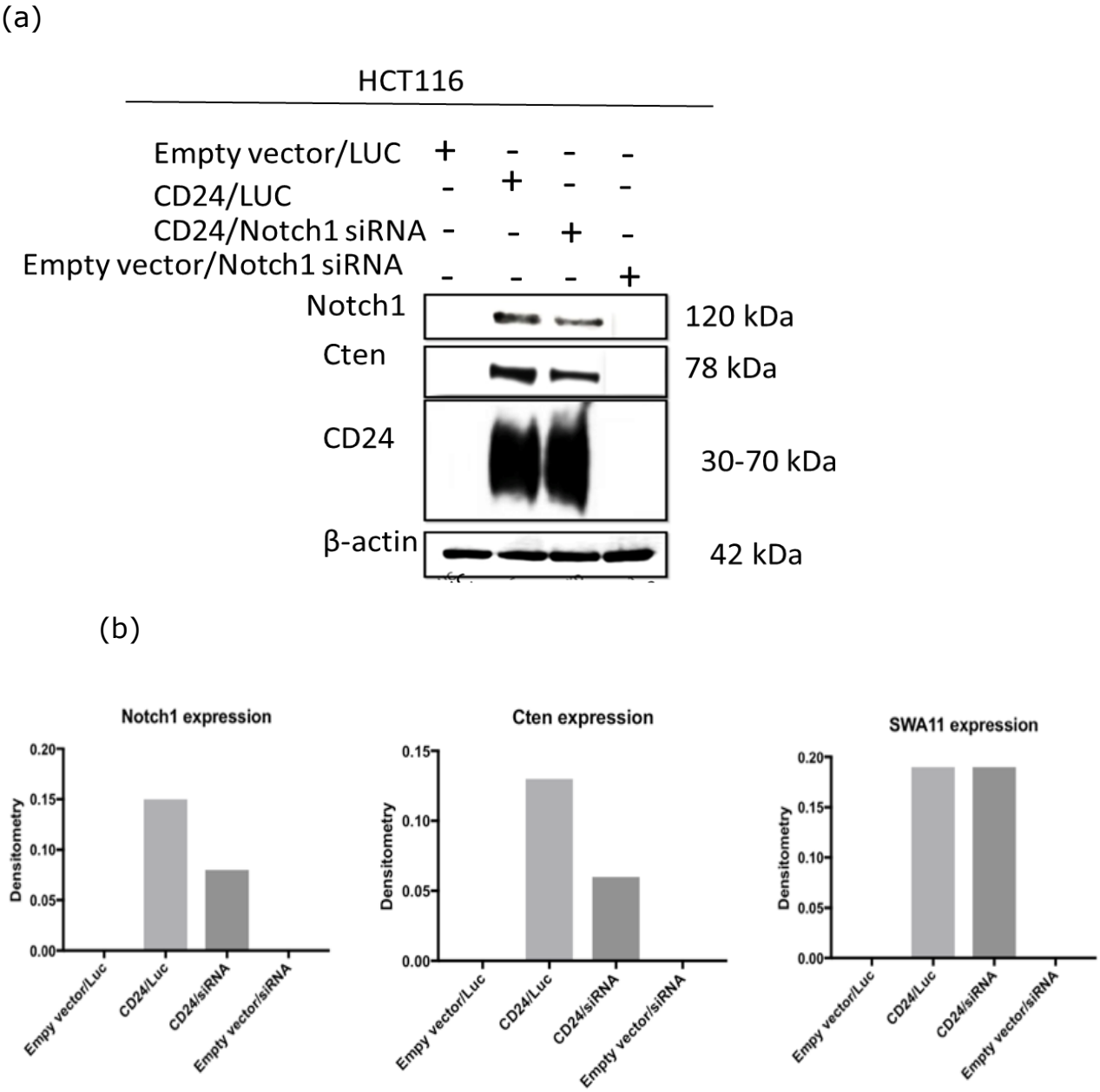


Figure 5-8: The CD24-Notch1-Cten pathway.

(a)HCT116 cells co transfected with construct causing ectopic expression of CD24 and concomitant Notch1-specific siRNA. The first lane was co-transfected with empty vector and scramble siRNA as a control. The second lane was co-transfected with CD24 and scrambled siRNA to up regulate Notch1 and Cten. The third lane was co-transfected with CD24 and concomitant Notch1 siRNA to test effect of knocking down of Notch1 on Cten. The fourth lane was co-transfected empty vector and Notch1-specific siRNA to confirm the reduced Cten was associated with knock down of Notch1 not with CD24 expression. (b) Densitometry of proteins normalised to β-actin.

5.3 Discussion:

Little is known about the mechanism of CD24 signalling and regulation. In this study, we investigated the signalling pathway of CD24 and whether any of its targets were related to its functional activity. Our hypothesis was that CD24 may signal thorough Notch1 and was based on published data in MCF7. Our experimental work was undertaken using a dual approach of forced expression (in a cell line does not express CD24) and gene knockdown (in a cell line with high expression of CD24). This approach does not only increase the number of cell lines tested, but also obviates over-interpretation of artefacts which are inherent within each of the individual technique. Our data have shown that, CD24 is an upstream regulator of Notch1 since forced expression of CD24 results in upregulation of Notch1 and knockdown of CD24 results in downregulation of Notch1. Interestingly, with mutation of the CD24 N-glycosylation sites, the induction of Notch1 was abrogated. Also, our data have shown that CD24 regulates Notch1 in lung cancer which could be an important pathway in this disease. More importantly, it suggests that the CD24-Notch1 signalling pathway is present in more than one organ system and it may be a generic pathway.

We investigated the mechanism through which CD24 may regulate Notch1. Quantification of Notch1 mRNA suggested that the regulation of CD24 to Notch1 is at the transcriptional level as CD24 forcibly expressed induced the mRNA level of Notch1 and CD24 knock down caused a reduction of the mRNA level of Notch1. A study done by Juyeon Lim [115] in MCF-7 cells showed that the regulation of CD24 to Notch1 mRNA was through p38MAPK. Previously, in our lab, we have shown (by Phospho-Kinase Array) that knockdown of CD24 in the CRC cell line G2PD altered the level

of activation of MAP kinase pathway. In particular, there was a change in p38MAPK which is a member of the pathway. These data were confirmed by the same group who showed that, in the MCF-7 cells, CD24 knockdown resulted in decreased p38MAPK phosphorylation. In addition, overexpression of p38MAPK resulted in increased Notch1 mRNA in MCF-7 cells. So, we assume that, CD24 may be inducing the level of Notch1 through the potential downstream target p38 MAPK.

We also investigated whether there was post-translational stabilisation of Notch1 by CD24. CD24 was shown to prevent the degradation of Notch1 protein by the Cycloheximide assay. Densitometry showed the decay of degradation of CD24 was the same whereas the degradation decay of Notch1 was quicker when CD24 was knocked down.

Following the investigation of protein regulation, a Co-IP was performed to investigate the binding interaction. CD24 did immunoprecipitate with Notch1 which indicates that these two proteins do physically interact.

The regulation of Notch1 at both transcriptional and post-transcriptional levels may be explained by feedback loops. One possible explanation is that CD24 forms a complex with Notch1 thereby stabilising Notch1. It may also have an activating effect on Notch1 by promoting proteolytic cleavage and released Notch-IC, when translocated into the nucleus, acts as transcriptional up regulator of itself as well as that of other target genes. A pathway of this type involving Notch1 already exists and involves Hes1 and , transcription factor RBP-Jk [139]. One possible explanation is as CD24 stabilising and activating Notch1 and after translocating into

the nucleus it might in turn activate the transcription of Notch1 as a result of positive feedback loop.

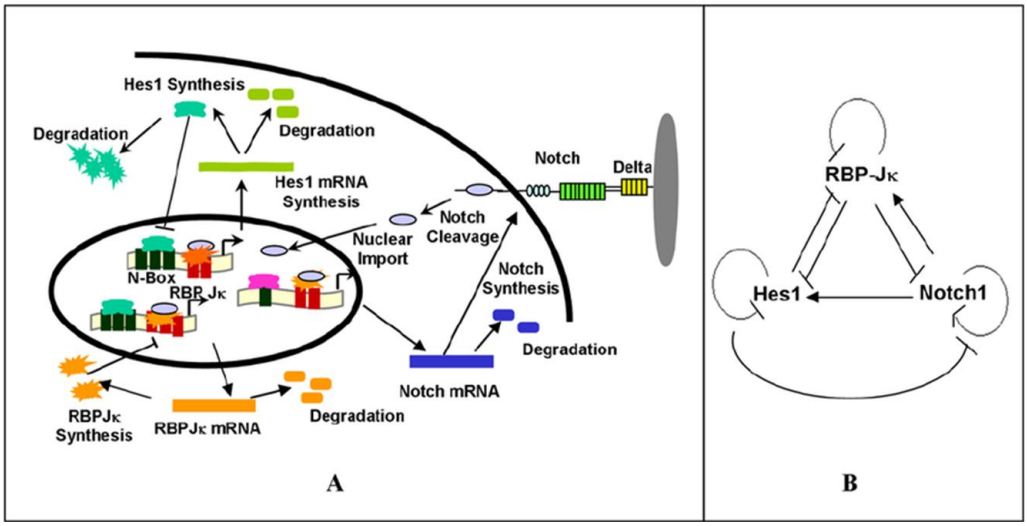


Figure 5-9 : Schematic of the Notch1-RBP-J k -Hes1 signaling network.

This figures illustrated a positive feedback loop of Notch1, following the activation of Notch1 and nuclear import of Notch1-IC into the nucleus it activates the target genes through RBP-Jk and hes1 which lead to activation of Notch1 mRNA and synthesis more Notch1 [139].

Cell fractionation technique have shown that CD24 and Notch1 localised into the cytoplasm and the nucleus and CO-IP have shown that CD24 did immunoprecipitate with Notch1 which indicate that these two proteins do physically interact and may form a complex to stabilising Notch1 as discussed previously.

Based on published data in MCF7, the role of Notch1 is in EMT-related functions such as cell migration. Having demonstrated that CD24 is a regulator of Notch1, we next investigated whether this interaction is functionally relevant. In order to achieve this, CD24 was forcibly expressed and Notch1 was simultaneously knocked down. We concluded that the positive regulation of CD24 to Notch1 is functionally relevant, as Notch1 knockdown resulted in a failure of CD24 to induce its usual effects.

Unpublished data from our lab have shown that CD24 up-regulates Cten and that induces the cell motility. These data are matching the data showing the interaction between CD24 and Notch1. Several studies have shown the regulation of Cten appears to be under the control of EGFR-Kras-mitogen activated protein kinase (MAPK) signalling pathway [140]. A study by Lim, have shown that p38MAPK which is a member of MAP kinase pathway is up regulator of Notch1 [115]. It prompted us to investigate whether there was a relationship between Cten and Notch1 or whether they interacted with CD24 independently of each other.

Modulation of Cten did not affect Notch1 levels indicating that it is not a regulator of Notch1. However, knockdown of Notch1 resulted in reduction of Cten, FAK, and ILK levels indicating that Notch1 can regulate Cten, FAK, and ILK. Forced expression of CD24 with simultaneous knock-down of Notch1 resulted in a loss of Cten induction by CD24 thereby suggesting a linear CD24-Notch1-Cten signalling pathway.

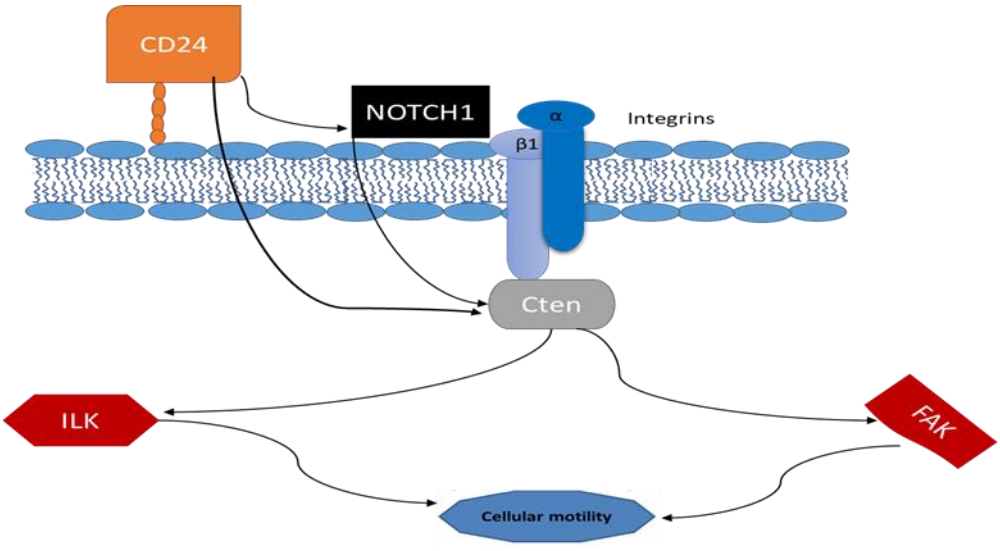


Figure 5-10 : Schematic diagram for proposed link between CD24 – Notch1-Cten-FAK-ILK.

In summary, a novel potential CD24-Notch1-Cten pathway has been discovered in colorectal cell lines, which acts to increase the cell migration. This finding sheds further light on networks regulating EMT processes in cell motility. Further work could lead to the identification of novel targets against cancer metastasis.

6. Extrinsic signalling of CD24

6.1 Introduction

Selectins are cell adhesion molecules and represent a family of molecules capable of binding to specific sugar elements on the surface of adjacent cells [141]. The selectins family has three members: P-selectin (CD62P), L-selectin (CD62L), and E-selectin (CD62E). P-selectin is expressed on the cell surface of endothelial cells and activated platelets [142]. The major ligand of P-selectin is P-selectin glycoprotein ligand-1 (PSGL-1), which is a 220 kD mucin-type glycoprotein and which carries a sulphated Tyr residue at the N-terminus. O-linked sialylLe^x glycans of the molecule seem to be important for its function [143, 144]. PSGL-1 is expressed on lymphocytes, neutrophils, CD34$^+$ early progenitor cells, and other hematopoietic cells [145]. It has been demonstrated that CD24 can act as a ligand of P-selectin [146] It has been shown that, on tumour cells, CD24 binds to P-selectin in activated platelets and endothelial cells and such binding is considered significant for breast cancer metastasis [147], [107]. In this chapter, we sought to investigate whether P-selectin represents an extrinsic signal that may stimulate CD24 signalling and whether this may occur through the N-glycosylation sites. To do so, we used recombinant P-selectin to stimulate a CD24-positive cell line (SW620) and a CD24 negative cell line (HCT116) in which CD24 had been ectopically expressed.

Aim of the study:
Investigate the extrinsic signalling of CD24.

6.2 Result:

6.2.1 Stimulating of SW620 with recombinant P-selectin

In order to ascertain whether P-selectin was able to stimulate and activate CD24 signalling, the CRC cell line SW620 (a high expressor of CD24) was exposed to recombinant P-selectin. The cells were treated with different concentrations of P-selectin (2 µg/ml, 5 µg/ml and
10 µg/ml diluted in PBS) for 30 minutes. PBS alone was used as a negative control. Since Notch1 is a target of CD24, Notch1 expression (by Western blot) was used as a downstream target of CD24 signalling. The 5 µg/ml and the 10 µg/ml concentrations resulted in an obvious increase in the expression level of CD24 and Notch1 whereas 2 µg/ml showed no effect compared to SW620 control cells stimulated with PBS only .(Figure 6-1).

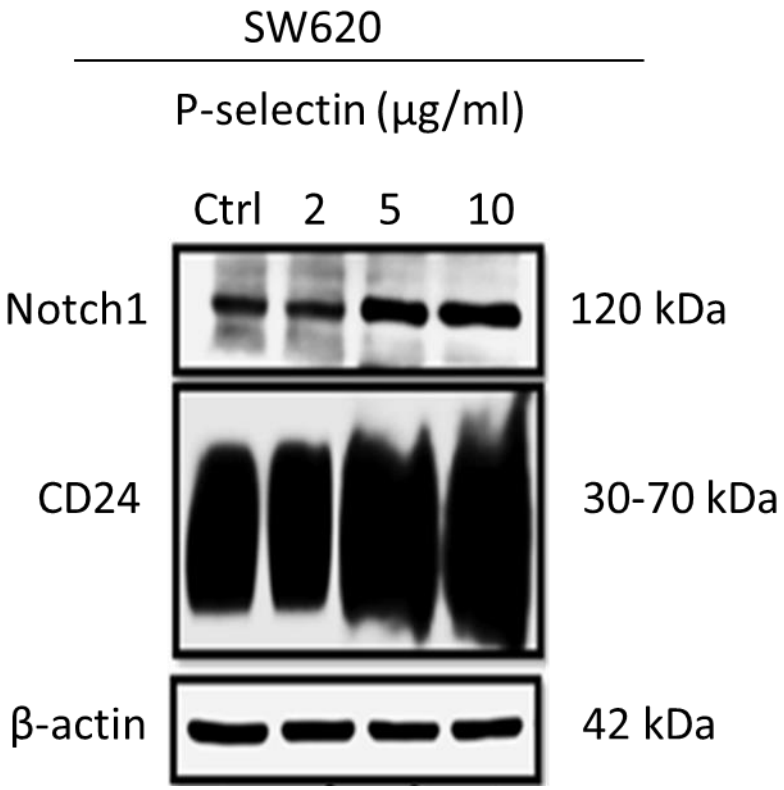


Figure 6-1: Stimulating SW620 with different P-selectin concentrations.

SW620 cell line where treated with recombinant P-selectin, cell was harvested 30 minutes after treatment and analysed by western blot. Results showed that, with

5 µg/ml and 10 µg/ml there were an obvious increase in the expression level of CD24 and Notch1 compared to control (SW620) treated with PBS only, where in 2 µg/ml there was no effect.

6.2.2 P-selectin enhances the cell motility

P-selectin was shown to up-regulate CD24 and Notch1 expression therefore suggesting it could stimulate cell motility. In order to test this, cell migration was assessed using a trans-well migration assay in a Boyden chamber and membranes. $5x10^5$ cells where seeded, and the number of migrated cells were evaluated after 48 hours. Results showed, with 5 µg/ml and 10 µg/ml, there was showed an increase in the number of cells migrating across the membrane, which was significant (p=0.0011 and, p=0.0006 respectively) whereas, with 2 µg/ml there was no effect no cell motility (p=0.7542) when compared to untreated SW620. Figure 6-2.

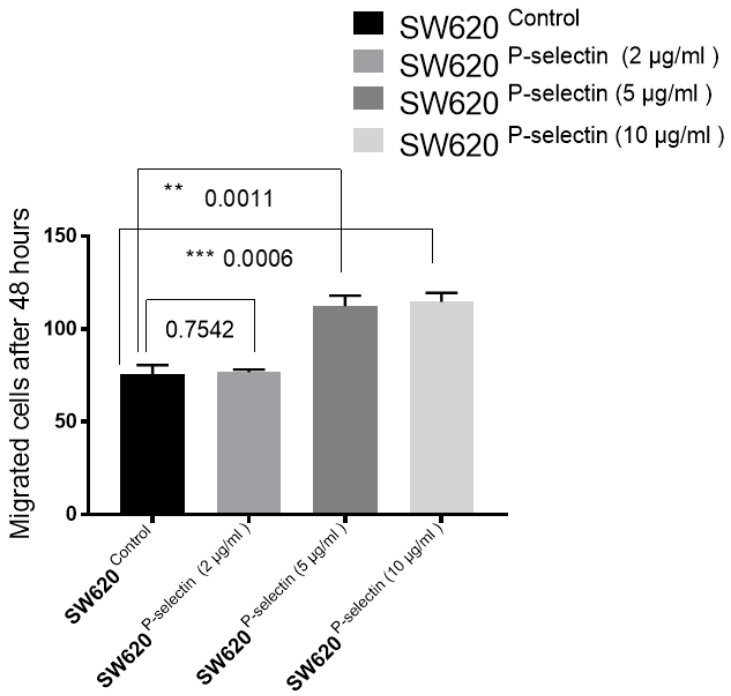


Figure 6-2 : The effect of P-selectin on the cell migration.

The 5 µg/ml and the 10 µg/ml showed increased in the cell number compared to 2 µg/ml and SW620 control treated with only PBS. All values were tested by t-test. Each experiment was repeated at least two times.

6.2.3 Cten mediates CD24/P-selectin induced motility

We were able to show that, in SW620, stimulation of CD24 with P-selectin resulted in up-regulation of Notch1 and enhanced the cell motility. We have previously shown a potential CD24-Notch1-Cten signalling pathway and, since Cten induces cell motility, it was reasonable to assume that P-selectin was stimulating this pathway. In the lab, we had available a variant of SW620 cell line which is identical to the parent SW620 except that both alleles of Cten have been mutated to make the cell line null for Cten expression ($SW620^{\Delta Cten)}$. If Cten is an important mediator of P-selectin induced motility, then $SW620^{\Delta Cten}$ should be non-responsive to stimulation with P-selectin. We sought to evaluate the effect of P-selectin on $SW620^{Cten}$ (with Cten) and $SW620^{\Delta Cten}$ (SW620 without Cten, Figure 6-4A). Cells were stimulated with P-selectin at a concentration of 10 µg/ml and harvested 30 minutes later. Western blots showed that P-selectin induced Cten expression in $SW620^{Cten}$ while $SW620^{\Delta Cten}$ showed complete absence of expression. The effect of P-selectin on cell motility was tested in this model. $5x10^5$ cells were seeded and, after 48 hours, cells which had migrated across the membrane were counted. The results showed, in $SW620^{Cten}$, there was an increase in cell migrated across the membrane treated with P-selectin compared with cells treated with carrier. In contrast, in $SW620^{\Delta Cten}$ was no change in cell motility when stimulated with P-selectin compared to stimulation with carrier (Figure 6-4B).

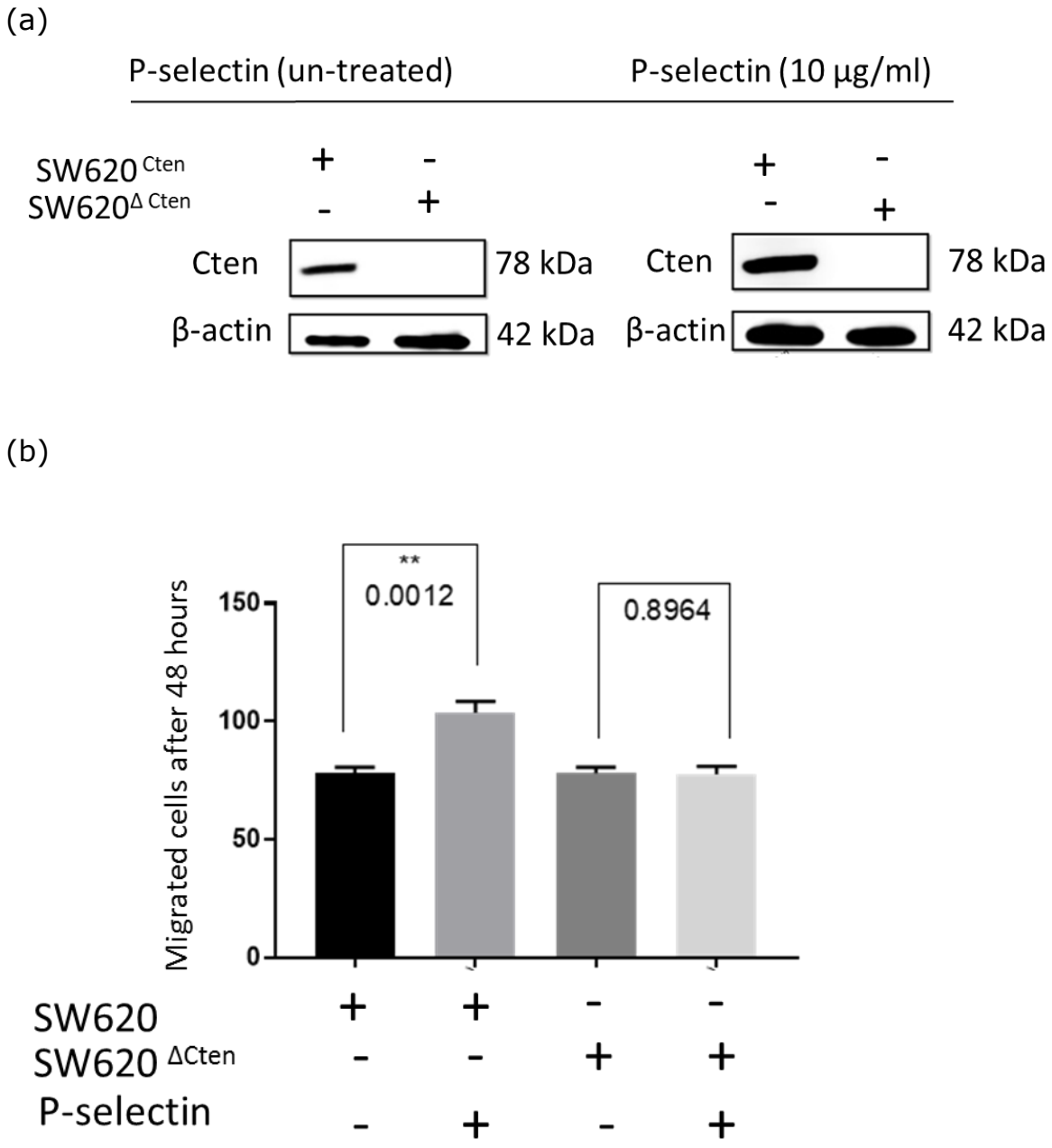


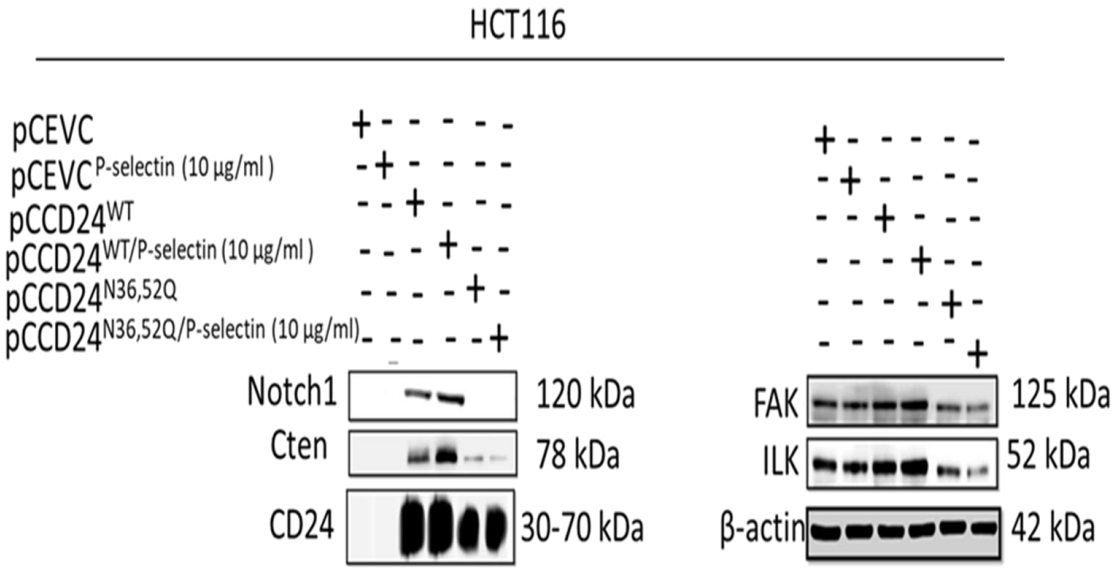
Figure 6-3 : The effect of Cten on CD24/P-selectin signalling.

(a) SW620^{Cten} and SW620$^{\Delta Cten}$ were treated with 10 ug/ml of P-selectin and analysed by western blot. Results showed, P-selectin induced Cten expression in SW620Cten while SW620$^{\Delta Cten}$ showed complete absence of expression. (b) Cell migration assay showed in SW620^{Cten} cells showed an increased in the number of migrated cells compared with carrier. In contrast, SW620$^{\Delta Cten}$ showed no change in cell motility when stimulated with P-selectin compared to stimulation with carrier.

6.2.4 The CD24/P-selectin pathway

We have shown previously that CD24 regulates Notch1, Cten, FAK, and ILK. Also, we have shown that stimulating CD24 with P-selectin increase the cell motility through Cten. Here, we sought to examine the effect of stimulating of CD24 with P-selectin on downstream targets of CD24 associated with cell motility. HCT116 cell line was transfected with the expression constructs pCCD24^{WT} (expressing CD24-wild type), pCCD24$^{N36, 52Q,}$ (expressing CD24 with loss of N-glycosylation sites) and empty vector pCEVC. Cells were treated for 30 minutes with 10 µg/ml of P-selectin and with PBS alone as control. The cells were analysed by western blot. Results showed, the HCT116 expressing wild type CD24, cells treated with P-selectin showed an obvious increase in the expression level of Notch1, Cten, FAK, and ILK compared with cells treated with PBS only. In contrast, in cells transfected with pCCD24$^{N36, 52Q}$ or with pCEVC, P-selectin stimulation had no effect on these downstream targets Figure 6-4.

(a)



(b)

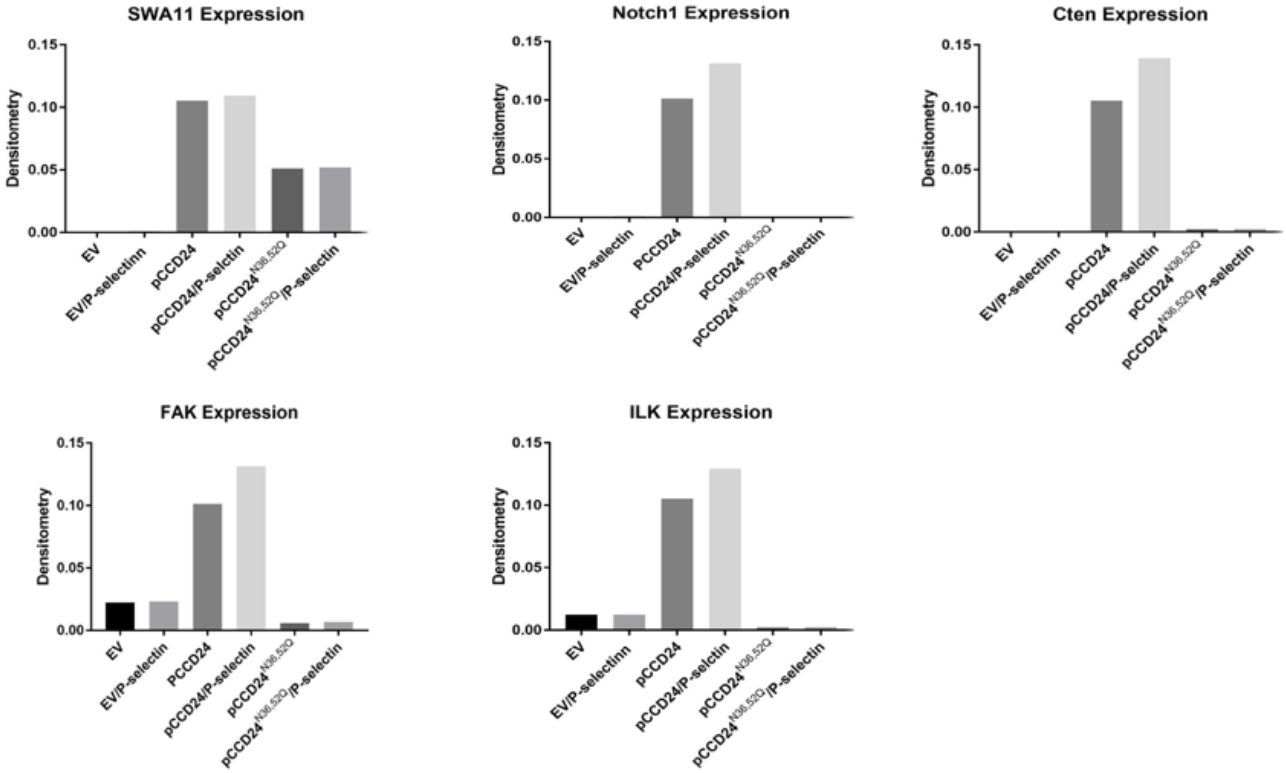


Figure 6-4: CD24/P-selectin pathway.

(a)Forced expression of pCCD24^{WT} and pCCD24$^{N36,\ 52Q}$ in HCT116 stimulated with P-selectin showed an increase in the protein level of Notch1, Cten, FAK, and ILK compared with HCT116 stimulated with PBS only. (b) Densitometry of each proteins normalised to β-actin.

6.3 Discussion

The present work was initiated by Peter Altevgot's observation [147] that CD24 acts as a ligand for P-selectin and CD24 on carcinoma cells can bind to P-selectin. In this study, we aimed to investigate the effect of stimulating CD24 with P-selectin and the effect on downstream targets associated with cell motility. Our hypothesis was that stimulating CD24 with P-selectin could increase the motility of carcinoma cells and thus enhance their ability to metastasise.

We found that, stimulating CD24 with P-selectin increased the expression level of CD24 and its downstream target Notch1. Moreover, the stimulation with P-selectin increased the motility of cells. Our observations would suggest that P-selectin, as well as promoting adhesion of CD24 bearing cells to the endothelium, is able to promote cell motility so that the cells are then more likely to migrate across the endothelium to form metastases. This hypothesis needs further testing with endothelial cells which are engineered to express P-selectin and endothelial cells in which P-selectin has been deleted.

Having shown that P-selectin induces motility in cells expressing CD24, we next investigated whether it would be through the signalling pathway we have identified. We have shown (unpublished data) that Cten is a downstream motility-inducing target of CD24 and we have shown that, a potential CD24-notch1-Cten signalling pathway. We found that Cten is an important mediator of P-selectin induced motility since SW620$^{\Delta Cten}$ (a cell line genetically identical to SW620 but null for Cten) was non-responsive to stimulation with P-selectin. We also tested the other targets known to be downstream of CD24 and we found that, on P-selectin stimulation, levels of Notch1, Cten, FAK, and ILK increased.

We have shown in the previous chapters that the N-glycosylation sites of CD24 are important for the motility-inducing activity of CD24 protein. Deletion mapping of CD24 had not identified any other functional domains but it is possible that the O-glycosylated regions could be important for signalling following binding of P-selectin. HCT116 was transfected with pCCD24^{WT} and pCCD24$^{N36, 52Q}$ to express wild type and N-glycosylation site-mutated CD24. It was responsible to assume since P-selectin enhances the cell motility it might have an effect to restore the motility. We found in CD24 with N-glycosylation mutant the protein was not responsive which indicate the motility function of CD24 is totally dependent on the N-glycosylation sites.

It can be conclude that, stimulating CD24 expressing cells with P-selectin increased the motility of the cells and may therefore enhance the ability to form metastasis. The signalling pathway of P-Seletin-CD24 appears to follow the pathway described in this thesis i.e. CD24 / Notch1 / Cten / FAK / ILK. Furthermore, the P-Seletin-CD24 signalling appears to be dependent on N-glycosylation.

7. General Discussion

7.1 Introduction

CD24 is a small (30-70 kDa), heavily glycosylated protein attached to cell membrane by a GPI anchor. Its encoding gene –is a single exon gene located on chromosome 6q21 and encodes 81 amino acids (30-70kDa). [61] Serine and threonine residues account for approximately half of the amino acids in CD24 protein [62], [63]. These represent potential sites of O-glycosylation. Additionally, there are potential sites of N-glycosylation due to the presence of asparagine. The differential glycosylation of CD24 is suggested as being the reason for variations in its molecular weight when analysed via Western blot [63], [64]. CD24 reportedly acts as a receptor for P-selectin and is expressed on a wide range of epithelial and non-epithelial cell types [65]. Recently, high CD24 expression has been reported by multiple authorities to be associated with poor outcomes in colorectal cancer [66, 67]. CD24 is broadly overexpressed in many types of tumour tissues Besides GI malignancies, CD24 expression is abundant in a variety of solid human cancers, such as squamous cell carcinoma ,gliomas, non-small-cell lung cancer, primary neuroendocrine carcinomas ,breast cancer, colorectal cancer, renal cell carcinoma, bladder carcinoma, ovarian cancer, prostate cancer [148].

7.2 Key findings

7.2.1 Removal of the N-glycosylation of CD24 caused a failure to induce the cell motility

The molecular weight of CD24 ranges from 30 to 70 kDa [149] , most of its weight is due to extensive N- and O-linked glycosylation, as it has potential O- and N-glycosylation sites. The extensive glycosylation renders to CD24 a similarity to mucin. Many studies have shown that glycosylation patterns vary widely between the tissues and these have been proposed as a factor responsible for

the broad spectrum of roles linked to CD24.Ranging from immune system regulation to auto-immune diseases, cancer cell migration, metastasis, and cancer stem cells etc [150]. There is evidence that fucosylated glycans present on CD24 enable CD24 to interact with P-selectins on endothelial cell and platelet surfaces and help in cancer cell metastasis [146]. Similarly, in neuronal tissue, the interaction between L1 and CD24 depends on α2,3-sialic acid present on CD24, and this interaction determines the CD24 induced and cell type-specific promotion or inhibition of neurite outgrowth [151]. TAG-1 and Contactin (lectin-like molecules present in lipid rafts) were also found to interact with CD24 in cerebellar and DRG(dorsal root ganglion) neurons through Lewis x glycan present on CD24 [152]. Another very recent evidence signifying role of sugars is the amelioration of sepsis by bacterial sialidases leading to the destruction of interaction between CD24-siglec-DAMP complex [153]. Protein glycosylation is seen in all eukaryotic cells. N-glycosylation of proteins is very significant and in some cases essential for cell viability. A multitude of enzymes are involved in this process and genes for these enzymes are fairly conserved amongst species. N-glycosylation is thought to help in very important physiological processes such as folding of proteins, maintaining their stability, conformation, and localization to cellular and subcellular sites. There is growing evidence about the link between N-glycosylation regulating genes and cellular growth, proliferation and various aspects of the cell cycle.

[98] . In addition, there are studies linking site specific N-glycans on proteins such as immunoglobulins and their function. Moreover increasing research have proposed a role of N-glycans in cancers [154] and based on above we hypothesized that being a heavily glycosylated molecule CD24 may also mediate its functions through its sugars. Hence, in this study, we aimed at mutating N-glycosylation sites. To achieve that, we used Site-directed

mutagenesis technique. Site-directed mutagenesis (SDM) has been a very important method to probe the function-structure relationship of proteins. So it was an ideal tool to test our hypothesis. We hypothesised removing the N-glycosylation of CD24 would result in silence or a failure to induce cancerous cells. We prevented the N-glycosylation of CD24 by site-directed mutagenesis (SDM) to remove the target Asparagine residues. This was followed by functional assays to explore the differences between the wild type CD24 protein (expressed by transfection with $pCCD24^{WT}$), CD24 protein with each of the N-glycosylation sites mutated individually (expressed through the constructs $pCCD24^{N36Q}$ and $pCCD24^{N52Q}$) as well as CD24 protein with both the N-glycosylation site mutated (expressed through the constructs $pCCD24^{N36,\ 52Q}$). The mutations induced were point mutation in which we removed asparagine and replaced it with another amino acid, glutamine. Importantly, because the glutamine has the same polarity charge as asparagine and O-glycosylation sites were not affected by these mutations as Glutamine does not bind to O-glycans [95]. The various constructs were created by site-directed mutagenesis, screened for mutation by HRM and mutations confirmed by sequencing.

The colorectal cell line, HCT116 (negative for CD24), was used for transient transfection. We forcibly expressed each of the constructs in HCT116 and performed functional assays including cell proliferation, cell motility, and cell invasion assay.

Forced expression of the CD24 which had lost one or both N-glycosylation sites ($pCCD24^{N36Q}$, $pCCD24^{N52Q}$ and $pCCD24^{N36,\ 52Q}$) in HCT116 was shown to have a significant increase in cell number compared to expression of wild type CD24 or transfection of empty vector (pCEVC). This effect was consistent in repeated experiments.

The effect of the mutation on the proliferation inducing activity of CD24 was totally unexpected. At this stage, we do not know why this is the case and we can only hypothesise that loss of the glycosylated residues may result in either escape from an inhibitor, or alternatively, the mutation may have induced this gain of a novel function through stimulating a new molecule or ligand. The latter may be more likely since we have subsequently showed that the Notch1 signalling was lost and thus it is unlikely (but not impossible) that loss of N-glycosylation would result in loss of Notch1 signalling but gain of another signalling pathway. One possibility is CD24 with loss of N-glycosylation activate PI3 kinase/AKT pathway to induce the cell proliferation as CD24-induced proliferation is dependent on the activation of PI3K/Akt [155].

We investigated the potential role of the N-glycosylation sites in the motility inducing activity of CD24. The data for both invasion and migration were similar. Ectopic expression of wild type CD24 in HCT116 was associated with an increase in cell motility when compared to the empty vector controls (pCEVC). When constructs pCCD24^{N36Q}, and pCCD24^{N52Q} were transfected into HCT116 each of the constructs induced motility compared to the empty vector controls. However the level of motility induction was significantly less than that induced by wild type CD24. When HCT116 was transfected with pCCD24$^{N36, 52Q}$ expressing CD24 with two mutated N-glycosylation sites, the level of motility was not different from that seen in the cells transfected with the empty vector controls, which conclude that the potential role of N-glycosylation is inducing cells to metastasis.

Another molecule that increases cellular characteristics quite similar

to CD24 is Cten also known as Tensin4. Recent research has shown Cten to bind with cytoplasmic tails of β integrin's cytoplasmic tail and to be present within the focal adhesions modulating proteins containing phosphorylated tyrosine residues like Focal adhesion Kinase(FAK),ILK, p130Cas and P13 kinase[138]. Our lab has identified Cten (C-terminal tensin-like) as a downstream motility inducing target of CD24 (unpublished data). We measured the level of Cten induction by western blot analysis and found that the mutations of the N-glycosylation sites reduced the Cten inducing activity of CD24. However, even with both sites mutated, Cten induction was not completely abrogated. These findings were reproducible over many experiments and seen with both mutations individually and combined.

Our observations suggest that the two N-glycosylation sites are important for CD24 function. When genes encoding them are mutated, there is loss of cell motility. At this stage we can only conjecture on the mechanism of activity. We would assume that the mutations result in loss of a ligand/receptor binding site although the nature of the ligands/receptors is not known. P-Selectin has been proposed as one possibility and this is explored in this thesis.

7.2.2 The O-glycosylation are not the functional parts of CD24

Base on the variation in molecular weight of CD24, which is due to extensive N- and O- liked glycosylation[69] and according to our previous findings on removal of the N-glycosylation which identified that the N-glycan are responsible for CD24's function. We followed our investigation to validate the N-glycosylation sites and to identify other functionality sites in CD24. We hypothesised that the N-glycosylation are responsible for CD24's function and O-glycosylation are not the functional parts of CD24. This was achieved by sequentially deleting seven amino acid segments of CD24 mature peptide without deleting the N-glycosylation sites. This was followed by functional assays to study the effect on each site segment and to explore the differences between $pCCD24^{WT}$, $pCCD24^{\Delta 7.1}$, $pCCD24^{\Delta 7.2}$, $pCCD24^{\Delta 7.3}$, and $pCCD24^{\Delta 4.4}$. The functional studies included the effect of the constructs on cell proliferation and cell motility. The constructs created by site directed mutagenesis were confirmed by sequencing.

Ectopic expression of ($pCCD24^{\Delta 7.1}$, $pCCD24^{\Delta 7.2}$, $pCCD24^{\Delta 7.3}$, and $pCCD24^{\Delta 4.4)}$ in HCT116 was shown to have no effect on cell number compared to expression of wild type CD24 or transfection of empty vector (pCEVC). This effect was consistent in repeated experiments. In cell motility, we investigated the effect of $pCCD24^{\Delta 7.1}$, $pCCD24^{\Delta 7.2}$, $pCCD24^{\Delta 7.3}$, and $pCCD24^{\Delta 4.4}$. $pCCD24^{WT}$ showed a significant increased effect on cell motility compared with an empty vector pCEVC.

We conclude from our results that N-glycosylation sites are responsible for the functionality of CD24 and the O-glycosylation are not important for defining the function of CD24. It does

however seem surprising that deletion of 7 amino acids from a 28 amino acid peptide has no effect on loss of function.

7.2.3 Notch1 is an important molecule in CD24 signalling

Although many new aspects of CD24 biology have emerged since its discovery, it is still uncertain how it mediates its effects without a transmembrane domain and much less is known about its exact signalling partners. Aberrant activation of Wnt signalling pathway is very well known and is found in almost 80% of colorectal carcinomas [156]. The presence of TCF/LEF consensus sequences in promoter region of CD24 suggests that it is target gene of Wnt signalling pathway and a recent study by Ahmed et al have shown the direct relationship between β-catenin confirming thereby CD24 as a target of Wnt signalling in the colon [157]. This association of CD24 and β-catenin has also being reported in hepatocellular carcinoma by Yang et al [158]. Being reported in hepatocellular carcinoma by Yang et al [159]Bauman et al showed that CD24 ectopic expression in breast cancer cells resulted in increased proliferation rates and the activation of the $a_3\beta_1$ and $a_4\beta_1$ integrins, which induce binding to selectins, collagen, and laminin and thus cell migration [160].

Runz et al showed that although no β1 integrin localizes to lipid raft domains in CD24-negative cells, transfection of CD24 induced the recruitment of β1 integrin into these, cholesterol and sphingolipid-enriched, membrane domains. Moreover, they also showed that CD24-transfectants increased both the invasiveness into a cushion of mixed collagens as well as the transmigration through a monolayer of endothelial cells [136] which they found to be dependent on β1 integrin. Given that CD24 is a major GPI-anchored and lipid rafts associated protein in many cell types, it might ,

therefore, act as a general "**gate-keeper''** to lipid rafts. In an attempt to further explore the downstream targets of CD24, Baumann et al in a very recent study found that in MTLy breast cancer cells CD24 interacts with and augments the kinase activity of c-src, this occurred within and was dependent upon intact lipid rafts. CD24-augmented c-src kinase activity increased the formation of focal adhesion complexes, accelerated phosphorylation of FAK and paxillin and consequently enhanced integrin-mediated adhesion [160]. Recent study has shown that Notch1 signalling activates β1-integrin which increase the celleualr adhesion to ECM [161]. CD24 reportedly regulates Notch1 in breast cancer [115]. We hypothesised that CD24 regulates Notch1 in colorectal cancer and tested it using a dual approach of forced expression and knockdown of CD24 in cell lines with low and high expressions of CD24 proteins. Forced expression of CD24 in HCT116 (a low expressor of CD24) resulted in upregulation of Notch1, and the reciprocal CD24 knockdown experiments in SW620 (a high expressor of CD24) resulted in the downregulation of Notch1.

Furthermore, these observations were also made in the lung cancer cell line A549. Based on our data and published data, it would seem that CD24 signals through Notch in at least colon, lung and breast. We can infer from this that CD24-notch1 signalling is a well conserved signalling pathway. We were able to further extend the study of CD24-Notch1 signalling and demonstrate that CD24 regulates Notch1 at transcriptional level as the mRNA level of Notch1 increased following forced expression of CD24 and decreased following knockdown of CD24.

We were also able to show that there was post-translational stabilisation of Notch1 by CD24 by the Cycloheximide assay. Densitometry showed the decay of Notch1 was quicker when CD24 was knocked down.

The direct regulation of Notch1 by up or down regulation of CD24 led us to ask whether these molecules physically interact. A co-immunoprecipitation technique showed a physical interaction between CD24 and Notch1.
Moreover, we found CD24 may regulate Notch1 in the cytoplasm and nucleus as both genes were localised into the cytoplasm and nucleus.

Having thus demonstrated that CD24 regulates Notch1, we tested the functional relationship between CD24 and Notch1 by forcibly expressing CD24 and knocking down Notch1 using a co-transfection technique. Knockdown of Notch1 resulted in a failure of the effect induced by CD24 forced expression, which showed the functional importance between CD24 and Notch1.

Our data shows that both Cten and Notch1 are downstream targets of CD24 although it was uncertain whether they represented independent signalling pathways or they were in a linear relationship. We investigated this using forced expression of Cten in HCT116 (a low expressor of Cten). Result of these experiments revealed that there is no change in the Notch1 protein level. We then knocked down Notch1 in SW620 (a high expressor of Notch1 and Cten) and found that Cten protein level decreased as Notch1 was knocked down, which suggests that Cten is a downstream target of Notch1.

As our findings indicate that Notch1 is a target of Cten, we hypothesised that Notch1 induces its functional activity through Cten. We tested this hypothesis using co-transfection where we forcibly expressed CD24 in HCT116 with a concomitant knock-down of Notch1. We found that the protein level of Cten decreased as well as FAK and ILK by knocking down Notch1, which suggests that Notch1 signals through Cten and induces its functional activity through it.

7.2.4 P-selectin stimulates CD24

One important investigation in this study was to identify CD24's extrinsic signals. A previous study found that CD24 acts as a ligand of P-selectin and shows binding as well. We hypothesised that this binding may affect CD24 signalling. This hypothesis was tested by treating cells with recombinant P-selectin and investigating the effects on downstream targets of CD24 associated with cell motility. The results showed stimulating CD24 with P-selectin enhances cell motility and induced expression of CD24. Since Cten is a target in signalling pathway of CD24, its role in CD24 signalling was tested by comparing the effect of P-selectin stimulation in SW620 (containing Cten) and SW620$^{\Delta\ Cten}$ (null for Cten). In the absence of Cten, the experiments showed cells were non-responsive to stimulation with P-selectin.

When we investigated the ability of P-selectin to activate the signalling pathway associated with cell motility we found CD24 stimulation with p-selectin induced the expression level of Notch1, Cten, FAK, and ILK.

Interestingly, we found the P-selectin could not restore the motility loss in CD24 N-glycosylation mutation as cells transfected with

pCCD24$^{N36,\ 52Q}$ were non-responsive to stimulation with P-selectin. This suggests that the functionality of CD24 may be dependent on the N-glycosylation sites.

7.3 Conclusion

To summarise, in this study we aimed to investigate the importance of CD24 N-glycosylation as functional parts of CD24. Our study has shown that the removal of N-glycosylation caused a failure to induce cell motility and cell invasion. Furthermore, we have validated the functional sites of CD24 by removing parts of the mature peptide of CD24 to map the functional sites of CD24, which revealed the N-glycosylation sites determine its functionality. Our study also showed that Notch1 is an important molecule in the signalling pathway of CD24 and represents a downstream target of CD24 and is also an up-stream target of Cten. Moreover, we found that P-selectin is a stimulator of CD24, which can increase cell motility and thus enhance the ability of carcinoma cell to metastasis.

7.4 Potential strengths

- This was the first study to investigate the N-glycosylation of CD24 *in vitro*.
- A minimum of two cell lines were used in most of the experiments.
- A dual approach of ectopic expression, knockdown and co-transfection, were sued to study CD24 signalling.
- This study was the first to show that NOTCH1 is a downstream target of CD24 in colorectal cancer and an upstream target of Cten as well as a motility inducing target.
- This also the first study to explore the effect of CD24/P-selectin on CD24's signalling pathway.

7.5 Potential weakness

- Xenografting models to study the effect of N-glycosylation *in vivo* by injecting mice with wild type CD24 and mutant CD24 and observing the live of the mice in term of cell motility and to validate the findings were obtained *in vitro*
- Due to time limitations of PhD coursework and as it was the final part of my project; I was not able to finish the CD24/P-selectin study which include CO-IP to study the physical interaction between CD24 and P-selectin.

7.6 Future suggestion and recommendation

- More cancer types' models could be used in studying the removal of N-glycosylation.
- Comparative expression profiling of cells transfected with wild type CD24 and N-glycosylation deficient CD24 (comparative expression profiling of cells transfected with wild type CD24 and N-glycosylation deficient CD24)
- Protein profiling using mass spectrometry; we could do 2D Western blotting as well.
- CD24/P-selectin needs more investigation.

8. References

1. Center, M.M., et al., *Worldwide variations in colorectal cancer.* CA Cancer J Clin, 2009. **59**(6): p. 366-78.
2. Brenner, H., M. Kloor, and C.P. Pox, *Colorectal cancer.* Lancet, 2014. **383**(9927): p. 1490-502.
3. Armaghany, T., et al., *Genetic alterations in colorectal cancer.* Gastrointest Cancer Res, 2012. **5**(1): p. 19-27.
4. Worthley, D.L. and B.A. Leggett, *Colorectal cancer: molecular features and clinical opportunities.* Clin Biochem Rev, 2010. **31**(2): p. 31-8.
5. Fearon, E.R. and B. Vogelstein, *A genetic model for colorectal tumorigenesis.* Cell, 1990. **61**(5): p. 759-67.
6. Montazer Haghighi, M., et al., *Four novel germline mutations in the MLH1 and PMS2 mismatch repair genes in patients with hereditary nonpolyposis colorectal cancer.* Int J Colorectal Dis, 2009. **24**(8): p. 885-93.
7. Boland, C.R. and A. Goel, *Microsatellite instability in colorectal cancer.* Gastroenterology, 2010. **138**(6): p. 2073-2087 e3.
8. Nazemalhosseini Mojarad, E., et al., *The CpG island methylator phenotype (CIMP) in colorectal cancer.* Gastroenterol Hepatol Bed Bench, 2013. **6**(3): p. 120-8.
9. Guinney, J., et al., *The consensus molecular subtypes of colorectal cancer.* Nat Med, 2015. **21**(11): p. 1350-6.
10. Chan, T.L., et al., *Early-onset colorectal cancer with stable microsatellite DNA and near-diploid chromosomes.* Oncogene, 2001. **20**(35): p. 4871-6.
11. Groden, J., et al., *Identification and characterization of the familial adenomatous polyposis coli gene.* Cell, 1991. **66**(3): p. 589-600.
12. Leach, F.S., et al., *Mutations of a mutS homolog in hereditary nonpolyposis colorectal cancer.* Cell, 1993. **75**(6): p. 1215-25.
13. Bronner, C.E., et al., *Mutation in the DNA mismatch repair gene homologue hMLH1 is associated with hereditary non-polyposis colon cancer.* Nature, 1994. **368**(6468): p. 258-61.
14. Grady, W.M. and J.M. Carethers, *Genomic and epigenetic instability in colorectal cancer pathogenesis.* Gastroenterology, 2008. **135**(4): p. 1079-1099.
15. Goel, A., et al., *The CpG island methylator phenotype and chromosomal instability are inversely correlated in sporadic colorectal cancer.* Gastroenterology, 2007. **132**(1): p. 127-138.
16. Walther, A., R. Houlston, and I. Tomlinson, *Association between chromosomal instability and prognosis in colorectal cancer: a meta-analysis.* Gut, 2008.
17. Bellam, N. and B. Pasche, *TGF-β signaling alterations and colon cancer*, in *Cancer Genetics*. 2010, Springer. p. 85-103.
18. Pritchard, C.C. and W.M. Grady, *Colorectal cancer molecular biology moves into clinical practice.* Gut, 2011. **60**(1): p. 116-129.
19. Chiaravalli, A.M., et al., *Immunohistochemical pattern of hMSH2/hMLH1 in familial and sporadic colorectal, gastric, endometrial and ovarian carcinomas with instability in microsatellite sequences.* Virchows Archiv, 2001. **438**(1): p. 39-48.
20. Vilar, E. and S.B. Gruber, *Microsatellite instability in colorectal cancer—the stable evidence.* Nature reviews Clinical oncology, 2010. **7**(3): p. 153.

21. Bellizzi, A.M. and W.L. Frankel, *Colorectal cancer due to deficiency in DNA mismatch repair function: a review.* Advances in anatomic pathology, 2009. **16**(6): p. 405-417.
22. Auclair, J., et al., *Intensity - dependent constitutional MLH1 promoter methylation leads to early onset of colorectal cancer by affecting both alleles.* Genes, Chromosomes and Cancer, 2011. **50**(3): p. 178-185.
23. Bacher, J.W., et al., *Development of a fluorescent multiplex assay for detection of MSI-High tumors.* Disease markers, 2004. **20**(4, 5): p. 237-250.
24. Guastadisegni, C., et al., *Microsatellite instability as a marker of prognosis and response to therapy: a meta-analysis of colorectal cancer survival data.* European journal of cancer, 2010. **46**(15): p. 2788-2798.
25. Halford, S., et al., *Low-level microsatellite instability occurs in most colorectal cancers and is a nonrandomly distributed quantitative trait.* Cancer research, 2002. **62**(1): p. 53-57.
26. Kim, Y.H., et al., *Sporadic colorectal carcinomas with low - level microsatellite instability in Korea: Do they form a distinct subgroup with distinguished clinicopathological features?* Journal of surgical oncology, 2009. **99**(6): p. 351-355.
27. Samowitz, W.S., et al., *Evaluation of a large, population-based sample supports a CpG island methylator phenotype in colon cancer.* Gastroenterology, 2005. **129**(3): p. 837-45.
28. Shen, L., et al., *Integrated genetic and epigenetic analysis identifies three different subclasses of colon cancer.* Proc Natl Acad Sci U S A, 2007. **104**(47): p. 18654-9.
29. Ogino, S., et al., *Correlation of pathologic features with CpG island methylator phenotype (CIMP) by quantitative DNA methylation analysis in colorectal carcinoma.* Am J Surg Pathol, 2006. **30**(9): p. 1175-83.
30. Dong, S.M., et al., *Progressive methylation during the serrated neoplasia pathway of the colorectum.* Mod Pathol, 2005. **18**(2): p. 170-8.
31. Petko, Z., et al., *Aberrantly methylated CDKN2A, MGMT, and MLH1 in colon polyps and in fecal DNA from patients with colorectal polyps.* Clin Cancer Res, 2005. **11**(3): p. 1203-9.
32. Ogino, S., et al., *Lymphocytic reaction to colorectal cancer is associated with longer survival, independent of lymph node count, microsatellite instability, and CpG island methylator phenotype.* Clin Cancer Res, 2009. **15**(20): p. 6412-20.
33. Spring, K.J., et al., *High prevalence of sessile serrated adenomas with BRAF mutations: a prospective study of patients undergoing colonoscopy.* Gastroenterology, 2006. **131**(5): p. 1400-7.
34. Torlakovic, E. and D.C. Snover, *Serrated adenomatous polyposis in humans.* Gastroenterology, 1996. **110**(3): p. 748-55.
35. Kambara, T., et al., *BRAF mutation is associated with DNA methylation in serrated polyps and cancers of the colorectum.* Gut, 2004. **53**(8): p. 1137-44.
36. Ogino, S., et al., *Molecular correlates with MGMT promoter methylation and silencing support CpG island methylator phenotype-low (CIMP-low) in colorectal cancer.* Gut, 2007. **56**(11): p. 1564-71.

37. Shima, K., et al., *MGMT promoter methylation, loss of expression and prognosis in 855 colorectal cancers.* Cancer Causes Control, 2011. **22**(2): p. 301-9.
38. Misale, S., et al., *Emergence of KRAS mutations and acquired resistance to anti-EGFR therapy in colorectal cancer.* Nature, 2012. **486**(7404): p. 532-6.
39. Spano, D., et al., *Molecular networks that regulate cancer metastasis.* Semin Cancer Biol, 2012. **22**(3): p. 234-49.
40. Lamouille, S., J. Xu, and R. Derynck, *Molecular mechanisms of epithelial-mesenchymal transition.* Nat Rev Mol Cell Biol, 2014. **15**(3): p. 178-96.
41. Bravo-Cordero, J.J., L. Hodgson, and J. Condeelis, *Directed cell invasion and migration during metastasis.* Curr Opin Cell Biol, 2012. **24**(2): p. 277-83.
42. Provenzano, P.P., et al., *Collagen reorganization at the tumor-stromal interface facilitates local invasion.* BMC Med, 2006. **4**(1): p. 38.
43. Yilmaz, M. and G. Christofori, *Mechanisms of motility in metastasizing cells.* Mol Cancer Res, 2010. **8**(5): p. 629-42.
44. Taddei, M.L., et al., *Mesenchymal to amoeboid transition is associated with stem-like features of melanoma cells.* Cell Commun Signal, 2014. **12**: p. 24.
45. Weidner, N., *New paradigm for vessel intravasation by tumor cells.* Am J Pathol, 2002. **160**(6): p. 1937-9.
46. Mukherjee, D. and J. Zhao, *The Role of chemokine receptor CXCR4 in breast cancer metastasis.* Am J Cancer Res, 2013. **3**(1): p. 46-57.
47. Murakami, T., et al., *The role of CXCR3 and CXCR4 in colorectal cancer metastasis.* Int J Cancer, 2013. **132**(2): p. 276-87.
48. Brabletz, T., et al., *Variable beta-catenin expression in colorectal cancers indicates tumor progression driven by the tumor environment.* Proc Natl Acad Sci U S A, 2001. **98**(18): p. 10356-61.
49. Tsai, J.H., et al., *Spatiotemporal regulation of epithelial-mesenchymal transition is essential for squamous cell carcinoma metastasis.* Cancer Cell, 2012. **22**(6): p. 725-36.
50. Paget, S., *The distribution of secondary growths in cancer of the breast. 1889.* Cancer Metastasis Rev, 1889. **8**(2): p. 98-101.
51. Kaplan, R.N., et al., *VEGFR1-positive haematopoietic bone marrow progenitors initiate the pre-metastatic niche.* Nature, 2005. **438**(7069): p. 820-7.
52. Pang, R., et al., *A subpopulation of CD26+ cancer stem cells with metastatic capacity in human colorectal cancer.* Cell Stem Cell, 2010. **6**(6): p. 603-15.
53. Hermann, P.C., et al., *Distinct populations of cancer stem cells determine tumor growth and metastatic activity in human pancreatic cancer.* Cell Stem Cell, 2007. **1**(3): p. 313-23.
54. Brabletz, T., et al., *Opinion: migrating cancer stem cells - an integrated concept of malignant tumour progression.* Nat Rev Cancer, 2005. **5**(9): p. 744-9.
55. Mani, S.A., et al., *The epithelial-mesenchymal transition generates cells with properties of stem cells.* Cell, 2008. **133**(4): p. 704-15.
56. Ocana, O.H., et al., *Metastatic colonization requires the repression of the epithelial-mesenchymal transition inducer Prrx1.* Cancer Cell, 2012. **22**(6): p. 709-24.
57. Shih, T. and C. Lindley, *Bevacizumab: an angiogenesis inhibitor for the treatment of solid malignancies.* Clin Ther, 2006. **28**(11): p. 1779-802.

58. Holland, S.J., et al., *R428, a selective small molecule inhibitor of Axl kinase, blocks tumor spread and prolongs survival in models of metastatic breast cancer.* Cancer Res, 2010. **70**(4): p. 1544-54.
59. Myers, S.H., V.G. Brunton, and A. Unciti-Broceta, *AXL Inhibitors in Cancer: A Medicinal Chemistry Perspective.* J Med Chem, 2015.
60. Springer, T., et al., *Monoclonal xenogeneic antibodies to murine cell surface antigens: identification of novel leukocyte differentiation antigens.* European journal of immunology, 1978. **8**(8): p. 539-551.
61. Kristiansen, G., M. Sammar, and P. Altevogt, *Tumour biological aspects of CD24, a mucin-like adhesion molecule.* J Mol Histol, 2004. **35**(3): p. 255-62.
62. *Recommendations for genetic counseling, molecular diagnosis and clinical management of familial adenomatous polyposis. Working group of the Special Project of the Italian Association for Cancer Research (AIRC) "Inherited Colon Cancer".* Tumori, 1997. **83**(5): p. 789-90.
63. Kay, R., F. Takei, and R.K. Humphries, *Expression cloning of a cDNA encoding M1/69-J11d heat-stable antigens.* J Immunol, 1990. **145**(6): p. 1952-9.
64. Kay, R., P.M. Rosten, and R.K. Humphries, *CD24, a signal transducer modulating B cell activation responses, is a very short peptide with a glycosyl phosphatidylinositol membrane anchor.* J Immunol, 1991. **147**(4): p. 1412-6.
65. Aigner, S., et al., *CD24, a mucin-type glycoprotein, is a ligand for P-selectin on human tumor cells.* Blood, 1997. **89**(9): p. 3385-95.
66. Sagiv, E., et al., *CD24 is a new oncogene, early at the multistep process of colorectal cancer carcinogenesis.* Gastroenterology, 2006. **131**(2): p. 630-9.
67. Weichert, W., et al., *Cytoplasmic CD24 expression in colorectal cancer independently correlates with shortened patient survival.* Clin Cancer Res, 2005. **11**(18): p. 6574-81.
68. Ahmed, F., et al., *GFP expression in the mammary gland for imaging of mammary tumor cells in transgenic mice.* Cancer Res, 2002. **62**(24): p. 7166-9.
69. Kay, R., P. Rosten, and R. Humphries, *CD24, a signal transducer modulating B cell activation responses, is a very short peptide with a glycosyl phosphatidylinositol membrane anchor.* The Journal of Immunology, 1991. **147**(4): p. 1412-1416.
70. Tan, Y., et al., *CD24: from a hematopoietic differentiation antigen to a genetic risk factor for multiple autoimmune diseases.* Clinical reviews in allergy & immunology, 2016. **50**(1): p. 70-83.
71. Fang, X., et al., *CD24: from A to Z.* Cellular & molecular immunology, 2010. **7**(2): p. 100-103.
72. Duckworth, C.A., D. Clyde, and D.M. Pritchard, *CD24 is expressed in gastric parietal cells and regulates apoptosis and the response to Helicobacter felis infection in the murine stomach.* American Journal of Physiology-Gastrointestinal and Liver Physiology, 2012. **303**(8): p. G915-G926.
73. Diaz-Gallo, L.-M., et al., *Analysis of the influence of two CD24 genetic variants in Crohn's disease and ulcerative colitis.* Human immunology, 2011. **72**(10): p. 969-972.

74. Suzuki, T., et al., *CD24 induces apoptosis in human B cells via the glycolipid-enriched membrane domains/rafts-mediated signaling system.* The Journal of Immunology, 2001. **166**(9): p. 5567-5577.
75. Li, O., P. Zheng, and Y. Liu, *CD24 expression on T cells is required for optimal T cell proliferation in lymphopenic host.* Journal of Experimental Medicine, 2004. **200**(8): p. 1083-1089.
76. Liu, Y., G.-Y. Chen, and P. Zheng, *CD24-Siglec G/10 discriminates danger-from pathogen-associated molecular patterns.* Trends in immunology, 2009. **30**(12): p. 557-561.
77. Valet, G., et al., *Pretherapeutic identification of high-risk acute myeloid leukemia (AML) patients from immunophenotypic, cytogenetic, and clinical parameters.* Cytometry B Clin Cytom, 2003. **53**(1): p. 4-10.
78. Lavabre-Bertrand, T., et al., *Quantification of CD24 and CD45 antigens in parallel allows a precise determination of B-cell maturation stages: relevance for the study of B-cell neoplasias.* Leukemia, 1994. **8**(3): p. 402-8.
79. Fogel, M., et al., *CD24 is a marker for human breast carcinoma.* Cancer Lett, 1999. **143**(1): p. 87-94.
80. Sorbello, V., et al., *Quantitative real-time RT-PCR analysis of eight novel estrogen-regulated genes in breast cancer.* Int J Biol Markers, 2003. **18**(2): p. 123-9.
81. Kristiansen, G., et al., *CD24 expression is a new prognostic marker in breast cancer.* Clin Cancer Res, 2003. **9**(13): p. 4906-13.
82. Al-Hajj, M., et al., *Prospective identification of tumorigenic breast cancer cells.* Proc Natl Acad Sci U S A, 2003. **100**(7): p. 3983-8.
83. Zheng, J., et al., *NDRG2 inhibits hepatocellular carcinoma adhesion, migration and invasion by regulating CD24 expression.* BMC Cancer, 2011. **11**: p. 251:1-9.
84. Aigner, S., et al., *CD24 mediates rolling of breast carcinoma cells on P-selectin.* FASEB J, 1998. **12**(12): p. 1241-51.
85. Lee, H.J., et al., *CD24, a novel cancer biomarker, predicting disease-free survival of non-small cell lung carcinomas: a retrospective study of prognostic factor analysis from the viewpoint of forthcoming (seventh) new TNM classification.* J Thorac Oncol, 2010. **5**(5): p. 649-57.
86. Fang, X., et al., *CD24: from A to Z.* Cell Mol Immunol, 2010. **7**(2): p. 100-3.
87. Kornfeld, R. and S. Kornfeld, *Assembly of asparagine-linked oligosaccharides.* Annu Rev Biochem, 1985. **54**: p. 631-64.
88. Tanner, W. and L. Lehle, *Protein glycosylation in yeast.* Biochim Biophys Acta, 1987. **906**(1): p. 81-99.
89. Kinoshita, T., N. Inoue, and J. Takeda, *Defective glycosyl phosphatidylinositol anchor synthesis and paroxysmal nocturnal hemoglobinuria.* Adv Immunol, 1995. **60**: p. 57-103.
90. Sagiv, E. and N. Arber, *The novel oncogene CD24 and its arising role in the carcinogenesis of the GI tract: from research to therapy.* Expert Rev Gastroenterol Hepatol, 2008. **2**(1): p. 125-33.
91. Varelas, X., M.P. Bouchie, and M.A. Kukuruzinska, *Protein N-glycosylation in oral cancer: dysregulated cellular networks among DPAGT1, E-cadherin adhesion and canonical Wnt signaling.* Glycobiology, 2014. **24**(7): p. 579-591.

92. Aebi, M., *N-linked protein glycosylation in the ER.* Biochimica et Biophysica Acta (BBA)-Molecular Cell Research, 2013. **1833**(11): p. 2430-2437.
93. Bennett, E.P., et al., *Control of mucin-type O-glycosylation: a classification of the polypeptide GalNAc-transferase gene family.* Glycobiology, 2011. **22**(6): p. 736-756.
94. Ma, J. and G.W. Hart, *O-GlcNAc profiling: from proteins to proteomes.* Clinical proteomics, 2014. **11**(1): p. 8.
95. Bause, E. and G. Legler, *The role of the hydroxy amino acid in the triplet sequence Asn-Xaa-Thr (Ser) for the N-glycosylation step during glycoprotein biosynthesis.* Biochemical Journal, 1981. **195**(3): p. 639-644.
96. Drake, R.R., et al., *Chapter Ten-Altered Glycosylation in Prostate Cancer.* Advances in cancer research, 2015. **126**: p. 345-382.
97. Pinho, S.S. and C.A. Reis, *Glycosylation in cancer: mechanisms and clinical implications.* Nature Reviews Cancer, 2015. **15**(9): p. 540.
98. Han, M., et al., *The role of N-glycosylation sites in the activity, stability, and expression of the recombinant elastase expressed by Pichia pastoris.* Enzyme and microbial technology, 2014. **54**: p. 32-37.
99. Brockhausen, I., J. Schutzbach, and W. Kuhns, *Glycoproteins and their relationship to human disease.* Cells Tissues Organs, 1998. **161**(1-4): p. 36-78.
100. Brockhausen, I., *Pathways of O-glycan biosynthesis in cancer cells.* Biochimica et Biophysica Acta (BBA)-General Subjects, 1999. **1473**(1): p. 67-95.
101. Sethi, M.K., et al., *In-depth N-glycome profiling of paired colorectal cancer and non-tumorigenic tissues reveals cancer-, stage-and EGFR-specific protein N-glycosylation.* Glycobiology, 2015. **25**(10): p. 1064-1078.
102. Kaprio, T., et al., *N-glycomic profiling as a tool to separate rectal adenomas from carcinomas.* Molecular & Cellular Proteomics, 2015. **14**(2): p. 277-288.
103. Padler-Karavani, V., *Aiming at the sweet side of cancer: aberrant glycosylation as possible target for personalized-medicine.* Cancer letters, 2014. **352**(1): p. 102-112.
104. Haakensen, V.D., et al., *Serum N‐glycan analysis in breast cancer patients–Relation to tumour biology and clinical outcome.* Molecular oncology, 2016. **10**(1): p. 59-72.
105. Bleckmann, C., et al., *Glycomic analysis of N-linked carbohydrate epitopes from CD24 of mouse brain.* Journal of proteome research, 2008. **8**(2): p. 567-582.
106. Kobata, A., *A journey to the world of glycobiology.* Glycoconjugate journal, 2000. **17**(7): p. 443-464.
107. Friederichs, J., et al., *The CD24/P-selectin binding pathway initiates lung arrest of human A125 adenocarcinoma cells.* Cancer research, 2000. **60**(23): p. 6714-6722.
108. Kneuer, C., et al., *Selectins–potential pharmacological targets?* Drug discovery today, 2006. **11**(21): p. 1034-1040.
109. Ohl, C., et al., *N-glycosylation patterns of HSA/CD24 from different cell lines and brain homogenates: a comparison.* Biochimie, 2003. **85**(6): p. 565-573.
110. Varki, A. and T. Angata, *Siglecs—the major subfamily of I-type lectins.* Glycobiology, 2005. **16**(1): p. 1R-27R.

111. Baumann, P., et al., *CD24 expression causes the acquisition of multiple cellular properties associated with tumor growth and metastasis.* Cancer research, 2005. **65**(23): p. 10783-10793.
112. Kadmon, G., et al., *Evidence for Cis Interaction and Cooperative Signalling by the Heat - stable Antigen Nectadrin (murine CD24) and the Cell Adhesion Molecule L1 in Neurons.* European Journal of Neuroscience, 1995. **7**(5): p. 993-1004.
113. Lieberoth, A., et al., *Lewisx and α2, 3-sialyl glycans and their receptors TAG-1, Contactin, and L1 mediate CD24-dependent neurite outgrowth.* Journal of Neuroscience, 2009. **29**(20): p. 6677-6690.
114. Kleene, R., et al., *The neural recognition molecule L1 is a sialic acid-binding lectin for CD24, which induces promotion and inhibition of neurite outgrowth.* Journal of Biological Chemistry, 2001. **276**(24): p. 21656-21663.
115. Lim, J., et al., *CD24 regulates stemness and the epithelial to mesenchymal transition through modulation of Notch1 mRNA stability by p38MAPK.* Archives of biochemistry and biophysics, 2014. **558**: p. 120-126.
116. Leong, K.G. and A. Karsan, *Recent insights into the role of Notch signaling in tumorigenesis.* Blood, 2006. **107**(6): p. 2223-2233.
117. Albasri, A., et al., *C-terminal Tensin-like (CTEN) is an oncogene which alters cell motility possibly through repression of E-cadherin in colorectal cancer.* J Pathol, 2009. **218**(1): p. 57-65.
118. Albasri, A., et al., *Cten signals through integrin-linked kinase (ILK) and may promote metastasis in colorectal cancer.* Oncogene, 2011. **30**(26): p. 2997-3002.
119. Al-Ghamdi, S., et al., *Cten Is Targeted by Kras Signalling to Regulate Cell Motility in the Colon and Pancreas.* PLoS ONE, 2011. **6**(6): p. e20919.
120. Bretz, N.P., et al., *CD24 controls Src/STAT3 activity in human tumors.* Cellular and Molecular Life Sciences, 2012: p. 1-17.
121. Lee, T.K., et al., *CD24(+) liver tumor-initiating cells drive self-renewal and tumor initiation through STAT3-mediated NANOG regulation.* Cell Stem Cell, 2011. **9**(1): p. 50-63.
122. Barbieri, I., et al., *Constitutively active Stat3 enhances neu-mediated migration and metastasis in mammary tumors via upregulation of Cten.* Cancer Res, 2010. **70**(6): p. 2558-67.
123. Schaller, M.D., et al., *pp125FAK a structurally distinctive protein-tyrosine kinase associated with focal adhesions.* Proc Natl Acad Sci U S A, 1992. **89**(11): p. 5192-6.
124. Scheswohl, D.M., et al., *Multiple paxillin binding sites regulate FAK function.* J Mol Signal, 2008. **3**: p. 1.
125. Wade, R., et al., *Paxillin enables attachment-independent tyrosine phosphorylation of focal adhesion kinase and transformation by RAS.* J Biol Chem, 2011. **286**(44): p. 37932-44.
126. Lark, A.L., et al., *Overexpression of focal adhesion kinase in primary colorectal carcinomas and colorectal liver metastases: immunohistochemistry and real-time PCR analyses.* Clin Cancer Res, 2003. **9**(1): p. 215-22.
127. Sulzmaier, F.J., C. Jean, and D.D. Schlaepfer, *FAK in cancer: mechanistic findings and clinical applications.* Nat Rev Cancer, 2014. **14**(9): p. 598-610.

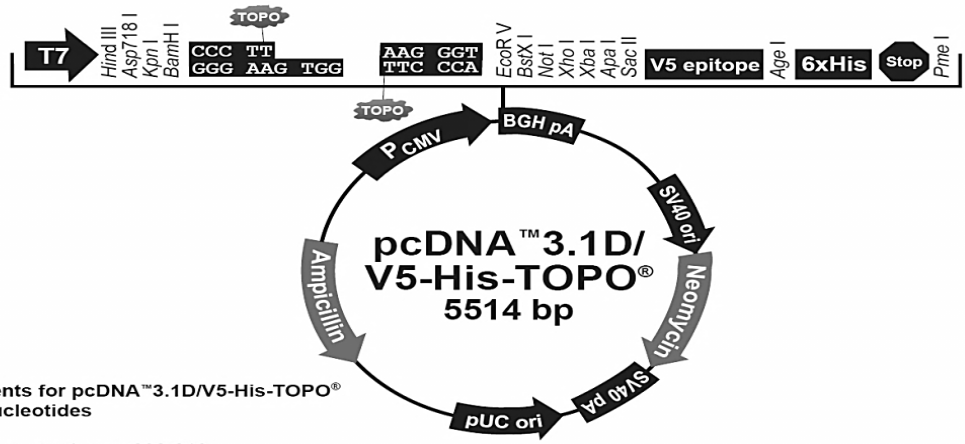
128. Baumann, P., et al., *CD24 interacts with and promotes the activity of c-src within lipid rafts in breast cancer cells, thereby increasing integrin-dependent adhesion.* Cellular and molecular life sciences : CMLS, 2011.
129. Persad, S. and S. Dedhar, *The role of integrin-linked kinase (ILK) in cancer progression.* Cancer and Metastasis Reviews, 2003. **22**(4): p. 375-384.
130. Han, K.S., et al., *Targeting Integrin-Linked Kinase Suppresses Invasion and Metastasis through Downregulation of Epithelial-to-Mesenchymal Transition in Renal Cell Carcinoma.* Mol Cancer Ther, 2015. **14**(4): p. 1024-34.
131. Elad, N., et al., *The role of integrin-linked kinase in the molecular architecture of focal adhesions.* J Cell Sci, 2013. **126**(Pt 18): p. 4099-107.
132. Bravou, V., et al., *ILK over‐expression in human colon cancer progression correlates with activation of β‐catenin, down‐regulation of E‐cadherin and activation of the Akt–FKHR pathway.* The Journal of pathology, 2006. **208**(1): p. 91-99.
133. Springer, T.A. and M.I. Cybulsky, *Traffic signals on endothelium for leukocytes in health, inflammation, and atherosclerosis.* Atherosclerosis and coronary artery disease, 1996. **1**: p. 511-38.
134. Sahai, E., et al., *Smurf1 regulates tumor cell plasticity and motility through degradation of RhoA leading to localized inhibition of contractility.* J Cell Biol, 2007. **176**(1): p. 35-42.
135. Schabath, H., et al., *CD24 affects CXCR4 function in pre-B lymphocytes and breast carcinoma cells.* Journal of cell science, 2006. **119**(2): p. 314-325.
136. Runz, S., et al., *CD24 induces localization of β1 integrin to lipid raft domains.* Biochemical and biophysical research communications, 2008. **365**(1): p. 35-41.
137. Scott, M.S., et al., *Refining protein subcellular localization.* PLoS computational biology, 2005. **1**(6): p. e66.
138. Albasri, A., et al., *Cten signals through integrin-linked kinase (ILK) and may promote metastasis in colorectal cancer.* Oncogene, 2011. **30**(26): p. 2997.
139. Lu, F.M. and S.E. Lux, *Constitutively active human Notch1 binds to the transcription factor CBF1 and stimulates transcription through a promoter containing a CBF1-responsive element.* Proceedings of the National Academy of Sciences, 1996. **93**(11): p. 5663-5667.
140. Chan, L.-K., et al., *Tensin4 is up-regulated by EGF-induced ERK1/2 activity and promotes cell proliferation and migration in hepatocellular carcinoma.* Oncotarget, 2015. **6**(25): p. 20964.
141. Bevilacqua, M.P. and R.M. Nelson, *Selectins.* Journal of Clinical Investigation, 1993. **91**(2): p. 379.
142. Larsen, E., et al., *PADGEM protein: a receptor that mediates the interaction of activated platelets with neutrophils and monocytes.* Cell, 1989. **59**(2): p. 305-312.
143. Moore, K.L., et al., *Identification of a specific glycoprotein ligand for P-selectin (CD62) on myeloid cells.* The Journal of cell biology, 1992. **118**(2): p. 445-456.
144. Moore, K.L., et al., *The P-selectin glycoprotein ligand from human neutrophils displays sialylated, fucosylated, O-linked poly-N-*

acetyllactosamine. Journal of Biological Chemistry, 1994. **269**(37): p. 23318-23327.
145. Zannettino, A., et al., *Primitive human hematopoietic progenitors adhere to P-selectin (CD62P).* Blood, 1995. **85**(12): p. 3466-3477.
146. Aigner, S., et al., *CD24, a mucin-type glycoprotein, is a ligand for P-selectin on human tumor cells.* Blood, 1997. **89**(9): p. 3385-3395.
147. Aigner, S., et al., *CD24 mediates rolling of breast carcinoma cells on P-selectin.* The FASEB journal, 1998. **12**(12): p. 1241-1251.
148. Overdevest, J.B., et al., *CD24 expression is important in male urothelial tumorigenesis and metastasis in mice and is androgen regulated.* Proc Natl Acad Sci U S A, 2012. **109**(51): p. E3588-96.
149. Coccia, E., et al., *Journal of Biological Regulators and Homeostatic Agents.* Differential regulation of ferritin expression in Friend leukemia cells by iron compounds, 1994. **8**: p. 81-87.
150. Motari, E., et al., *Analysis of recombinant CD24 glycans by MALDI-TOF-MS reveals prevalence of sialyl-T antigen.* American journal of biomedical sciences, 2009. **1**(1): p. 1.
151. Kleene, R., et al., *The neural recognition molecule L1 is a sialic acid binding lectin for CD24, which induces promotion and inhibition of neurite outgrowth.* Journal of Biological Chemistry, 2001.
152. Hennen, E. and A. Faissner, *LewisX: A neural stem cell specific glycan?* The international journal of biochemistry & cell biology, 2012. **44**(6): p. 830-833.
153. Paulson, J.C. and N. Kawasaki, *Sialidase inhibitors DAMPen sepsis.* Nature biotechnology, 2011. **29**(5): p. 406.
154. Bironaite, D., et al., *N-Glycans influence the in vitro adhesive and invasive behaviour of three metastatic cell lines.* Tumor biology, 2000. **21**(3): p. 165-175.
155. Nakamura, K., et al., *CD24 expression is a marker for predicting clinical outcome and regulates the epithelial-mesenchymal transition in ovarian cancer via both the Akt and ERK pathways.* Oncology reports, 2017. **37**(6): p. 3189-3200.
156. Takahashi-Yanaga, F. and M. Kahn, *Targeting Wnt signaling: can we safely eradicate cancer stem cells?* Clinical cancer research, 2010: p. 1078-0432. CCR-09-2943.
157. Ahmed, M.A., et al., *CD24 is upregulated in inflammatory bowel disease and stimulates cell motility and colony formation.* Inflammatory bowel diseases, 2009. **16**(5): p. 795-803.
158. Yang, X.-R., et al., *CD24 is a novel predictor for poor prognosis of hepatocellular carcinoma after surgery.* Clinical Cancer Research, 2009: p. 1078-0432. CCR-09-0151.
159. Yang, X.R., et al., *CD24 is a novel predictor for poor prognosis of hepatocellular carcinoma after surgery.* Clinical Cancer Research, 2009. **15**(17): p. 5518-5527.
160. Baumann, P., et al., *CD24 interacts with and promotes the activity of c-src within lipid rafts in breast cancer cells, thereby increasing integrin-dependent adhesion.* Cellular and Molecular Life Sciences, 2012. **69**(3): p. 435-448.

161. Hodkinson, P.S., et al., *Mammalian NOTCH-1 activates β1 integrins via the small GTPase R-Ras.* Journal of Biological Chemistry, 2007. **282**(39): p. 28991-29001.

9. Appendices

9.1 Vector map of His Topo Cloning Vector 3.1.



Comments for pcDNA™3.1D/V5-His-TOPO®
5514 nucleotides

CMV promoter: bases 232-819
T7 promoter/priming site: bases 863-882
TOPO® recognition site 1: bases 930-934
Overhang sequence (complementary strand): bases 935-938
TOPO® recognition site 2: bases 939-943
V5 epitope: bases 1011-1052
Polyhistidine (6xHis) tag: bases 1062-1079
BGH reverse priming site: bases 1102-1119
BGH polyadenylation signal: bases 1108-1332
SV40 early promoter and origin: bases 1833-2142
Neomycin resistance gene: bases 2217-3011
SV40 early polyadenylation signal: bases 3189-3319
pUC origin: bases 3700-4373 (complementary strand)
Ampicillin (*bla*) resistance gene: bases 4518-5378 (complementary strand)
bla promoter: bases 5379-5477 (complementary strand)

Invitrogen™
life technologies

9.2 BCA protein assay Kit standard preparation guidelines.

Preparation of Standards and Working Reagent (required for both assay procedures)

A. Preparation of Diluted Albumin (BSA) Standards

Use Table 1 as a guide to prepare a set of protein standards. Dilute the contents of one Albumin Standard (BSA) ampule into several clean vials, preferably using the same diluent as the sample(s). Each 1mL ampule of 2mg/mL Albumin Standard is sufficient to prepare a set of diluted standards for either working range suggested in Table 1. There will be sufficient volume for three replications of each diluted standard.

Table 1. Preparation of Diluted Albumin (BSA) Standards

Dilution Scheme for Standard Test Tube Protocol and Microplate Procedure (Working Range = 20-2,000µg/mL)

Vial	Volume of Diluent (µL)	Volume and Source of BSA (µL)	Final BSA Concentration (µg/mL)
A	0	300 of Stock	2000
B	125	375 of Stock	1500
C	325	325 of Stock	1000
D	175	175 of vial B dilution	750
E	325	325 of vial C dilution	500
F	325	325 of vial E dilution	250
G	325	325 of vial F dilution	125
H	400	100 of vial G dilution	25
I	400	0	0 = Blank

Dilution Scheme for Enhanced Test Tube Protocol (Working Range = 5–250µg/mL)

Vial	Volume of Diluent (µL)	Volume and Source of BSA (µL)	Final BSA Concentration (µg/mL)
A	700	100 of Stock	250
B	400	400 of vial A dilution	125
C	450	300 of vial B dilution	50
D	400	400 of vial C dilution	25
E	400	100 of vial D dilution	5
F	400	0	0 = Blank

B. Preparation of the BCA Working Reagent (WR)

1. Use the following formula to determine the total volume of WR required:

   (# standards + # unknowns) × (# replicates) × (volume of WR per sample) = total volume WR required

   Example: for the standard test-tube procedure with 3 unknowns and 2 replicates of each sample:

   (9 standards + 3 unknowns) × (2 replicates) × (2mL) = 48mL WR required

   Note: 2.0mL of the WR is required for each sample in the test-tube procedure, while only 200µL of WR reagent is required for each sample in the microplate procedure.

2. Prepare WR by mixing 50 parts of BCA Reagent A with 1 part of BCA Reagent B (50:1, Reagent A:B). For the above example, combine 50mL of Reagent A with 1mL of Reagent B.

9.3 Cell line mutation profiling

Table 9-1 : The mutation status of CRC cell lines for commonly mutated genes in CRC.

	KRAS **Exon 2**	*KRAS* **Exon 4**	*BRAF* **Exon 11**	*BRAF* **Exon 15**	*PIK3CA* **Exon 20**	*PTEN* **Exon 3**	*TP53* **Exon 6**
HCT116	Mutant	Wt.	Wt.	Wt.	Mutant	Wt.	Wt.
RKO	Wt.	Wt.	Wt.	Mutant	Mutant	Wt.	Wt.
C32	Wt.	Wt.	Wt.	Wt.	Wt.	Wt.	Wt.
CACO2	Wt.	Wt.	Wt.	Wt.	Wt.	Wt.	Mutant
SW480	Mutant	Wt.	Wt.	Wt.	Wt.	Wt.	Wt.
SW620	Mutant	Wt.	Wt.	Wt.	Wt.	Wt.	Wt.
DLD1	Mutant	Wt.	Wt.	Wt.	Wt.	Wt.	Wt.

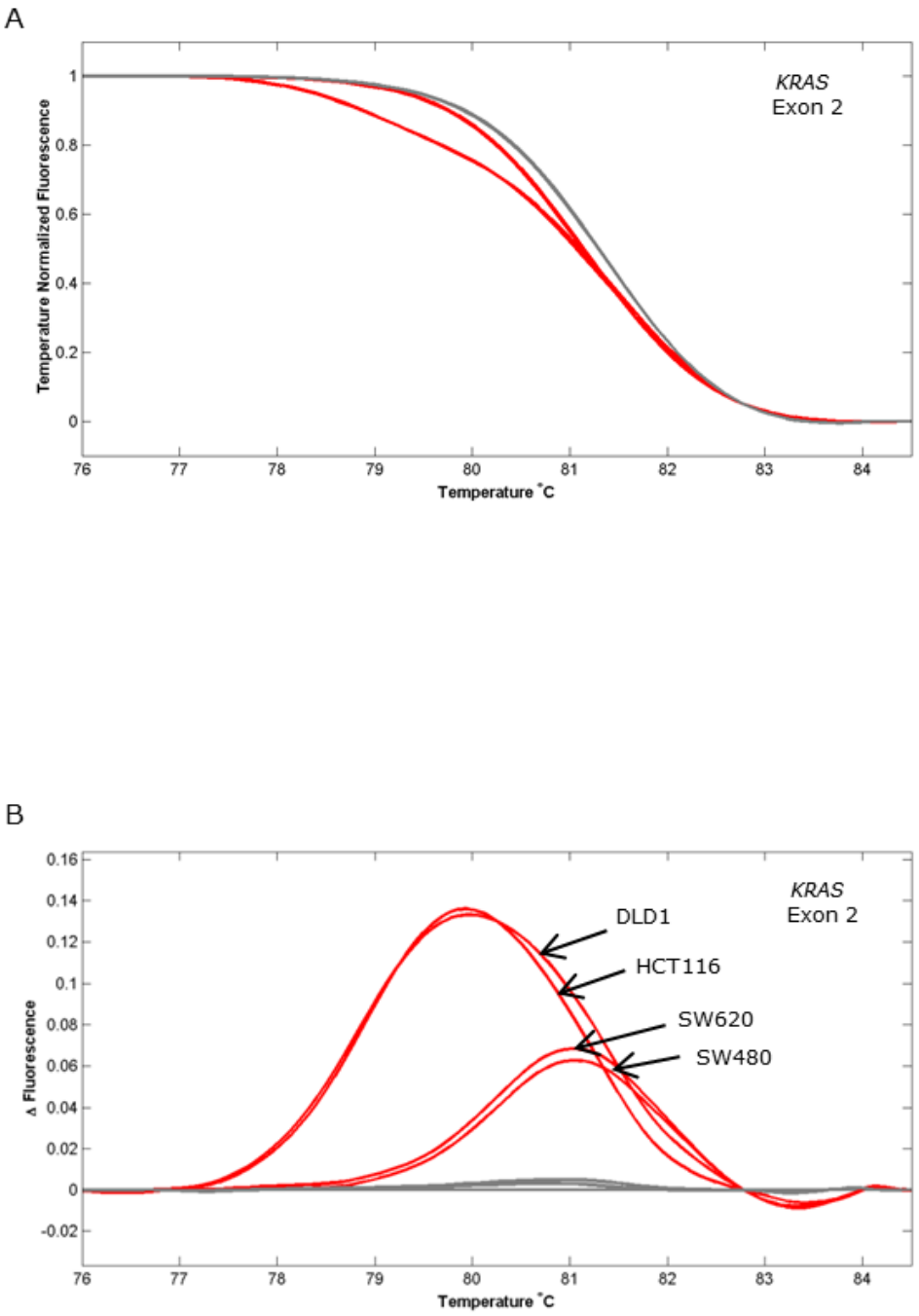


Figure 9-1 : The screening of CRC cell lines for a mutation in KRAS exon2. A) KRAS exon 2 shifted melting curve for HCT116, Caco-2, RKO, DLD1, C32 SW480 and SW620. B) The difference plot for Kras exon 2 revealed that DLD1, HCT116, SW620 and SW480 displayed a mutation in this exon.

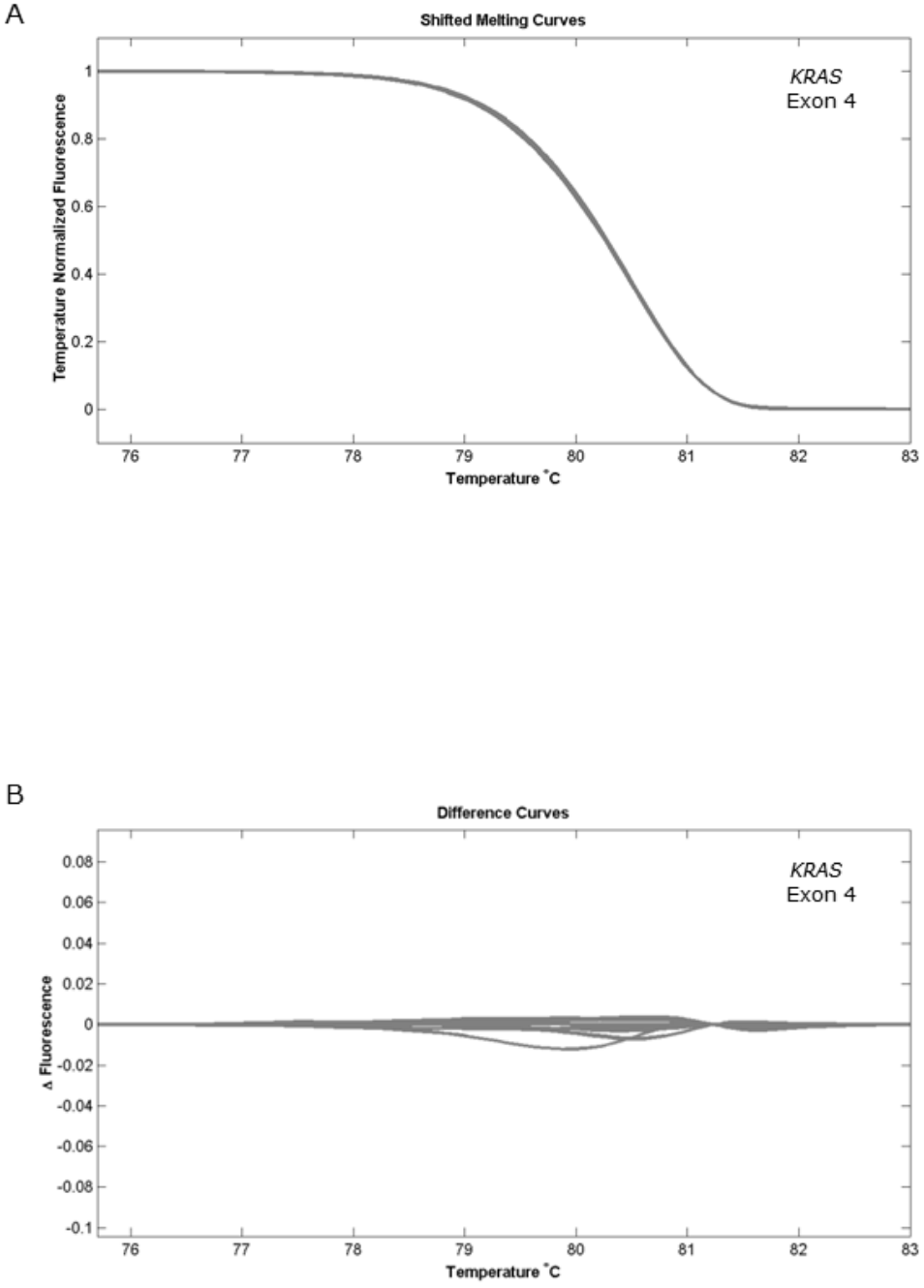


Figure 9-2 : The screening of CRC cell lines for a mutation in KRAS exon4. A) KRAS exon 4 shifted melting curve for HCT116, Caco-2, RKO, DLD1, C32 SW480 and SW620. B) The difference plot for Kras exon 4 revealed that all cell lines were wt. for this exon.

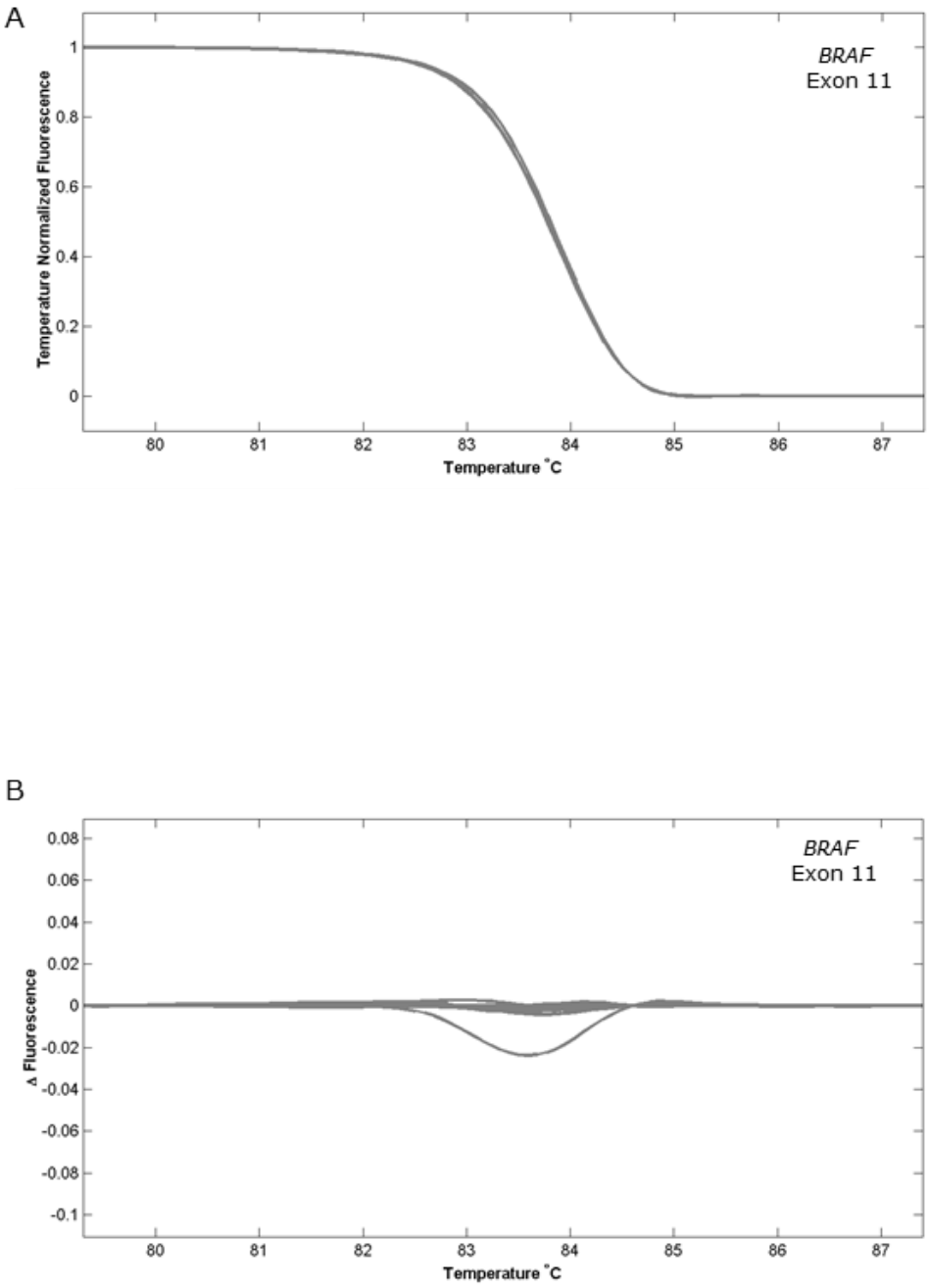


Figure 9-3 : The screening of CRC cell lines for a mutation in BRAF exon 11. A) BRAF exon 11 shifted melting curve for HCT116, Caco-2, RKO, DLD1, C32 SW480 and SW620. B) The difference plot for BRAF exon 11 revealed that all cell lines were wt. for this exon.

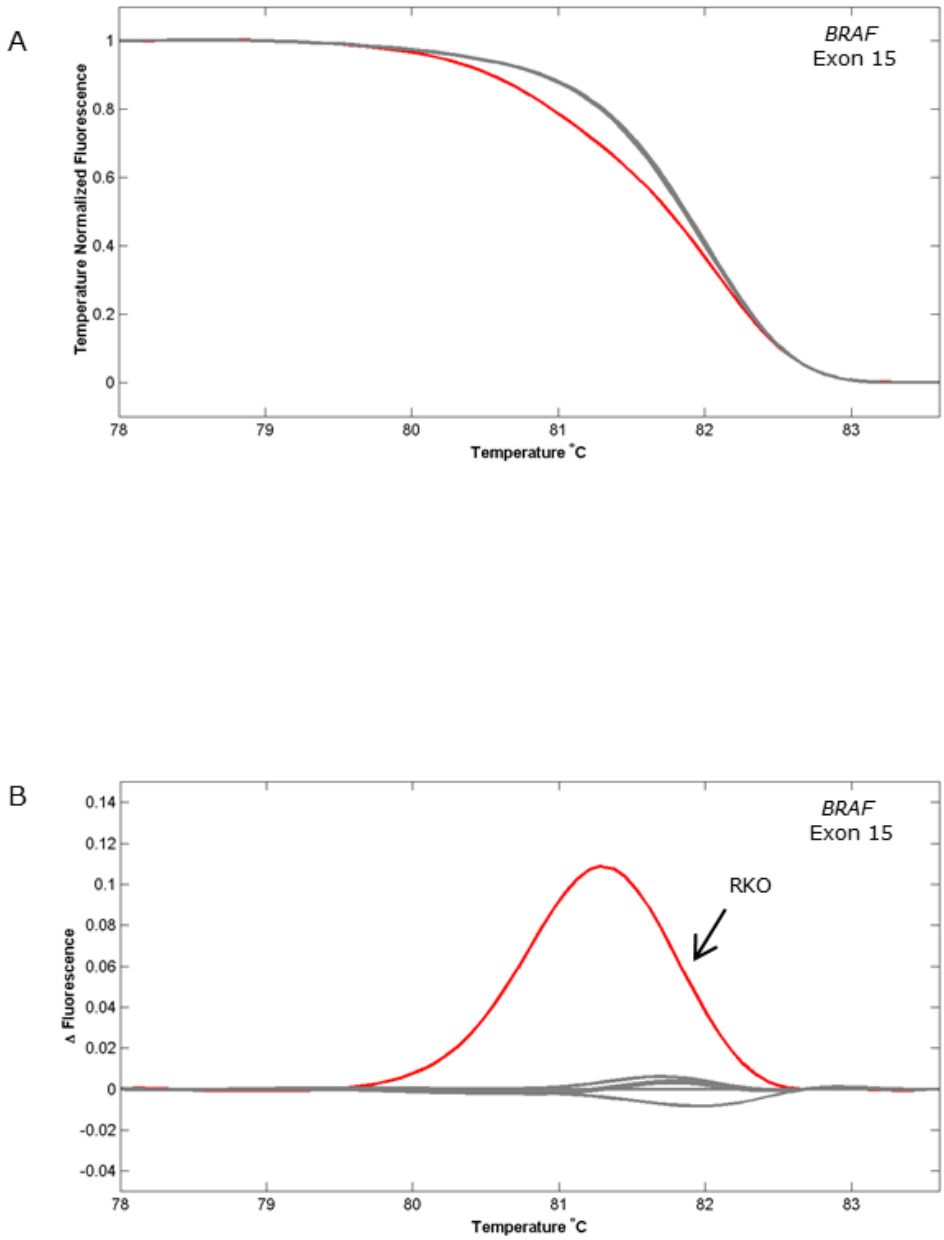


Figure 9-4 : The screening of CRC cell lines for a mutation in BRAF exon 15. A) BRAF exon 15 shifted melting curve for HCT116, Caco-2, RKO, DLD1, C32 SW480 and SW620. B) The difference plot for BRAF exon 15 revealed that only RKO displayed a mutation in this exon.

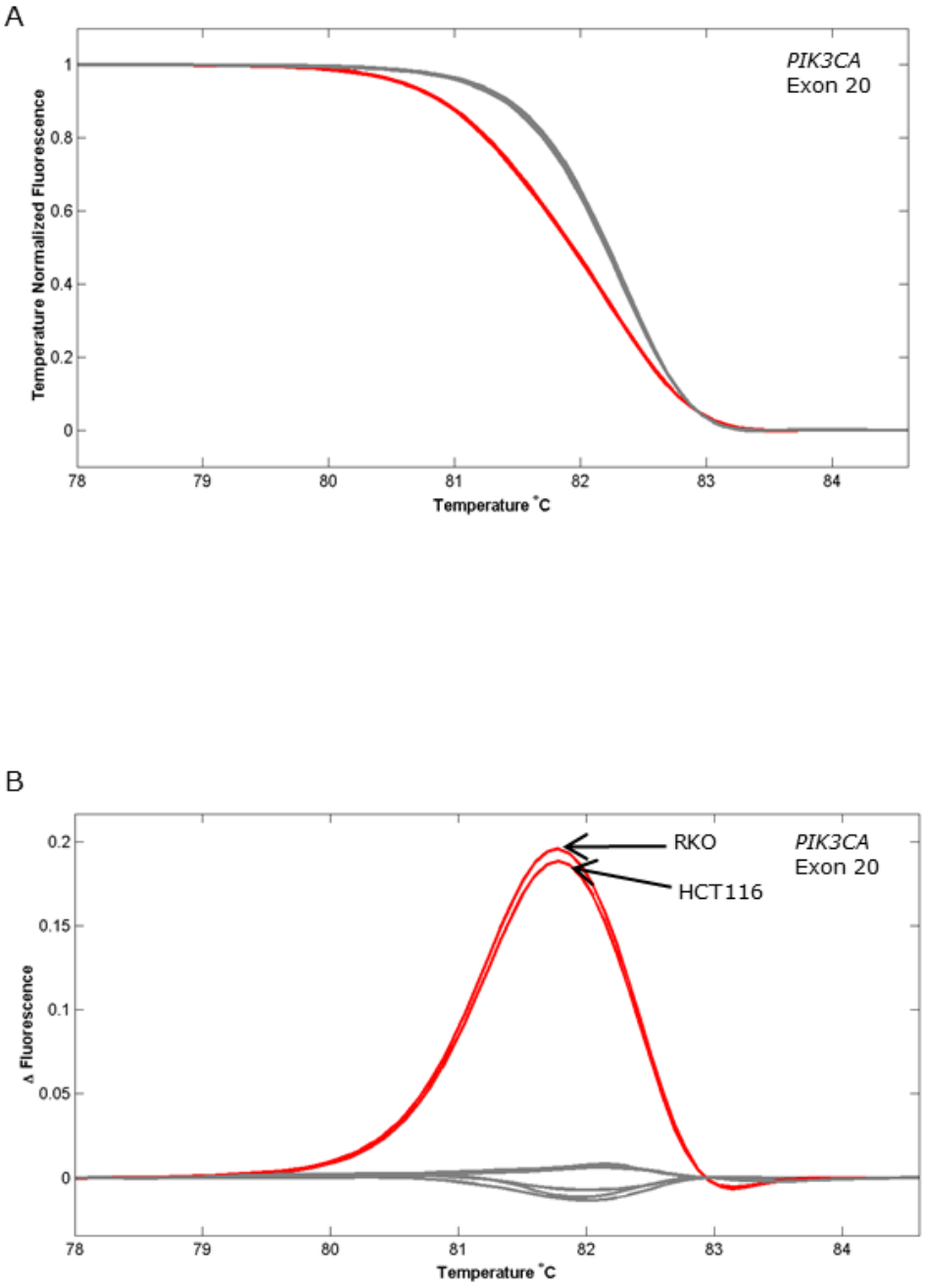


Figure 9-5 : The screening of CRC cell lines for a mutation in PIK3CA exon 20. A) PIK3CA exon 20 shifted melting curve for HCT116, Caco-2, RKO, DLD1, C32 SW480 and SW620. B) The difference plot for PIK3CA exon 20 revealed that HCT116 and RKO displayed a mutation in this exon.

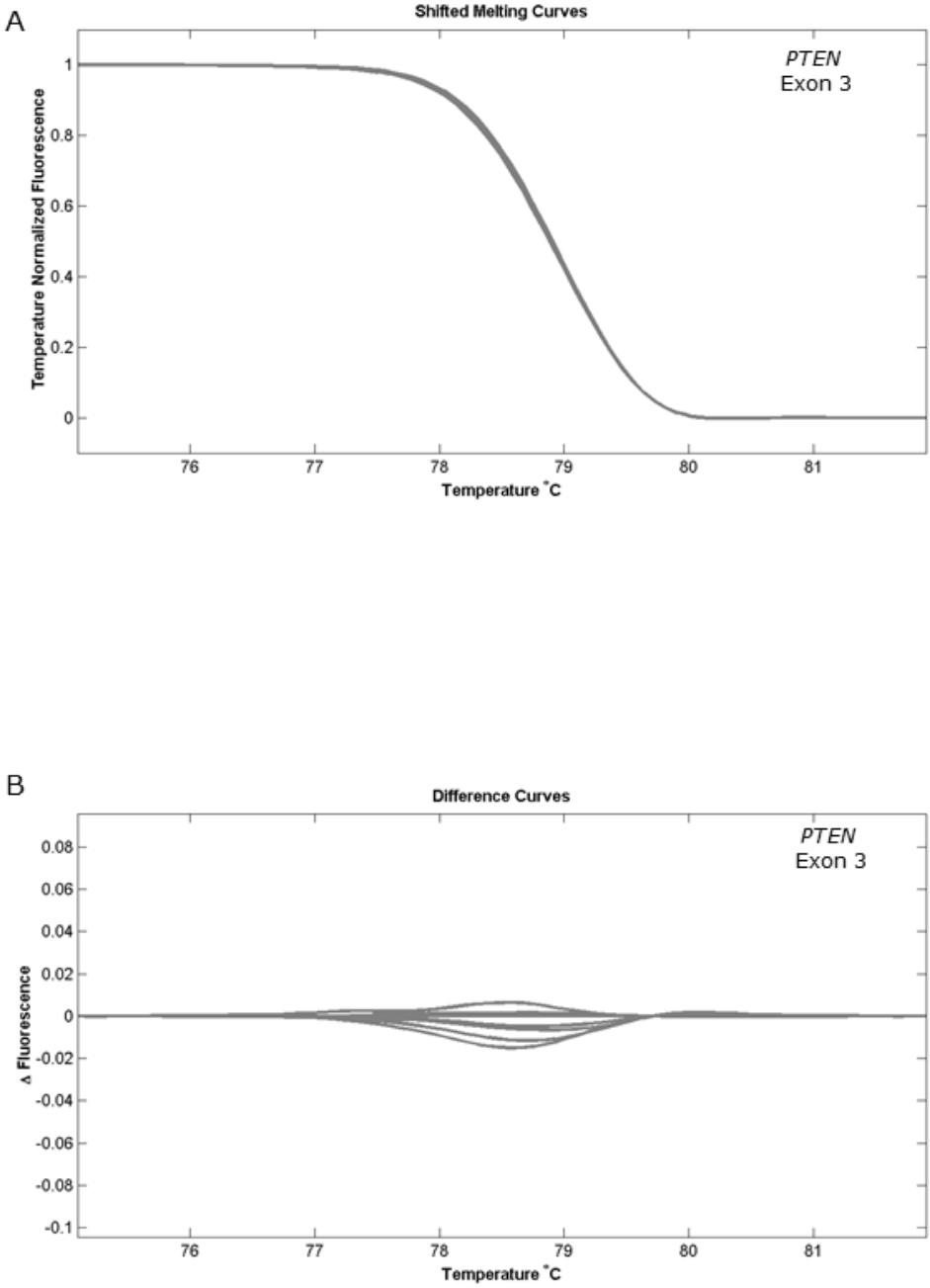


Figure 9-6 : The screening of CRC cell lines for a mutation in PTEN exon 3. A) PTEN exon 3 shifted melting curve for HCT116, Caco-2, RKO, DLD1, C32 SW480 and SW620. B) The difference plot for PTEN exon 3 revealed that all cell lines were wt. for this exon.

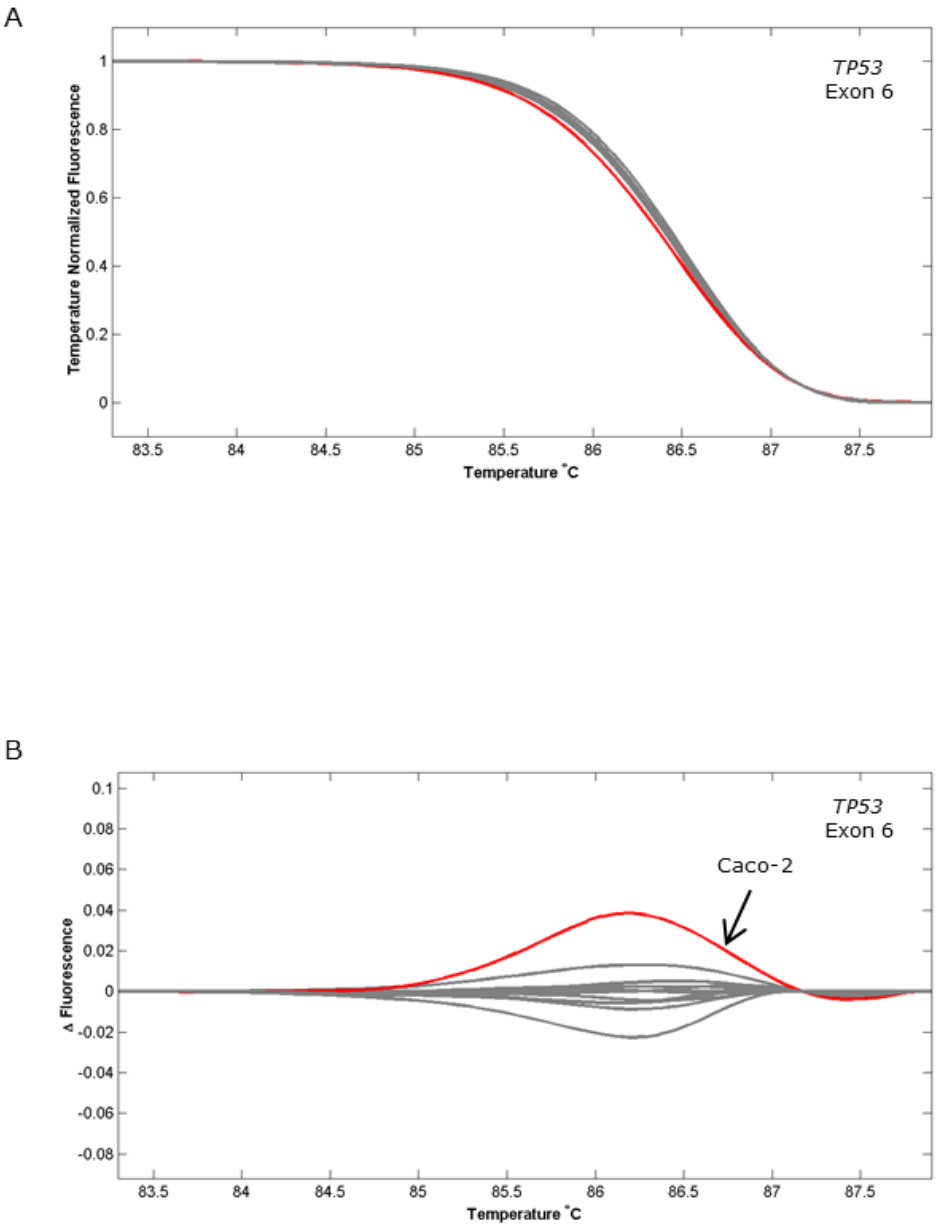


Figure 9-7 : The screening of CRC cell lines for a mutation in TP53 exon 6. A) TP53 exon 6 shifted melting curve for HCT116, Caco-2, RKO, DLD1, C32 SW480 and SW620. B) The difference plot for TP53 exon 6 revealed that only Caco-2 displayed a mutation in this exon.